IFS, Massey University, New Zealand

&

Fonterra, New Zealand

Investigations of the behaviour of pectin in casein micelle systems and their analogues

Thesis presented by:

Aurélie Suzanne Bernadette CUCHEVAL

For the degree of Doctor of Philosophy in Physics

Research conducted at the Institute of Fundamental Sciences, Massey University of Palmerston North

Supervision by: **Dr. Martin A.K Williams**
Co-supervision by: **Dr. Yacine Hemar and Dr. Don Otter**

May 28, 2009

Abstract

Firstly, the effect of pectin on acid milk gels in concentrated, quiescent systems was investigated by passive microrheology using two complementary techniques: diffusive wave spectroscopy (DWS) and multiple particle tracking (MPT). DWS, by allowing probing the mechanical properties of the network at high frequency, gave information on its microstructure. The addition of high methoxyl pectins was shown to change the network structure which has been explained by bridging of the casein micelles by the polymer as the system was undergoing acidification. On the other hand, the presence of low methoxyl pectin in the acid milk gel was shown to have no effect on the microstructure of the network at low concentration of polymer (0.1%w/w) which has been attributed to the sensitivity of this low DM pectin to calcium: LM pectin are trapped by calcium and not able to interact with casein micelles anymore. Multiple particle tracking was used to probe the effect of pectin on the heterogeneity of the system by following the distribution of the displacements of added micro beads at a given time lag during the gelation using the Van Hove distribution. Furthermore, the surface chemistry of the probes was modified in an attempt to control their location in the system. Finally, the mean square displacements of the casein micelles obtained by DWS and, of κ-casein coated particles obtained by MPT were shown to give good agreement for the same acid milk system.

Having established that the interaction between casein micelles and low methoxyl pectin is prevented by the pectin sensitivity to calcium, the effect of the pectin fine structure was investigated on the interaction between κ-casein and pectin by surface plasmon resonance (SPR). The amount of pectin binding on a κ-casein coated gold surface was shown to be strongly dependant on the pectin fine structure. It was concluded that small negative patches on the pectin backbone, likely to comprise of around two consecutive unmethylesterified galacturonic acid, are the most effective for pectin binding to κ-casein. The effect of the direct interaction between pectin and κ-casein on 'calcium-free casein micelle mimics' in pectin solution was then investigated using coated latex beads. A pectin structure with a limited number of negative patches on its backbone was also shown to limit the potential for destabilization via bridging.

Acknowledgements

I better first start with the VIPs…Bill Williams, Don Otter and Yacine Hemar. Yacine; thanks for always being here, always being available for questions…and answering fast a bit in a 'Lucky Luck' way…thanks for all your good ideas… and thanks as well for believing in me and for your encouragements… Don; thanks for all interesting and helpful discussions and good ideas…and thanks for your milk knowledge. Bill, if I say Super Bill, you will tell me to not take the mickey, but it is in a good way….thanks for all your help, your passion for pectin, your hidden passion for milk….and your enthusiasm all the way. I enjoyed all these discussions in your office…even what you call 'wibbles' …now I know the proper way to communicate with (swearing) English people.

I would also like to thank all the members of the Biopolymer group for ideas exchange, discussions…and good moments. Medhat Al-Ghobashy, I better confess, I am really impressed by your lab organization and your knowledge of techniques, thanks a lot to have let me in your lab and initiate me to the Biacore. Dr RRR Vincent, work with you was fun even if we didn't agree too often…your physics knowledge (in a no stamp collection way) was much appreciated…and thanks for your special way to always see the positive side of each problem…thanks Bro. Motoko, thanks to have taken time to show me the NMR techniques and to have shared with me the PME experience. Erich, going with you and Bill to the synchrotron was cool (far from 'boring'), thanks for your help to prepare the samples there…Erich and Steve, thanks for the 'social pressure', you know what I mean…

I would like to thank all the people from Fonterra who helped me, especially Rob Hunter, Skelte Anema and Steve Taylor.

Chère 'familie', que pouvais je faire de pire que de partir aux 'antipodes' (comme papa aime a le répéter) et pourtant vous m'avez supporté tout du long, et vous êtes même venu en expédition organisée…merci, merci beaucoup...

Moncheri, pour les nombreux aller-retour à la fac à pas d'heure, les multiples problèmes et fins du monde que je te ressasse, pour t'avoir ignoré quelquefois, tu dessers une médaille pas de crapauds mais de charming prince!

Abbreviations

MPT	Multiple Particle Tracking
DWS	Diffusive Wave Spectroscopy
HG	Homogalacturonan
DM	Degree of Methylesterification
HM pectin	High-Methoxy pectin
LM pectin	Low-Methoxy pectin
DB	Degree of Blockiness
RGI	RhamnoGalacturonan I
RGII	RhamnoGalacturonan I
AFM	Atomic Force Microscopy
PME	Pectin Methyl-Esterase
f-PME	Fungal Pectin Methyl-Esterase
p-PME	Plant Pectin Methyl-Esterase
NMR	Nuclear Magnetic Resonance
PL	Pectin Lyase
PG	PolyGalacturonase
Mw	Molecular weight
PGA	PolyGalacturonic Acid
$G'(\omega)$	Elastic modulus
$G''(\omega)$	Viscous modulus
f	Frequencies
k	Boltzmann constant
T	Temperature
$<r_2(\tau)>$	Mean Square Displacement

PEG	PolyEthylene Glycol
τ	Time lag
$g_1(\tau)$	Field autocorrelation function
$g_2(\tau)$	Intensity autocorrelation function
l*	Light mean free path
z_0	Penetration depth
L	DWS (cell) sample thickness
T0, T1, T2	Treatment 0, 1, 2
SPR	Surface Plasmon Resonance
RU	Resonance Unit
D	Diffusion coefficient
DAm	Degree of amidation
GDL	Glucono-δ-lactone
pC	Cirtical pH
a	Radius of particle
LMA pectin	Low Methoxyl Amidated pectin
CE	Capillary Electrophoresis
HG	Homogalacturonan
Dabs	Absolute Degree of blockiness

Table

Chapter 1

Background

1 Pectin

Pectin is a structural carbohydrate rich in galacturonic acid. An important component of the primary cell walls of plants, pectin plays a major role as a cementing material in the middle lamella through its interaction with cellulose and hemicelluloses (Marry *et al.*, 2006, Willats *et al.*, 2001) as well as contributing to pH and ionic strength control in the plant cell (Nussinovitch, 1997, Limberg *et al.*, 2000). Pectin is also determinant for the mechanical properties of the plant cell through its interaction with calcium and its ability to form a network. Pectin biosynthesis requires the action of at least 53 different enzymes (Mohnen, 1999) while other enzymes modify and regulate the pectin fine structure in location and time (Ström and Williams, 2004). Pectins are secreted into the wall as highly methylesterified forms. They can be subsequently modified by pectin methylesterase (PME) which deesterifies the pectin into pectic acid and methanol (Micheli, 2001). Pectin is arguably the most complex polymer of the plant cell polysaccharides.

In a normal western diet around 4-5g of pectin are consumed each day. Worldwide annual consumption is estimated at around 45 million kilograms (Willats *et al.*, 2006). Indeed pectin is used in the food industry for jam production (Pilgrim *et al.*, 1991), but also to stabilise cloudiness in beverages and to stabilise proteins in acid milk products (Nussinovitch, 1997, Glahn, 1982). There are not any specific limitations or guidelines for the use of pectin in food product (Food and Drug Administration) (Nussinovitch, 1997), and the recommended daily intake of soluble dietary fibre which includes pectin is 35g per day (Thebaudin *et al.*, 1997). Pectin has been shown to have health benefits, as it has a positive effect on cholesterol regulation (Keys *et al.*, 1961), hypoglycaemic control (Marles, 1995), immunostimulation (Inngjerdingen *et al.*, 2007) and induces apoptosis of prostate cancer cell (Jackson *et al.*, 2007).

Pectins are polymolecular and polydispersed, exhibiting significant heterogeneity with respect to both chemical structure and molecular mass (Perez *et al.*, 2000). The composition of pectin varies with sources, extraction process and location (Braccini and Perez, 2001).

1.1 Pectin structure

Pectin describes a family of oligosaccharides and polysaccharides that have common features, but are extremely diverse in their fine structure. The Food and Agriculture Organization of the United Nations (FAO) definition of pectin is given by its galacturonic acid content which should be superior to 65% (Willats *et al.*, 2006).

At first sight, pectin is essentially a linear heteropolysaccharide consisting mainly of polymerized, partly methanol-esterified (1-4)-linked α-D-galacturonic acid with a small fraction of rhamnose and small side chains formed by other sugars (Capel *et al.*, 2005, Morris *et al.*, 1982). The chemical structures of (1-4)-linked α-D-galacturonic acid and [→4)- α-D-GalA-(1→2)-α-L- rha-(1→] are shown in figure 1. The pectin pKa depends of the dissociation degree, the degree of methylesterifiaction and the intramolecular distribution of the methylester group along the pectin chain. But at a degree of dissociation equal to 0, the pKa is about 2.9 whatever the degree of methylesterification (DM) and the charge distribution along the pectin chain (Ralet *et al.*, 2001).

Pectin is characterized by its degree of methylesterification (DM) and in some cases, when the pectin backbone has been amidated in vitro, by its degree of amidation (DA) (Capel *et al.*, 2005). However, pectin methylester intramolecular distribution is difficult to characterise. Two approaches have been investigated. The calculation of the degree of blockiness (DB), determined by Daas and co-worker (Daas *et al.*, 1999) is obtained by analysis of the digest of pectin by a degrading enzyme. DB is the percentage of the unesterified GalA residues released from pectin samples that are fully digested by the endoPG enzyme (Ström, 2006). Another more direct method has been pursued by Nuclear Magnetic Resonance (NMR) where the frequencies of the possible triad sequences of residues within the chain are measured (Kim *et al.*, 2005).

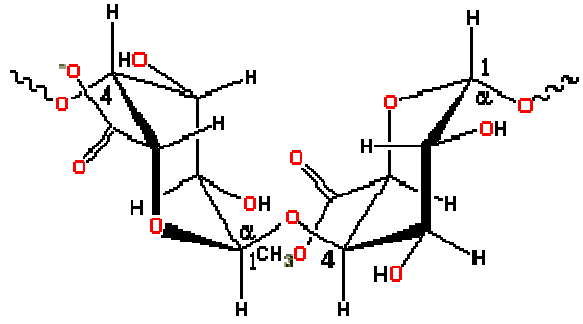

Figure 1a: (1-4)-linked α-D-galacturonic acid

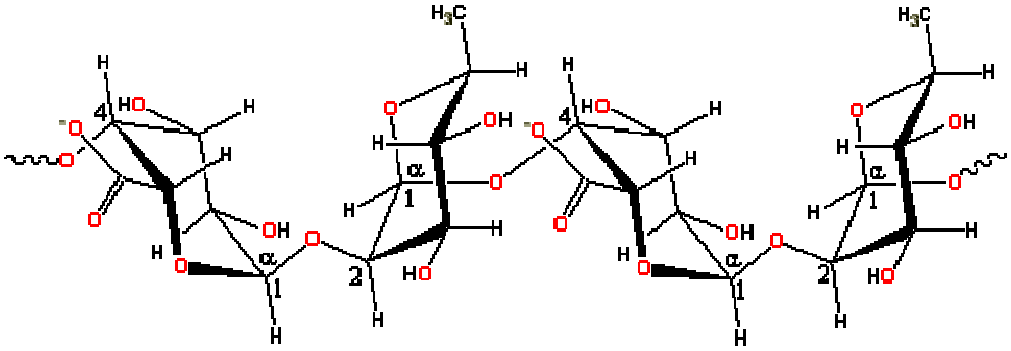

Figure 1b: [→4)- α-D-GalA-(1→2)- α-L- rha-(1→]

In more details, pectin contains 3 pectic polysaccharides (Willats *et al.*, 2006, Ström, 2006):

- Homogalacturonan (HG): linear polymer of (1-4)-linked α-D-galacturonic acid
- Rhamnogalacturonan I (RGI): repeating disaccharide [→4)- α-D-GalA-(1→2)- α-L- rha-(1→] backbone with glycan (principally arabinan, arabinogalactan and galactan) side chains attached to the Rha residues at C-4. The side chains have a length of 1-20 residues.
- Rhamnogalacturonan II (RGII): backbone of HG (1,4-linked α-D-GalA), with complex sugars side chains attached to the GalA residues. The side chains are composed of sugar as xylose, galactose, rhamnose and unusually fucose and apiose.

The region of the backbone consisting of homogalacturonan is often considered as the 'smooth' area, whereas the ones containing rhamnogalacturonan are 'hairy': sugar side chains are attached to the rhamnosyl residues of the backbone (Limberg *et al.*, 2000, Schmelter *et al.*, 2002). Two models are proposed for the pectin fine structure. In the conventional one (figure 2A), rhamnogalacturonan and galacturonan domains form the 'backbone' of pectic polymer. In the recently proposed one, the backbone is a long chain of rhamnogalacturonan I (figure 2B) (Willats *et al.*, 2006). The extraction process modifies the pectin fine structure, notably decreasing the number of side chains. Indeed, commercially extracted pectins consist mainly of homogalacturonan and 5-10% of neutral sugar (Ridley *et al.*, 2001, Willats *et al.*, 2006).

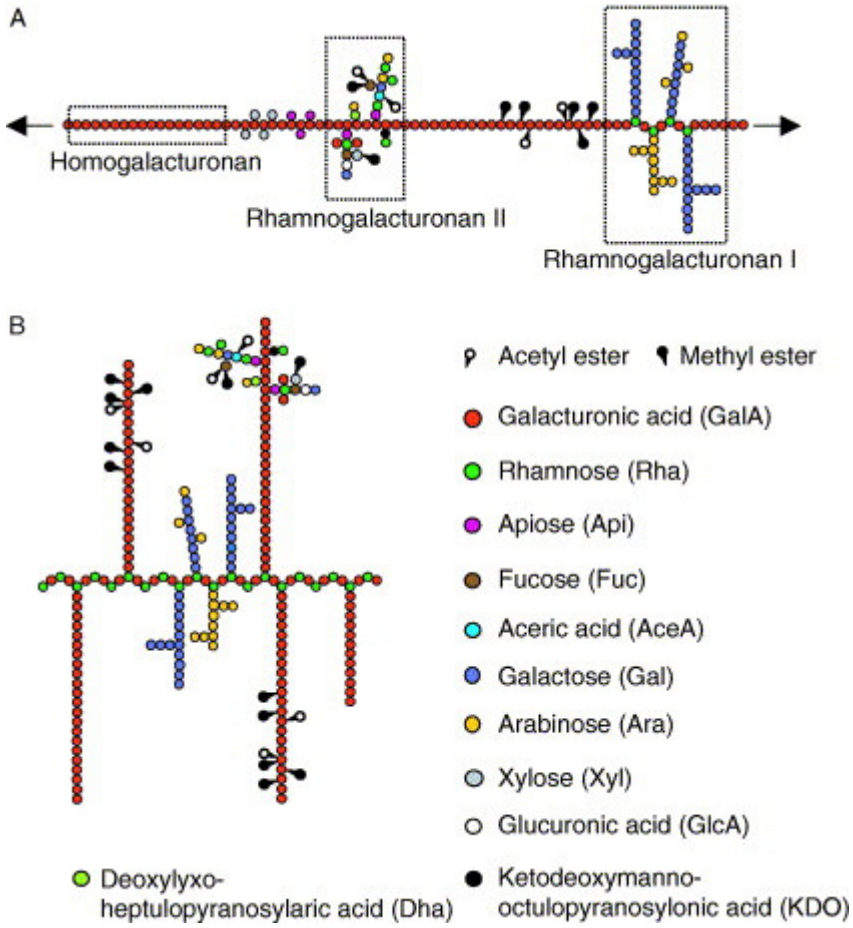

Figure 2: Schematic representations of the conventional (A) and recently proposed alternative (B) structures of pectin (Willats *et al.,* 2006).

1.2 Pectin fine structure modification

Pectin can be deesterified by the action of enzymes: pectin methylesterase (PME) or chemically by the addition of alkali or acid. In presence of ammonia, the de-esterification is a way to convert some of the methyl-ester groups to amide groups (Ström, 2006). Designing pectins with amide groups on their backbone is an effective way to reduce the kinetics of gelation as it introduces positive charges on the polymer.

1.3 Enzymatic deesterification: pectinesterase

Pectinesterase follows the catalysis reaction:

$$RCOOCH_3 + H_2O \rightarrow RCOOH + CH_3OH$$

1.3.1 Plant Pectinesterase

Enzymatic deesterification in planta is in general a sequential process (Taylor, 1982). Pectinesterase initiates its action adjacently to a free carboxyl group or at the free reducing end, and proceeds along the chain in a stepwise fashion, producing blocks of free carboxyl groups (Morris *et al.*, 1982). The PME mechanisms result in the consecutive removal of a number of neighbouring methyl ester groups and the formation of 'blocky pectin' (Hotchkiss *et al.*, 2002). PME treatment increases rapidly the calcium sensitivity of the polymer (Hotchkiss *et al.*, 2002, Ralet *et al.*, 2001). Pectin samples treated with plant PME have also a broader DM distribution than those produced with fungal PME or alkali treatment (Ström, 2005).

Pectinesterase generally follows Michaelis-Menton kinetics, but it has isozymes with different pH optima and kinetic properties (Sajjaanatakul and Pitifer, 1991). The enzyme activity is dependant on pH, cations and temperature (Sajjaanatakul and Pitifer, 1991). Monovalent and divalent cations enhance the enzyme activity with an optimal cation concentration under specific condition for an optimal activity. PME activity is inhibited by a block of free carboxyl groups in the pectin chain. The optimal pH for PME activity

depends on its origin. Plant PMEs show a broad optimum between pH 6.5 and 9.5 (Sajjaanatakul and Pitifer, 1991). Commercial orange peel enzyme (Sigma), the most commonly used in research, has a broad range of activity and a maximum activity at pH 9 in absence of salt and pH 6 in presence of 1.2% NaCl (Savary *et al.*, 2002).

1.3.2 Fungal pectinesterase

Fungal pectinesterase (F-PME) is believed to act with a multiple chain mechanism which leads to a random removal of methyl ester groups. If the DM stays above 50%, the calcium sensitivity is not improved by f-PME treatment (Limberg *et al.*, 2000). The optimal pH for F-PME activity is 4.0-5.2 (Sajjaanatakul and Pitifer, 1991).

1.4 Alkaline deesterification

Chemical de-esterification uses base catalysis. Alkaline deesterification is believed to produce random esterified pectin as f-PME (Limberg *et al.*, 2000). In alkaline condition (pH10-11), the reaction of de-esterification by saponification is in competition with the β-elimination which digests the pectin chain. The reaction of saponification is favoured by increasing the pH and the reaction of β-elimination by increasing the temperature (Renard and Thibault, 1996).

1.5 Backbone degradation by polygalacturonase (PG)

Polygalacturonases catalyse the hydrolysis of glycosidic bonds between de-esterified galacturonide residues in pectin (Nussinovitch, 1997). The different esterification patterns influence the way hydrolytic enzymes like PGI or PGII cleave the HG backbone (Limberg *et al.*, 2000) and hence they have been used to determine pectin intramolecular structure (Hunt *et al.*, 2006, Williams *et al.*, 2001).

The substrate binding site of PGII (the PG commonly used in this thesis), is made up of seven subsists. The enzyme is believed to tolerate some esterified residues in the subsite and to be able to "chop-up" a polymer shorter than the subsite length. The subsite size is believed to be 7, from -5 to +2. Subsite -1 and +1 must be unesterified for enzymatic action to occur. But PGII is able to bind a methylgalacturonate at the subsite -2 even if the hydrolysis rate is above 5 times higher for the unesterified oligomers (Kester *et al.*, 1999, Singh and Rao, 2002).

PGII (from *Aspergillus Niger*) has an optimum pH of 3.8-4.3 and a maximal activity at a temperature between 45 and 51 ˚C. The enzyme follows Michaelis–Menton kinetics (Singh and Rao, 2002).

1.6 Pectin gels

A pectin gel is formed when portions of homogalacturonan are cross-linked to form a 3D network in which water and solutes are restricted (Willats *et al.*, 2006). The methyl ester content and the distribution of the methylester group on the pectin backbone are the main parameters determining under which conditions a pectin network is formed (Ström, 2007). Gelation of low methoxyl pectin with DM<50% and blocky pectin with higher DM is induced by presence of calcium ions often by controlled calcium release methods (Ström, 2003, Stokke *et al.*, 2000). In this case, the pectin junction zones are formed by calcium cross-linking between free carboxyl groups (Willats *et al.*, 2006). Pectin can form gels at low pH in the absence of calcium. LM pectins with a blocky pattern (Morris *et al.*, 1982, Vincent *et al.*, 2008) are able to gel without added sugar and HM pectin requires the addition of a sufficient amount of sugar (Thebaudin *et al.*, 1997). The junction zones are formed by the cross-linking of homogalacturonan by hydrogen bridges and hydrophobic forces between methoxyl groups.

1.6.1 Calcium gels

Pectin-Ca^{2+} networks are formed in two stages: a formation of strongly linked and specific dimer associations followed by the formation of weak interdimer aggregation exerted by less-specific non-ionic intermolecular interactions, hydrophobic interactions and hydrogen bonds (Cardoso *et al.*, 2003, Braccini and Perez, 2001). This interdimer association leads to the approximate doubling in the amount of Ca^{2+} that is bound co-operatively (Morris *et al.*, 1982). The 'egg box' conformation has been attributed to this specific dimer association (figure 3): the calcium chelating with two acid functions from different pectic chains, is a bridge between two adjacent chains, zipping galacturonate unit together (Morris *et al.*, 1982, Flutti, 2003, Rees *et al.*, 1975). However this conformational model hasn't been validated by structural information and molecular dynamics simulations have shown that the egg box model is not the most energetically favourable (Braccini, 2001). Indeed a shift between the two chains leads to an efficient association with numerous van der Waals interactions (Braccini, 2001). Nevertheless, the egg box model is a good starting point to better understand the network microstructure for calcium pectin gels.

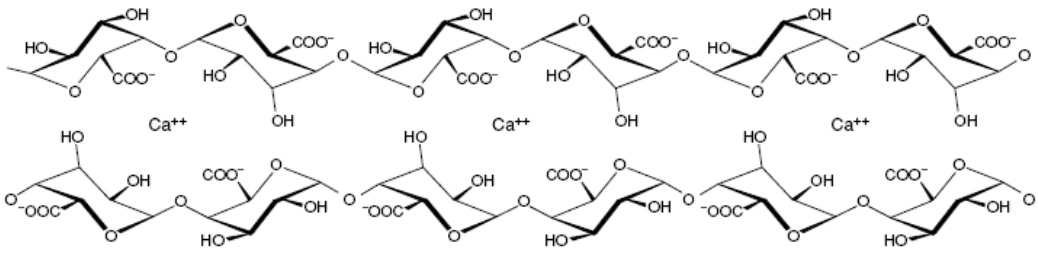

Figure 3: The egg box model (Flutti, 2003)

A minimum number of consecutive charges are believed to be required for a stable calcium-junction. This number has been estimated from 9 to 16 residues (Kohn, 1975, Powell *et al.*, 1982, Liners *et al.*, 1992). One could presume then that the number of charges present on the backbone (DM) and their intermolecular and intramolecular distribution will play an important role in the polymer affinity to calcium and the gel formation. Indeed, the pectin

chain affinity towards calcium increases with the decreasing degree of methylesterification (Cardoso *et al.*, 2003). Ström *et al.* (2006 & 2007) found a good correlation between the small deformation rheological response and the absolute degree of blockiness for enzymatically and alkali modified pectin. The DB_{abs} is defined as the amount of monomer, dimer and trimer obtained by PGII digestion divided by the total amount of galacturonate (Guillotin *et al.*, 2005). The pectin chain affinity towards calcium also increases with decreasing the ionic strength, and with increasing the polymer concentration (Cardoso *et al.*, 2003).

The rheological properties of calcium induced gels have been extensively studied. The gelation kinetics of the storage modulus as a function of curing time (at 1Hz, at temperature constant within 5-20˚C) is typical of that of other gelling biopolymers. *G'* and *G"* increase first rapidly and subsequently more slowly approaching pseudo-equilibrium, whereas the loss modulus *G"* is always lower than *G'* (Cardoso *et al.*, 2003).

Recently, microrheology studies of pectin gel have given insight into the microstructure of the network with measurements at high frequency (10^4-10^6Hz) (Vincent *et al.,* 2007 & 2009, Williams *et al.*, 2008). Calcium gels made with high methoxyl pectin (blocky pattern, DM62%) exhibited behaviour indicative of semi-flexible polymer network as observed for actin solutions (Xu *et al.*, 1998). Subsequently by varying polymer and calcium concentration, gels were formed from the same pectin that showed the signatures of chemically cross-linked network of flexible polymer with short ion-binding blocks.

1.6.2 Acid gels

At low pH and decreased water activity, the intermolecular electrostatic repulsions are minimized and chain-chain interactions are more favourable than chain-solvent interaction. The methoxyl groups are stacked together through hydrophobic interactions and hydrogen bonding between protonated carboxyl groups. This promotes the gel formation without the addition of calcium. This type of interaction is favoured by a high degree of esterification in presence of sugar because the ester groups contribute to the stability of the

interchain junctions and decrease the charge density. In absence of sugar, only the LM pectins are able to form gel at low pH. In this case, the gel is formed predominantly through hydrogen bonding (Morris *et al.*, 1980, Walkinshaw and Arnott, 1981).

2 Milk protein

2.1 Milk composition

2.1.1 General

Milk contains an oil-in water emulsion with fat as the dispersed phase, a colloidal suspension of casein micelles, globular proteins and lipoprotein particles and a solution of lactose, soluble proteins, minerals, vitamins and other components in the aqueous phase (Swaisgood, 1996).

The general composition of milk of western cows (in weight %) is (Corbin and Whittier, 1965) :

Water 86.6 %

Milk fat 4.1 %

Protein 3.6%

Lactose 5%

Minerals (Ca, P, citrate, Mg, K, Na, Zn, Cl, Fe) 0.65%

Acids (citrate, formate, acetate, lactate, oxalate) 0.18%

Enzymes- peroxidase, catalase, phosphatase, lipase

Gases: oxygen, nitrogen

Vitamins: A, D, E,

2.1.2 Milk lipids

The main milk lipids are triglycerides (93.8%). Milk contains also small amounts of di- and monoacylglycerols, free fatty acid, phospholipids (0.8%) and cholesterol (0.3%) (Varnam and Sutherland, 1994).

Milk lipids are in the form of globules which are fat droplets covered by a thin membrane (8 to 10 nm). The globule size is in the range of 0.1-15 μm, and the major components of the thin membrane are proteins and phospholipids. The thin membrane decreases the lipid-water phase interfacial tension and limits the flocculation and coalescence between the fat globules (Varnam, 1994, Swaisgood, 1996).

2.2 Milk protein composition and structure

The nitrogen content of milk is distributed among caseins (76%), whey protein (18%), and non-protein nitrogen (6%). The caseins can be separated from the other proteins by precipitation at pH 4.6 (Swaisgood, 1996).

2.2.1 Caseins

Casein molecules are small proteins (molecular mass between 20-25kDa). They behave like heterogeneous copolymers, with a strong tendency for self assembly and for adsorbing strongly to hydrophobic surfaces (Jenness *et al.*, 2001, Dickinson, 2006).

Individual caseins

The casein proteins are phosphoproteins. There are 4 different forms of casein: α_{s1}-casein, α_{s2}-casein and β-casein which are calcium sensitive, and κ-casein which is calcium insensitive. The κ-caseins in solution stabilise the presence of calcium-sensitive group of the other caseins avoiding the precipitation with calcium (Swaisgood, 1996, Horne, 2006). Calcium sensitive caseins, which are highly phosphorylated, are able to bind calcium by their phosphate group. The phosphate group is on the hydroxyl groups of serine.

Phosphoserine residues are concentrated in cluster of 2, 3, or 4 of such residues and are responsible for the existence of hydrophilic areas with strong negative charge (Swaisgood, 1996, Jenness *et al.*, 2001, Horne, 2006).

Caseins are flexible and disordered due to the presence of proline which inhibits the formation of α-helices, β-sheets and β-turns. Without a tertiary structure, the hydrophobic residues are exposed which gives a strong association reaction and a low solubility in water (Swaisgood, 1996, Dickinson, 2006).

The charge characteristics and the phosphate content of the different casein forms are presented in the following table (Swaisgood, 1996):

Protein	Isoionic pH	Charge density at pH 6.6 ($mC.m^{-2}$)	Number of phosphate group
α(s1)-casein	4.94	-21.9	8-9
α(s2) casein	5.37	-13.8	10-13
β-casein	5.14	-13.3	5
κ-casein	5.90	-2.0	1

Table 1: Charge characteristics of the caseins (Swaisgood, 1996)

Casein forms are differentiated by their calcium sensitivity and their charge distribution (Varnam, 1994, Jenness *et al.*, 2001, Fox and Kelly, 2004, Dickinson, 2006):

- α_{s1}-casein contains two hydrophobic regions separated by a polar region, large numbers of proline residues inhibit the formation of secondary structure and promote the exposition of nonpolar groups at the surface. They associate into long chain-like aggregates by electrostatic and hydrophobic interactions.
- α_{s2}-casein: The negative charges are concentrated near the N-terminus and positive charges near the C-terminus. It is the most hydrophilic of the caseins and contains three anionic clusters.
- β-casein, a very amphiphilic protein, includes a highly charged N-terminal region which is mainly hydrophilic, and a hydrophobic C-terminal region. There are a large number of β-turns leading to the exposure of a considerable number of the nonpolar groups. The β-casein self-assembles into surfactant like micelles above a certain critical concentration.

- κ-casein is a heterogeneous mixture of polymers linked together by intermolecular disulfide bonds with mean molecular weights of 88,000 to 118,000. The N-terminal portion is hydrophobic and the C-terminal portion is hydrophilic. It is the only glycosylated casein. It contains only one proline residues and a charged oligosaccharide. The protein includes both α-helical and β-sheet motifs.

Casein micelles

The amphiphilic nature of caseins and their phosphorylation facilitate interactions with each other and with calcium phosphate to form highly hydrated spherical complexes known as micelles. The diameter is around 200 nm on average (Hansen *et al.*, 1996). The protein content of the casein micelles is 92%, composed of αs1-, αs2-, β- and κ-caseins in an average ratio of 3:1:3:1. The remaining 8% is made of inorganic constituents, primarily colloidal calcium phosphate (CCP) (Dickinson, 2006), which is considered as the cementing material holding together the micelle (Varnam, 1994, Horne, 2006).

The detailed internal structure of the native casein micelle is still a source of controversy (Dickinson, 2006). It seems accepted that the κ-casein forms a hairy layer on the exterior of the assembly ensuring the stability of the casein micelle through a steric stabilisation mechanism (Swaisgood, 1996). Indeed, κ-casein can stabilize about 10 times its own mass of Ca-sensitive caseins (Fox and Kelly, 2004).

The prominent models for the casein micelle are the submicelle model and the dual binding model. In the submicelle model first proposed by Waugh (Waugh, 1971), the casein micelle is composed of small aggregates of whole casein, containing 15 to 20 casein molecules and with a diameter of 10-15 nm, called submicelles. The calcium phosphate and αs-, β-caseins are linked by the intermediary of the phosphoserine residues in the structure of the calcium phosphate. The CCP acts as cement between the hundreds or even thousands of submicelles that form the casein micelle. The κ-casein is positioned at the surface of the micelle, with its hydrophobic part bound to the core of the micelle, while the hydrophilic macropeptide forms a hairy layer, at least 7 nm

thick and protruding into the aqueous phase. This hairy layer limits the micelle aggregation by increasing the steric repulsion between micelles. Although explaining the principal features of the casein micelle, the main limitation of this model is the non explanation of the κ-casein segregation at the surface of the micelle (Horne, 2002 & 2006). Furthermore, recent electron microscopy studies didn't confirm the presence of sub-micelles (Dalgleish *et al.*, 2004).

Holt and co-workers (Holt, 1992) proposed a more open and fluid structure, perhaps a 'bowl of spaghetti' type model. Polypeptide chains in the core are partly cross-linked by nanometer sized clusters of Ca-phosphate, the interaction sites on the caseins are the phosphoseryl clusters of the calcium-sensitive caseins (Holt, 1994, Horne, 2002 & 2006, Fox and Kelly 2004). The casein micelle in this model is a tangled web of flexible casein molecules forming a gel-like structure (Swaisgood H.E., 1996). The main limit of this model is the non existence of a mechanism for limiting gel growth and there is no substantial role for the κ-casein (Horne, 2002).

In the dual binding model proposed by Horne (Horne, 1998 & 2002); the micelle growth involved two types of bonding: cross linking through hydrophobic regions of the caseins and bridging with calcium phosphate clusters. In this model, α_{s1}-casein has two hydrophobic regions and one hydrophilic region including the cluster. α_{s2}-casein has two hydrophobic regions and two clusters, and β-casein has only one hydrophobic group and one phosphoseryl group. The caseins form a network by the combination of the 2 interaction types: between 2 hydrophobic regions and between 2 hydrophilic regions. The growth of the casein micelle is limited by the κ-casein which can interact with the other casein with its hydrophobic terminal region but has no phosphoseryl cluster, thus no other possibility to interact a second time. Therefore the κ-casein is on the surface of the micelle and plays its role of providing a hairy stabilizing layer (Fox and Kelly, 2004, Horne, 2002).

2.2.2 Whey protein

The whey proteins are the proteins present in the supernatant (serum) of milk after precipitation of the caseins at pH 4.6. They are typical compact

globular proteins, more water soluble than caseins and heat sensitive. They have a reasonably uniform sequence distribution of nonpolar, polar and charged residues. The formation of disulphide bond between the cystein residues buries most of the hydrophobic residues in the interior of the molecules which limits their aggregation. The whey proteins are composed of mainly of β-lactoglobulin and alpha-lactalbumin but also bovine serum albumin (BSA) and immunoglobulins (Ig) (Varnam, 1994, Swaisgood, 1996).

The main whey protein is lactoglobulin which exists as two main forms: α and β lactoglobulin and self associate to monomer, dimer or octomer as a function of the pH (Swaisgood., 1996, Jenness *et al.*, 2001). It has a molecular weight of 18,350 Da (Girard, 2002). The tertiary structure of β-lactoglobulin contains a β-barrel structural motif and a single short α-helix lying on its surface. The centre of the β-barrel forms a hydrophobic pocket which enables the binding of many small hydrophobic molecules with varying affinities. Another hydrophobic pocket may also exist between the β-barrel and the α-helix. The presence of two disulfide bonds and a partially buried sulfhydryl group is also important for the protein functionality and its structure. Furthermore, it enables sulfhydryl-disulfide interchange reaction with itself or with other protein such as κ-casein (Swaisgood, 1996, Girard, 2002).

Alpha-lactalbumin exists primarily as a nearly spherical, compact globular monomer in neutral and alkaline media. At pH values below the isoionic point, alpha-lactalbumin associates to form dimers and trimers and can become aggregated into polymers (Jenness *et al.*, 2001).

3 Acid milk gels

3.1 General

As reported above, casein micelles in milk are sterically stabilized by a hairy layer of κ-casein present at their surface. Milk gels are formed by the destabilisation of this steric barrier which initiates the colloidal aggregation and the formation of a network consisting primarily of aggregated micelles. Thus,

milk gels are built of a three dimensional network of chains and clusters of milk proteins, which at a smaller scale retain some of the integrity of the particulate micellar form (Kalab *et al.*, 1983).

Two main mechanisms are used to disturb the κ-casein hairy brush:

- An acidification of the system below pH 5 induces an electrostatic collapse of the κ-casein (Tuinier *et al.*, 2002).
- The cleavage of the κ-casein by 'chymosin', an enzyme present in rennet, which removes the hydrophilic part of the κ-casein and thus reduces the net negative charge and steric repulsion (Lucey, 2002)

Industrially, acid milk gels are produced by fermentation of milk with lactic acid bacteria; *Lactobacillus bulgaricus* and *Streptococcus thermophilus* which transform lactose into lactic acid. Glucono-δ-lactone (GDL) which slowly produces gluconic acid has been used to mimic the gradual pH decrease observed with bacteria culture. The acidification rate is faster at the beginning of the reaction with GDL which is rapidly hydrolyzed. In contrast, when the bacteria starter is added the pH doesn't evolve much at the beginning (Amice-Quemeneur *et al.*, 1995, Lucey *et al.*, 1998). Acid milk gels acidified with GDL and lactic acid bacteria have been compared (Amice-Quemeneur *et al.*, 1995, Lucey 1999). Amice-Quemeneur (1995) observed similar rheological properties for both methods of acidification, while Lucey *et al.* (1998) concluded that there are differences in the rheological and physical properties of these acid gels.

A high temperature treatment (90 °C, 10 min) of milk before acidification increases the pH of gelation and the gel strength of the final gel system (Horne and Davidson, 1993). Horne and Davidson (1993) showed that during the preheating of milk above 75 °C, the whey proteins are denatured and form a whey protein/casein complex on the casein micelles surface (Horne and Davidson, 1993). The denaturation of whey protein exposes their hydrophobic domains enhancing the protein-protein interaction near their isoelectric pH and including them in the protein network (Lucey *et al.*, 1997). Without heat treatment at high temperature, the gel networks could be considered as mainly made of caseins.

3.2 Effect of acidification on micellar state

At its physiological pH (6.7), milk is a stable dispersion of casein micelles which have an average diameter of ~200 nm (Hansen *et al.*, 1996). 70% of the calcium present is in the micellar fraction. As the pH decreases to pH 5, the casein micelles undergo important changes in their composition, size and stability (Lucey *et al.*, 1997). Gastaldi *et al.* (1996) studied the effect of acidification (at slow rate to allow equilibrium) by GDL at 20°C on the micellar state of unheated skim milk. Between pH 6.7 and 5.8, the micellar calcium phosphate is slowly released into the serum but the casein micelles retain their shape and individuality (Gastaldi *et al.*, 1996). A slight size decrease in the average diameter of 10 nm has also been observed by light scattering measurement (De Kruif *et al.*, 1996) which corresponds to the collapse of the κ-casein brush on the surface of the micelle. At pH 5.8 the micelles start to be closer and aggregate, while retaining their shape. Between pH 5.8 and 5.1, the release of calcium phosphate in the serum is intensified, and at pH 5.1 only 20% of the calcium remain in the micellar fraction. A small fraction of caseins from the micelles migrates to the serum with a maximum release of caseins to the serum occurring at pH 5.4. Indeed the soluble fraction for the 3 caseins is around 5% at pH 6.7. At pH 5.4, it reaches 9-10% for α- and κ-casein and 20% for β-casein. At pH 5, almost all caseins reintegrate into the global network (only around 1% remains soluble). Between pH 5.5 and 5.3 casein micelles appeared deformed and stretched as the pH decreases further. Around pH 4.8, the caseins seemed to reassume a more spherical shape and form a three dimensional network of chains and clusters (Gastaldi *et al.*, 1996).

The casein micelle undergoes similar changes at higher and lower temperature of acidification but the extent of casein release into the serum is greatly influenced by the gelation temperature: at 30˚C the liberation of caseins in the serum is negligible, at 4˚C, 40% of the caseins are in the serum at around pH 5.5 (Lucey *et al.*, 1997). The pH of gelation isn't however influenced by the temperature of acidification between 20 and 40˚C (Lucey *et al.*, 1997). The liberation of calcium phosphate into the serum is also not temperature dependent in the range of 4-30˚C (Dalgleish and Law 1989).

Light scattering methods (DLS, DWS) have been used to follow the micellar state during acid milk gelation (Hemar *et al.*, 2004, Alexander and Dalgleish, 2004, Donato *et al.*, 2007, Dalgleish and Horne, 1991, Dalgleish *et al.* 2004). Alexander and Dalgleish (2004) recorded the evolution of the apparent radius of the casein micelle/aggregate during the acid gelation of unheated milk at 30 ˚C. Between 6.7 and 5.6 they observed a slight decrease of 10-15 nm corresponding to the collapse of the κ-casein brush on the casein micelle. Between pH 5.6 and 5.1, the size of the casein micelle increases slowly, at pH 5 a marked growth was observed and was attributed to the gel point (Alexander and Dalgleish, 2004).

3.3 Rheology and microstructure of acid milk gels

Acid milk gels are irreversible, particulate gels formed by the aggregation of protein particles (Lucey, 2002). The strength of the network is dependent on the number and nature of bonds between the casein particles, on their structure and on their spatial distribution (Roefs and van Vliet, 1990). At low acidification rates for skim milk (1-2% GDL), it has been reported that *G'* increases rapidly after the gelation point and reaches a plateau of a few Pa characteristic of a weak gel (Lucey *et al.*, 1997). Microscopic observation of acid milk gels highlights the heterogeneity of the system including a coarse particulate network and voids where the aqueous phase is confined (Lucey *et al.*, 1997). The size of these pores varies from 1 to 30 μm, and increases with the gelation temperature.

Varying the gelation temperature between 20 and 40°C has an important effect on the final gel (Lucey *et al.*, 1997) for sodium caseinate gels at low acidification rate (1.3% GDL). Higher values of the storage modulus are observed for gels formed at lower temperature (Lucey *et al.*, 1997). At 20°C, microscopy observation revealed a homogeneous network with small pores. At 40°C, the gel was coarser with bigger pores. (Lucey *et al.*, 1997). At high temperature more hydrophobic bonds caused the particles to shrink and leaded to smaller contact zones and then weaker interactions. The protein particles might undergo more rearrangement as the interactions are weaker (Lucey,

1997). It has been reported that the acidification rate (in the GDL range 3-6 % at 30ºC) also plays a role on the final gel strength (Horne, 2003): at higher acidification rate, higher maximum complex moduli are observed for acid milk gels which has been explained by a kinetic competition between the calcium, and to some extent, casein protein leaking out of the casein micelle and the network formation (Horne, 2003).

3.4 Rearrangement

Acid milk gels are dynamic; they undergo important rearrangements after the gel point. The mechanism of acid milk gelation as the κ-casein brush collapsing at a critical pH, aggregation and gelation is a simplified version of a complex mechanism (Horne, 2001). Syneresis observed in acid gels formed at high temperature (above 40°C) is related to the rearrangement of the casein particles (van Vliet *et al.*, 1997). The existence of one maximum (at high acidification rate) at low temperature (20°C) and 2 maxima at high temperature (45°C) in the complex modulus G* profile during the gelation also shows than the system undergoes rearrangement after the gel point. The profile of G* has been explained by Horne (1993). During the acidification, the calcium phosphate migrates to the serum leaving the casein micelle among other things more negatively charged. If the micellar aggregation is initiated when the release of the calcium phosphate is not complete, calcium phosphate will continue to migrate to the serum decreasing the micellar integrity and thus weakening the gel network. But as the pH is going through the pI, more bonds are formed and the gel stiffness increases (Horne, 2001).

The degree of the rearrangement in acid milk gels is strongly linked to the gelation temperature. Syneresis is much stronger at 40°C than 20°C. Van Vliet *et al.* (1997) showed that there is no extensive rearrangement during gel formation at 20°C which could be explained by the formation of dense aggregates or by the fusion of particles. (van Vliet *et al.*, 1997).

Four levels of rearrangement have been proposed by Mellema *et al.* (2002):

- Subparticle or intraparticle rearrangements: fusion of particles
- Interparticle rearrangement: change in the mutual position of particles
- Cluster rearrangement leading to denser aggregates and larger pores
- Syneresis at the macroscopic level of the gel

3.5 Models applied to acid milk gels and gelation

Two main theoretical models have been applied to acid milk gels: the adhesive sphere model (De Kruif *et al.*, 1992, De Kruif, 1997) and the fractal model (Bremer *et al.,* 1989).

3.5.1 Adhesive sphere model

In the adhesive sphere model, casein micelles behave as hard spheres stabilized by a hairy layer of κ-casein (Holt, 1975). This brush has been described as 'salted brush' as it is screened by salt ions (Israels *et al.*, 1994). This brush collapses at a low charge density (at the critical pH: pC) which is related to the pKa value along the hairy brush (de Kruif, 1999). If the distance is large between the micelles there is no interaction and if it is very short, there is a strong repulsion. But in between there is short range with a pair attractive potential which is modulated by the state of the brush related to the pH in acid milk gelation (de Kruif, 1997, 1999):

$$\frac{\varepsilon}{kT} = \frac{1}{pC - pH} \qquad (1)$$

with ε, the strength of the interaction between the micelles, k, the Boltzmann constant and T, the absolute temperature, pC, the critical pH value at which the hairy layer collapses.

The hard sphere model is a thermodynamic model and doesn't give any information on the kinetics of the gelation. It is applicable only if the attractions are weak between the particles, which means that it could be most

applicable to describe the approach to gelation at the critical point (Horne 1999 & 2003).

3.5.2 Fractal models

Fractals models describe the geometry of the gel network and predict gel properties from the composition of the gel (Horne, 1999). In the fractal model applied by Bremer to acid milk gel (Bremer *et al.*, 1989 & 1990), the aggregation of particles follows the scaling relation:

$$N_p = (R/a)^D \tag{2}$$

with N_p, the number of particles in an aggregate of radius R, a, the radius of the particles and D, the fractal dimension (constant). The number of sites for particles in an aggregate is equal to $(R/a)^3$ which allows the calculation of the volume fraction of particle aggregates (Φ_a) as follows:

$$\Phi_a = \frac{N_p}{N_s} = (R/a)^{D-3} \quad \text{with D<3} \tag{3}$$

As the aggregation proceeds Φ_a will increase to be equal to the volume fraction Φ at the gelation point (Bremer *et al.*, 1989). The radius of the aggregates R_g at the gelation point is defined as:

$$R_g = a\Phi^{1/(D-3)} \tag{4}$$

For acid milk gels, the fractal dimension has been found to be ≈2.3 (Bremer *et al.*, 1989). At high frequency, for a fractal system the mean square displacement of the aggregates is predicted to follow a power law with an exponent of 0.7. This behaviour has indeed been observed for acid milk gel (gelation temperature 30°C, unheated milk) by diffusing wave spectroscopy (DWS) (Schurtenberger *et al.*, 2001, Mezzenga *et al.*, 2005).

Horne (1999) highlights 2 limits of the fractal model as applied to acid milk gel. A fractal cluster decreases in density as it grows, which means holes are observable in the cluster which is not the case for acid milk gel experimentally.

Furthermore, the definition of the gel point as volume aggregates equal to the volume fraction is in disagreement with rheology. Indeed, if the gel point is also defined as the cross over of *G'* and *G''* by bulk rheology, *G'* still increases after the gel point which implied rearrangement occurs or more particles are integrated in the network (Horne, 1999).

4 Pectin-casein micelle interaction

Pectin is commonly used in the food industry and has been nominally attributed two distinct functions: a 'stabilizer' (Glahn, 1982, Glahn and Rollin, 1994), inhibiting gel formation in acid milk drinks or a 'thickener', forming a serum gel in other dairy desserts (Matia-Merino *et al.*, 2004). The interaction between pectin and casein micelles has been the subject of many works that are reported in this section and is believed to be largely of electrostatic nature. The isoelectric point of the casein micelle is 4.6 (Swaisgood, 1996), 5.9 for κ-casein and the pKa of the pectin carboxylic group is between 2.9 and 4.5 (Zhong *et al.*, 1997). As pectin is polyelectrolyte, its pKa depends of the dissociation degree, the degree of methylesterification and the intramolecular distribution of the methylester group along the pectin chain.

4.1 The Effect of pectin on the properties of acid milk gels and rennet induced gels

The effect of pectin on milk gel properties has been mostly studied by rheology and microscopy. It has been found to be strongly dependant on the pectin concentration (Lucey *et al.*, 1999), and the amount of charge on the pectin backbone (evaluated by the degree of methylesterification and the pH of the system).

4.1.1 Rennet gels

Rennet induced gels are formed at the natural pH of milk: 6.7. At this pH, pectin and casein micelles are both substantially negatively charged. Depending on the position of a system relative to the phase diagram, there is a kinetic competition between phase separation due to the presence of the polysaccharide, and gelation induced by the enzyme (Corredig *et al.*, 2008). For low concentrations of HM pectin (equal to ~ 0.1%w/w or below, for ~10%w/w skim milk powder), the syneresis in gels is decreased and the gel strength increased (higher G') by the polysaccharide addition. However, confocal pictures have shown that the microstructure of this gel is similar with or without the polysaccharide (Tan *et al.*, 2007). Furthermore, the spatial correlation of casein micelles recorded with ultrasound spectroscopy on a similar low pectin concentration system (0.04% pectin, skim milk) is unchanged by the presence of pectin as well as the kinetics of the gel formation followed by DWS (Corredig *et al.*, 2008). At higher concentration (0.15%w/w, skim milk) of HM pectin, the casein micelles can be subject to depletion flocculation induced by the polymer present in solution and are not distributed uniformly in the sample but in pockets of high density. In such circumstances, the polysaccharide can inhibit the formation of a continuous network (Corredig *et al.*, 2008). This open network with less interconnectivity and with large voids for similar HM pectin concentration (0.2%w/w pectin, skim milk) has been observed by confocal microscopy (Fagan *et al.*, 2006). Above 0.2% w/w, the network is further reduced: only localised clusters are observed and segregative phase separation may occur before significant viscoelastic evolution can restrict it. Under these conditions, the final gels were weaker than the control gels without the polysaccharide (Fagan *et al.*, 2006).

4.1.2 Acid milk gels

The effect of pectin on acid milk gels has mostly been studied on 'secondary gels' obtained by shearing of a primary gel, i.e. stirred yoghurt type acid milk gel. This secondary gel is weaker than the primary one. The standard procedure in the food industry is formation of an acid milk gel, homogenisation

in presence of pectin or homogenisation followed by mixing with pectin. The polysaccharide is then used as a stabilizer which limits the reformation of a 'secondary gel' with a self supporting network. The final system is composed of casein aggregates (or fragments from the primary casein gel) stabilized in a pectin matrices. Confocal microscopy has shown that pectin can have an important effect on the development of the secondary gel but that this effect is dependant on the concentration of the polysaccharide (Lucey *et al.*, 1999). Indeed, HM pectin at low concentration (0.1%w/w and below) in a concentrated milk protein system (6.5%wt/wt milk solid) has little influence on the microstructure of the final system (pH 4.0) where a 'secondary gel network' is formed. At higher concentration (0.2%), some large aggregates are observed but not a self supporting network. When the polysaccharide concentration is increased further (above 0.3%) only small protein particles were observed (Lucey *et al.*, 1999). Particle size measurements by dynamic light scattering have also shown the ability of pectin to decrease the size of the aggregates resulting from the breaking of the primary gel (Nakumara, 2006, Liu *et al.*, 2006). Such efficiency of pectin is dependant of the pH: at pH 4.2 the size distribution of casein particles is monomodal, but bimodal below this pH with the appearance of a population with a larger size, which increased as the pH decreases. This indicates that the interaction between the caseins and the HMP are weaker at pH below 4.2 (Nakumara, 2006). HM pectin also has an influence on the whey separation. At high concentration of pectin (at 0.3% or above for 6.5%w/w non fat milk solid), whey separation is considerably decreased. Furthermore, the polysaccharide affects the rheology of the sample depending on its concentration. For a similar concentrated system (8.5% w/w non fat milk solid), by adding HM pectin at increasing concentration, the viscosity of the system first decreased following a pseudoplastic (up to a concentration of 0.1%) and then a Newtonian behaviour (0.1%-0.125%); and then increased following a pseudo-plastic behaviour (above 0.125%) (Boulenguer and Laurent, 2003, Parker *et al.*, 1994).

4.2 Interaction of pectin with casein micelles & casein micelle 'aggregates' and the localisation of pectin in acid milk systems

The interaction of casein micelles with pectin has mostly been investigated in diluted systems by dynamic light scattering. The size of the casein micelle or micelle aggregates has usually been probed against pH, and small increases in size in the presence of the polysaccharide have been explained by the presence of a pectin layer absorbed on the casein aggregates.

4.2.1 Interaction with casein micelle

At the natural pH of milk: 6.7, pectin and casein micelles are both significantly negatively charged. The apparent particle size of casein micelles dispersion has been found not to change on adding pectins of different fine pectin structure (LM, HM and LMA). The polymer does not absorb onto casein micelles and above a certain concentration (HM and LMA 0.2% pectin, LM 0.1% for skim milk), depletion flocculation, which leads to phase separation, is observed (Maroziene and de Kuif, 2000). At pH values close to 5, above but close to the isoelectric point of the casein micelles, but below the pI of the κ-casein (5.9), pectin molecules (still strongly negatively charged) adsorb onto the casein micelles, before protein aggregation, by electrostatic interactions (Leskauskaité *et al.*, 1998, Tuinier *et al.*, 2002). Indeed, caseins as unfolded proteins tend to form a maximum number of contacts with oppositely charged polysaccharide (Tolstuguzov, 2001). This adsorption can cause bridging flocculation if the polymer concentration is below full coverage. A maximum size of aggregate is observed for a concentration of pectin which corresponds to the half coverage of the protein hydrocolloid (Maroziene and de Kruif, 2000, Tuinier *et al.*, 2002). At full coverage the particles can be stericly stabilised with some measurements probing the increase in diameter of the micelles generated by HM pectin addition at some 60 nm. The full coverage of casein micelles by pectin occurs at lower concentrations for HMP (1mg/m^2 of casein micelle) than LMP. The absorbed amount of pectin for a given pH depends on its degree of methyl esterification. However the role of calcium is not clear

here and will form part of our investigation in this thesis. Furthermore, adsorption of pectin is a reversible process: if the pH is increased back to 6.8, pectin slowly desorbs from the casein micelle (Maroziene and de Kruif, 2000). By lowering the pH from 5 to 3.5, the pectin layer on the casein micelle increases: multilayers of pectin on the casein micelle are observed and aid stabilization (Tuinier *et al.*, 2002). At low pH (below 5), pectin once adsorbed can prevent the flocculation of the casein by steric hindrance: the polysaccharide absorbed on the casein micelle via its charged blocks, the other part of the molecule will protrude in solution as loops and tails (de Kruif and Tromp, 2008). At higher pectin concentration, phase separation results from depletion flocculation by the non adsorbed pectin (Einhorn-Stoll *et al.*, 2001).

4.2.2 Interaction with casein aggregates

In standard acid milk preparation, the primary acid milk gel is broken and pectin is then added to the system. The polysaccharide is thus interacting with fragments of protein network or casein micelles aggregates which have already been subjected to an acidification process (to pH 3.7-4.6). The casein micelles have by then undergone important changes (Gastaldi *et al.*, 1996): most of the micelle calcium has leaked in the serum and the κ-casein hairy layer has collapsed on the surface of the micelles. However, pectin absorbs on the casein aggregates as on casein micelle by electrostatic interactions at low pH at which the primary acid milk gel has been acidified (around pH 4). Indeed, the zeta potential of casein aggregates in acid milk drink changed from positive to negative at pH 4 with addition of HM pectin, due to electrosorption of the pectin (Sejersen *et al.*, 2006). Furthermore, the zeta potential become more negative with increasing pectin concentration which supports the theory of multilayer adsorption of pectin on the casein aggregate as observed with pectin and casein micelle (Tuinier *et al.*, 2002). However, it was shown that the zeta potential of casein aggregates coated by HM pectin (0.2% in skim milk) can not be at the origin of the required repulsion force for the hydrocolloid stabilization (Parker *et al.*, 1994). One should also consider the decrease of the charge strength on carboxyl group of pectin at low pH (pKa~3.5). Pectin stabilizes the casein aggregates by steric repulsion: it is the same mechanism,

when the polymer is in presence of the casein micelle during the acidification process. A thick layer of pectin on the casein aggregates will hold the casein particles at a distance far enough to inhibit aggregation by van der Waals attraction (Kravtchenko *et al.*, 1994). Arltoft *et al.* (2007) have probed the location of pectin in acid milk system and observed pectin as small entities in the vicinity of the protein networks in acid milk drink (AMD) with monoclonal pectin antibodies (Arltoft *et al.*, 2007 & 2008).

4.2.3 Casein micelle / aggregates sterically stabilized by a pectin layer supported by serum pectin or pectin / casein mixed gel

Boulenguer and Laurent (2003) recently suggested a more complex mechanism as the origin of the stabilization of acid milk drink by pectin. Indeed, they found that not all the pectin was active, e.g. interacting with the casein aggregates, and that removing the non-absorbed serum pectin of the final system didn't alter its stability (Boulenguer and Laurent, 2003, Tromp *et al.*, 2004). Nonetheless, the presence of this inactive pectin during the process was found to be necessary to obtain a stable system. It was suggested that a weak gel inhibits the sedimentation of the casein aggregates (Boulenguer and Laurent, 2003). The nature of this weak gel is still controversial. Boulenguer and Laurent (2003) proposed that the weak gel was made by a pectin network (Boulenguer and Laurent, 2003) and Tromp *et al.* (2004), the existence of a self-supporting mixed network of pectin-coated casein aggregates which doesn't requires the serum pectin for stability. However, all pectins seem to be incorporated in a network, despite the removal of some not being a determining factor, by investigating the degree of mobility of pectin in AMD using a fluorescence recovery after photobleaching (Tromp *et al.*, 2004).

4.3 The interaction of pectin with casein molecules in the absence of calcium

Certain pectin structures (LM or HM blocky pectin) are highly sensitive to calcium and it has recently been shown that low DM pectins can be gelled with serum extracted from milk at increasing stages of acidification (Harte *et al.*, 2007). In the literature, there are different milk protein systems in which the interaction of pectin with calcium has been eliminated as a complicating factor, allowing the investigation of the interaction of pectin and casein directly: these are using (1) acid sodium caseinate gel in presence of pectin, (2) oil in water emulsions stabilized by sodium caseinate and (3) pectin-casein mixtures.

4.3.1 Acidified sodium caseinate gels with pectin

In the presence of LM and HM pectin (1% for 2.5% sodium caseinate), proteins aggregates, obtained by breaking and homogenizing the primary acid sodium caseinate gel, are smaller; both LM and HM pectin fine structures are thus inhibiting the re-association of the protein network. However, sedimentation is observed after centrifugation for LM pectin and not HM pectin at low pH (3.8 and 4.8): HM pectin stabilized more effectively sodium caseinate dispersion. But it is worth mentioning that both, the degree of esterification and molecular weight were different for the two pectins investigated (Pereyra *et al.*, 1997).

The addition of LMA pectin (0-1%w/v) to sodium caseinate (2%w/v) before acidification changed the evolution of the gel strength with pH (Matia-Merino *et al.*, 2004). Indeed, without pectin, *G'* during acidification reaches a maximum and decreased to a lower plateau: below pH 4.6, the proteins are negatively charged and the repulsive interactions weaken the network. When pectin is added (at 0.05% w/v or above), the maximum after the gelation point (taken as time at which G' equal G'') is not observed anymore: the repulsive interactions seem to be reduced. Furthermore, as the pectin concentration is increased, the final gel strength decreased and above 0.8%, the system doesn't gel anymore. Calcium has been added to the same system with the effect that at low pectin concentration (below 0.2% w/v), caseinate gel with and without

calcium have similar rheological profile but at higher polymer concentration (0.2%w/v and above), syneresis with gel shrinkage is observed in the presence of calcium.

4.3.2 Thermodynamic compatibility of pectin / casein mixtures

Four different regimes are observed on mixing protein with an anionic polysaccharide as a function of the pH and ionic strength (Weinbreck *et al.*, 2003, de Kruif *et al.*, 2004):

- At pH above the isoelectric point of the protein and the polysaccharide and at low ionic strength, protein and polysaccharides are both negatively charged and cosoluble.
- At pH close or below the isoelectric point of the protein and above the isoelectric point of the polysaccharide, the formation of soluble protein/polysaccharides complexes occurred.
- By lowering the pH, the amount of positive net charge on the protein and negative charge on the polysaccharide are becoming similar. The soluble complexes could aggregate and form complex coacervates.
- At pH values below the pKa of the polysaccharide, the acidic groups on the polysaccharides are less charged and the complexes can be dissolved.

However, pectin-caseinate mixtures as polysaccharide-protein mixtures are unstable and phase separation occurs above a certain polymer concentration. Depending on the pH, two different interactions lead to phase separation: repulsive (segregative) or attractive (associative) interactions (Tolztoguzov, 1991, Schmitt *et al.*, 1998, Turgeon *et al.*, 2003, Redigueri, 2007). At pH 6.8, pectin and caseinate charges are of opposite sign. Pectin doesn't adsorb to the caseinate, and the non-absorbing polymer is depleted from the surrounding of the colloids. This depletion by segregation leads to phase separation (Rediguieri *et al.*, 2007). The thermodynamic compatibility increases with increasing the pH from 6 to 8 (Einhorn-Stoll *et al.*, 2001). This has been explained by an increasing of the repulsion force between the proteins

themselves and unfolding of these proteins which give more sites for weak interaction between pectin and caseinate involving opposites charged patches (Einhron-Stroll, 2001). Below pH 5.5, pectin and caseinate concentrate in a single phase which is characteristic for complexation (Redigueri, 2007). This complexation is reversible with pH but is resistant to high ionic strength (Redigueri, 2007). At low concentration of polymer and protein (0.9% each), the pectin caseinate system is phase separating but only at the microscopic scale (de Kruif and Tromp, 2008). Depending on the pH and the respective phase diagrams, caseinate droplets in pectin solution (at pH 5.38 and above) or droplets of pectin-caseinate complexes (at pH 5.22 and below) are observed (de Kruif and Tromp, 2008).

4.3.3 Oil in water emulsions stabilized by sodium caseinate containing pectin

Pectin inhibits the aggregation of sodium caseinate-coated droplets at pH 5 and below (Dalgleish and Hollocou, 1997). At pH 7, pectin doesn't adsorb onto the caseinate layer covering the oil droplet and at a certain concentration of polymer, flocculation and coalescence is observed resulting from depletion exerted by pectin (Dickinson *et al.*, 1998, Surh *et al.*, 2006). At pH 5.5, the zeta potential which was positive with only casein is negative in the presence of pectin: the polymer adsorbs to the surface of the oil droplets (Dickinson *et al.*, 1998). The interaction of pectin with the caseinate covered oil droplet involves relatively weak and reversible interactions (Dickinson *et al.*, 1998). Pectin reduces droplet aggregation but doesn't eliminate it: unabsorbed polymer is still reported to induce destabilization by depletion. At pH 4 and below, extensive droplet flocculation is observed in presence of pectin, due to adsorption, which might reduce the magnitude of the zeta-potential and thus the electrostatic repulsion between the droplets and/or the polymer might bridge the droplets (Surh *et al.*, 2006). For the stabilization of caseinate coated oil droplet by pectin, there seems to be little effect of the pectin fine structure (LM or HM).

5 Instrumentation

This section briefly reviews the techniques and instrumentation which will be used in this thesis. Further details of the different experimental methodologies are reported in the relevant chapters.

5.1 Method to study pectin fine structure: capillary electrophoresis (CE)

The first method commonly used to determine pectin degree of methylesterification (DM) was a classical titration method. Since then, many techniques have been developed: chromatography, nuclear magnetic resonance and FTIR to name a few (more details are described in chapter 2).

The main advantage of capillary electrophoresis (CE), as an inherent separation method, is that the intermolecular methylester distribution is systematically measured. The intramolecular distribution is still not literally resolved; but an indirect assessment of this intramolecular distribution can be made by determinating the 'degree of blockiness' (Goubet *et al.*, 2005). Two approaches have been taken: fragmentation of the pectin backbone by an enzyme or NMR on the intact polymer (Kim *et al.*, 2005). Fragmentation relies on the enzymatic cleavage being dependant of the methylester sequence and on the ability to resolve the released oligomers (which CE can also do).

5.1.1 CE general

Capillary electrophoresis describes a family of techniques used to separate a variety of compounds. The separation is driven in narrow tubes (25-100 μm) by an electric field. The mobility results from its attraction to the electrode of opposite charge, electroosmotic flow and frictional forces. Bare silica capillaries generate an electroosmotic flow upon the application of a voltage so that all analytes are dragged one way in the capillary.

The CE instrumentation consists of a high voltage power supply, electrolyte reservoir, a DAD ultraviolet detector and a capillary (figure 3).

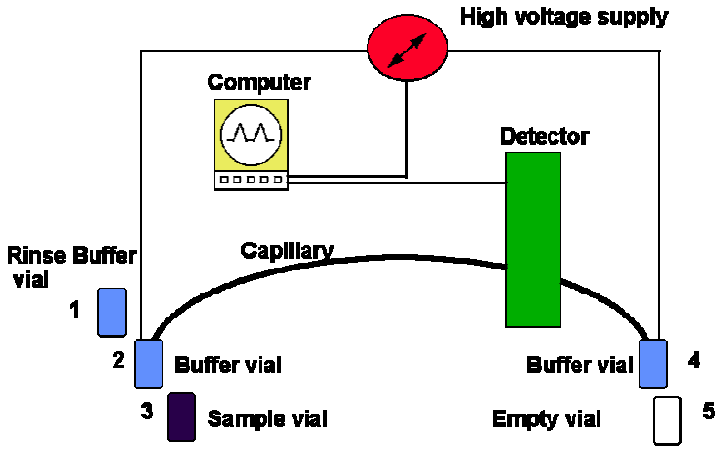

Figure 3: CE instrumentation (http://www.ceandcec.com/ce_theory.htm)

The mobility μ is determined from the migration time t of the molecule analysed and the migration time t_0 of a neutral maker, using the equation:

$$\mu = \mu_{obs} - \mu_{eo} = (lL/V)\,(1/t - 1/t_0) \qquad (5)$$

with L: total length of the capillary, l: the distance from the inlet to detector μ_{obs}: observed mobility, μ_{eo}= electroosmotic mobility (Zhong *et al.*, 1998 & 1997).

5.1.2 Capillary electrophoresis studies of pectins

Pectin was analysed by CE first in 1997 by H-J Zhong *et al*. While most carbohydrates lack chromophores, the carboxylate group of the galacturonic acid unit is a UV chromophore which can be used for the CE analysis. Furthermore, pectin is a charged molecule with a pKa between 2.9 and 4.5 depending on its degree of ionisation and methylesterification. Its charge density depends of the degree of methylesterification (DM) (Zhong *et al.*, 1997).

When the degree of polymerisation (DP) is smaller than 10-20, the electrophoretic mobility depends on both the DP and DM of the pectin chain allowing resolution of oligomers released for example from pectin digestion. The quantification is complicated by the fact that the methylesterified residues

have a significantly lower absorbance than their unmethylesterified counterparts. However, taking this into account samples of mixed DPs and DMs can be quantitatively analyzed. The DP and DM of the different fragments of the sample analysed can be calculated by reference to standard samples (Ström and Williams, 2004).

Under the same CE experimental conditions, when the DP is higher than ~25, the electrophoretic mobility does not depend anymore on the DP but only on the pectin DM. The pectin DM can thus be determined by CE. The DM has been calculated by comparison with standard samples of known DM. A linear fit between the DM and the reduced electromobility ($1/t - 1/t_0$) has been used to determine the pectin DM. The use of standards is obviously valid if the pectins tested have the same galacturonic content than the standards but Zhong *et al.* (1997) also found that the neutral sugars content did not significantly alter the hydrodynamic properties of the molecules and thus didn't affect the electrophoretic mobility. One of the main advantages of CE over the conventional methods is the possibility to access the DM distribution by direct measurement; indeed the peak shape reflects the intermolecular methylester distribution of the sample (Zhong *et al.*, 1998&1997, Ström *et al.*, 2005).

The electrophoretic mobility of pectin has been reported to be not significantly influenced by the methylester intramolecular distribution in typical running conditions: little difference has been observed between pectins with random and blockwise distribution (Zhong *et al.*, 1997, Ström *et al.*, 2005).

In addition, CE is an efficient tool to determine the intramolecular distribution of methylesterified residues in pectic substrates by analysing the endo-polygalacturonase digest pattern. Indeed, the high enzyme-substrate specificity allows indirect but useful information about the pectin fine structure to be obtained by analysing the PG digest pattern (Ström and Williams, 2004).

CE has recently also proved to be an alternative method to determine the degree of amidation of pectin (a commercial modification previously described in the introduction) by Guillotin *et al.* (2006). Indeed the methyl ester group and the amide group have the opposite effect on the electrophoretic mobility.

Therefore the degree of amidation can be determined by measuring the electromobility of the pectin sample before and after saponification which remove all the methylester groups. The comparison between the two obtained electromobility gives the DAm (Guillotin *et al.*, 2006).

5.2 Microrheology

Microrheology is the study of the mechanical properties of materials at small length scales: in the micrometer range (Gardel *et al.*, 2005). Micron size probes, usually added to the system, locally deform the sample. Microrheology allows probing the system with a small volume of sample (around 100 µl). Microrheology techniques can either be passive or active. In active techniques, the probes are subjected to external and local applied forces using magnetic fields, electric fields, or micromechanical forces. The advantage is the possibility to apply larges stresses to stiff materials. Passive microrheology consists of recording the passive motion of particles undergoing Brownian motion where the local deformation is simply induced by the mobility of the particle due to thermal fluctuations. Thus, passive methods are non-invasive. Brownian motion first observed by Brown in 1827 has been linked to the mechanical properties of the system (viscosity) by Einstein in 1905. The diffusion coefficient *D* is related to the mean square displacement (MSD) in 2D by the following equation (Berg, 1993):

$$\left\langle r^2 \right\rangle = 4Dt \tag{6}$$

with $\left\langle r^2 \right\rangle = \left\langle r_x^2 \right\rangle + \left\langle r_y^2 \right\rangle$ mean square displacement in 2 dimensions (m^2), *t*, time lag (s) and D, the diffusion coefficient for purely viscous system. The Stokes Einstein equation links the mechanical properties of the system to the diffusion coefficient and the thermal energy through:

$$D = \frac{kT}{6\pi\eta r_h} \tag{7}$$

with kT, thermal energy, η, viscosity of the system and $r_{h,}$ the hydrodynamic radius. For viscoelastic materials, a frequency dependant modification is used (Weitz *et al.*, 1993).

Tracking particles undergoing Brownian motion is typically done by light scattering or microscopic or laser interferometric methods. In this thesis, two passive microrheological methods will be used and compared. These methods are multiple particle tracking (MPT) and diffusive wave spectrometry (DWS).

5.2.1 MPT

Multiple particles tracking (MPT) consists of recording the Brownian motion of fluorescent latex beads, added to samples as tracer particles. The trajectories of the probes are obtained by visualising them by fluorescence microscopy and by analysing the recorded images with a tracking analysis software (figure 4). The motions of single probes are obtained in this way and can be used to calculate the ensemble average mean square displacement for a group of probes. Indeed, as MPT enables the study of the motion of single probe particles, it allows monitoring the heterogeneity of the system. Analysing the tracking data using the Van Hove correlation function, which is the probability distribution of particle displacement for a given time lag gives information on the spread of the MSD and thus on the heterogeneity of the system (Wong *et al.*, 2004, Oppong *et al.*, 2006).

The frequency at which the system is studied by MPT is limited by the speed at which the camera can take pictures of the system: around 45Hz for CCD camera used in this work.

In MPT well defined probes are added to the system, but their location in a complex system requires further analysis with microscopy techniques (Confocal microscopy) (Moschakis *et al.*, 2006). In some cases the location of the probe has been controlled by modifying their surface chemistry by binding of molecules of interest at their surface (Valentine *et al.*, 2004).

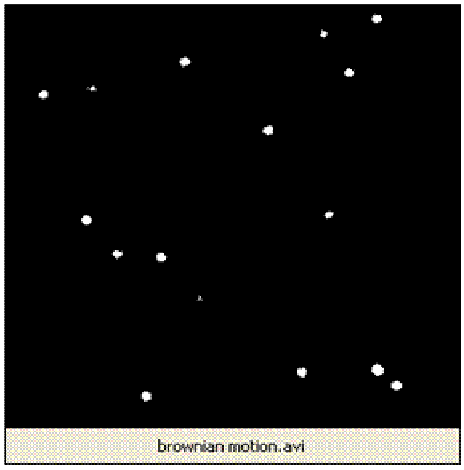

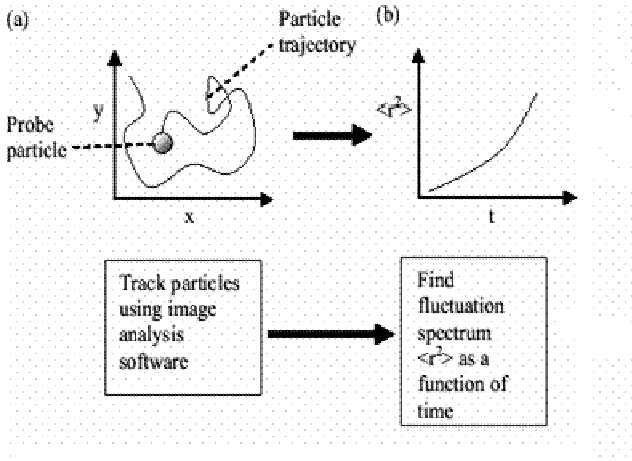

Figure 4: (i) 500 nm latex beads in solution (ii) MPT principle

5.2.2 DWS

Diffusive wave spectroscopy (DWS) is a light scattering based method. The light is multiple scattered to such an extent that the path of each photon is considered random. This method can be applied to turbid and concentrated systems. The light is typically scattered by probes (e.g. latex beads) added to the sample. However in this thesis casein micelles/casein aggregates themselves were, in some cases, used as probes.

Figure 5 shows a schematic of the method. A laser beam is shone through the sample, the light is multiple scattered by the probes naturally present or added to the system and the intensity versus time is recorded by a detector: an optic fiber fed to a photodiode and then a correlator. As the particles diffuse and rearrange in the sample, the intensity of light that reaches the detector fluctuates in time. These intensity fluctuations as a function of time, *I(t)*, allow calculating the correlation function, $g_1(\tau)$:

$$g_1(t) \equiv \frac{1}{\beta}\left(\frac{\langle I(t)I(0)\rangle}{\langle I\rangle^2} - 1\right)^{1/2} \tag{8}$$

where β is a constant, characteristic of the optics, and $I(0)$ and $I(t)$ the intensity of the detected light at the time zero and t. As the correlation function can also be expressed as a function of the mean square displacement (Weitz *et al.*,

1993), the experimentally determined correlation function (equation 8) can lead to the plot of MSD versus lag time (as discussed in chapter 4).

DWS allows studying the mechanical properties of the system at high frequency (limit 1-10 MHz) which gives insight to the microstructure of the network. The high frequency limit is governed by the condition that the inertia of the probes is negligible.

Since DWS intrinsically gives an ensemble average, it doesn't allow probing the heterogeneity of the system.

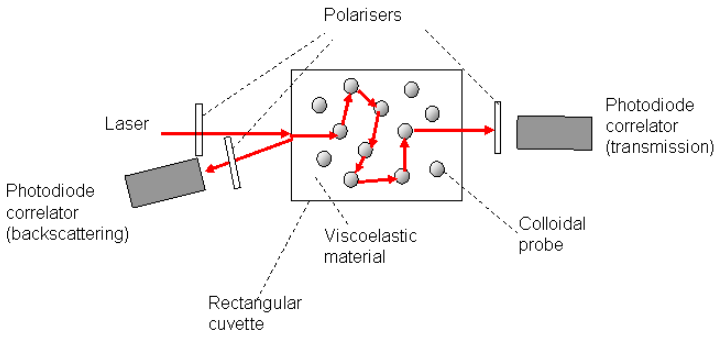

Figure 5: Schematic of the experimental set up for DWS

5.3 Surface Plasmon Resonance

Surface plasmon resonance (SPR) is an optical method which allows the study in real time of interactions between a flowing analyte and an ligand immobilized on a metal surface. Surface plasmons are surface electromagnetic waves with a parallel propagation to the metal interface. These waves are sensitive to any change in the refractive index on the metal surface. Molecule absorption will produce such a refractive index change. Surface plasmons are excited by a light beam (figure 6). The light is almost totally reflected but the evanescent wave penetrates a distance of the order of one wavelength into the buffer and is able to interact with free-oscillating electrons (plasmons) present in the metal film surface and generates SPR. A photodetector is used to monitor the reflected light intensity which provides the resonance angle and then the refractive index of the solution close to the metal film. The change in the refractive index gives information on the number of molecules bounds to

the ligand on the coated surface but also on the state of the ligand e.g. conformation, as the analyte is flown over.

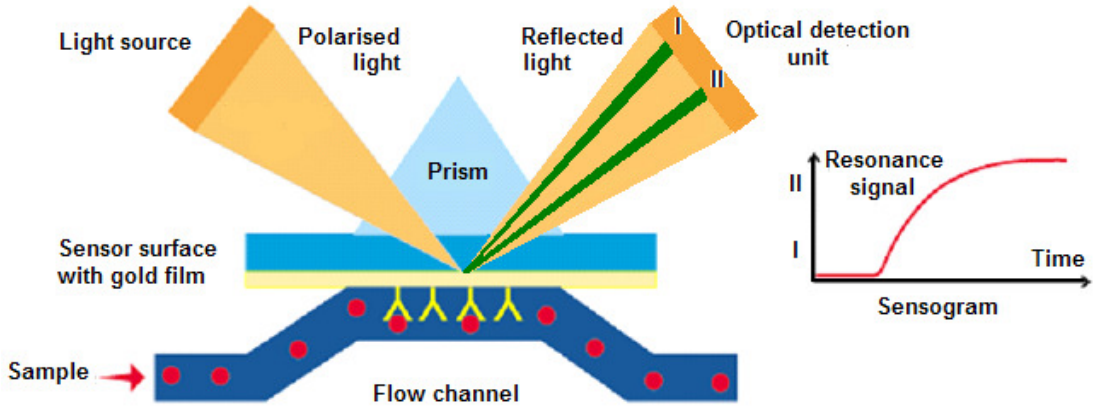

Figure 6: Schematic of the experimental set up for SPR (GE Healthcare, Biacore manual)

6 Aims of the thesis

The interaction between pectin and κ–casein is crucial for the food industry in dairy products where it has found wide utility; low methoxypectin as a 'thickener' and high methoxyl pectin as a 'stabilizer'. As one would expect, the study of this interaction has been the topic of many previous papers and as such it is not a novel system *per-se*. However, the methods that are used in this thesis haven't been applied to study the interaction previously, which has mainly been studied on diluted systems using dynamic light scattering (DLS) or in concentrated systems using microscopy and bulk rheology. In this work, the two main methods used to probe the interaction are microrheology and surface plasmon resonance (SPR), which can offer new insights into the microscopic interactions in these systems.

A further strategy to gain a better understanding of the interaction was to investigate the effect of the pectin fine structure. In chapter 2, we first aimed to study the degree of methylesterification and its pattern (random or blockwise) on a number of selected pectins. Furthermore, the intermolecular distribution for DM pectins with either a random or blocky intramolecular distribution of

charges was investigated. We characterized the pectin fine structures, designed for their interaction with milk protein, by intermolecular and intramolecular distributions of the methylester group using capillary electrophoresis (coupled with digestion of the pectin backbone with endoPGII). We also further investigated the intermolecular distribution as bearer of information on the intramolecular distribution.

Microrheology allowed us to study the effect of pectin on acid milk gels in concentrated and undisturbed systems. In chapter 3, using DWS, the system was probed at high frequency, allowing to investigate the effect of the polymer on the microstructure of the network. This was complemented by the use of multiple particle tracking studies, which allowed probing the mechanical heterogeneity of the system (chapter 4). On the other hand, surface plasmon resonance which is the object of chapter 5, gave us insight into the interfacial interaction between κ-casein and pectin. Finally, the study of the motion of model 'calcium-free casein micelles' (κ-casein coated latex particles) in pectin solutions is investigated in chapter 5. To summarize, the aim of this thesis is to study the interaction of pectin and casein micelles at different levels and by linking the results obtained, gain a better understanding of the effect of pectin addition to milk.

References

Alexander M., Dalgleish D.G. (2004) Application of transmission diffusing wave spectroscopy to the study of gelation of milk by acidification and rennet. *Colloids and surfaces B-Biointerfaces* **38**(1-2):83-90

Amice-Quemeneur N., Haluk J-P., Hardy J. (1995) Influence of the acidification process on the colloidal stability of acidic milk drinks prepared from reconstituted nonfat dry milk. *Journal of dairy science* **78**:2683-2690

Arltoft D., Madsen F., Ipsen R. (2007) Screening of probes for specific localisation of polysaccharides. *Food Hydrocolloids* **21**(7):1062-1071

Arltoft D., Madsen F., Ipsen R. (2008) Relating the microstructure of pectin and carrageenan in dairy desserts to rheological and sensory characteristics. *Food Hydrocolloids* **22**(4):660-673

Berg H.C. (1993) In *Random Walks in Biology*, Princeton: Princeton University Press

Boulenguer P., Laurent M.A. (2003). Comparison of the stabilisation mechanism of acid dairy drinks (ADD) induced by pectin and soluble soybean polysaccharide (SSP). In Voragen F., Schols H. & R. Visser (Eds.). *Advances in Pectin and Pectinase Research*, Dordrecht: Academic Publishers, 467–480

Braccini I., Perez S. (2001) Molecular basis of Ca^{2+}-Induced gelation in alginates and pectins: the egg-box model revisited. *Biomacromolecules* **2**:1089-1096

Bremer L.G.B., van Vliet T., Walstra P. (1989). Theoretical and experimental study of the fractal nature of the structure of casein gels. *Journal of the Chemical Society: Faraday Transactions* **85**:3359-3372

Bremer L.G.B., Bijsterbosch H., Schrijvers R., van Vliet T., Walstra P. (1990) On the fractal nature of the structure of acid casein gels. *Colloids and Surfaces* **51**:159-170

Capel F., Nicolai T., Durand D., Boulenguer P., Langendorff V. (2005) Calcium and acid induced gelation of (amidated) low metoxyl pectin. *Food hydrocolloids* **20**:901-907

Cardoso S.M., Coimbra M.A., Lopes da Silva J.A. (2003) Temperature dependence of the formation and meeting of pectin-Ca2+ networks: a rheological study. *Food hydrocolloids* **17**:801-807

Corbin E.A., Whittier E.O. (1965). The composition of milk. In Webb B.H., Johnson A.H. (Eds.). *Fundamentals of Dairy Chemistry,* Westport: CT, 1-36

Corredig M., Lopez A., Alexander M. (2008) Diffusing wave spectroscopy and ultrasonic spectroscopy: advantages of these non invasive techniques in food colloid research illustrated by rennet-induced gelation of skim milk in the presence of pectin. *Agro Food Industry Hi-Tech* **19**(3):54-57

Daas P.J., Meyer-Hansen K., Schols H.A., De Ruiter G.A., Voragen A.G.J (1999) Investigation of the non-esterified galacturonic acid distribution in pectin with endo-polygalacturonase. *Carbohydrate Research* **318:**135-145

Dalgleish D.G., Law A.J.R. (!989) pH-induced dissociation of bovine casein micelles. II. Mineral solubilization and its relation to casein release. *Journal of dairy research* **56:**727-735

Dalgleish D.G., Horne D.S. (1991) Studies of gelation of acidified and renneted milks using diffusing wave spectroscopy. *Milchwissenschaft-Milk science international* **46**(7):417-420

Dalgleish D.G., Hollocou A.L. (1997) Stabilization of protein-based emulsions by means of interacting polysaccharide. In Dickinson E. and Bergenstahl B.(Eds.). *Food colloids: Proteins, lipids and polysaccharides*, Cambridge: Royal Society of Chemistry,. 236–244

Dalgleish D.G., Alexander M., Corredig M. (2004) Studies of the acid gelation of milk using ultrasonic spectroscopy and diffusing wave spectroscopy. *Food hydrocolloids* **18**(5):747-755

Dalgleish D.G., Spagnuolo P.A., Goff H.D. (2004) A possible structure of the casein micelle based on high-resolution field-emission scanning electron microscopy. *International dairy journal* **14**(12):1025-1031

de Kruif C.G., Jeurnink T.J.M., Zoon P. (1992) The viscosity of milk during the initial stages of renneting. *Netherlands Milk and Dairy Journal* **46**:123-137

de Kruif C.G., Ekatherina B., Zhulina B. (1996) K-casein as a polyelectrolyte brush on the surface of casein micelles. *Colloids and Surface A: Physicochemical and Engineering Aspects* **117**:151-159

de Kruif C.G. (1997). Skim milk acidification. *Journal of Colloid and Interface Science* **185**:19-25

de Kruif C.G. (1999) Casein micelle interactions. *International Dairy Journal* **9**:183-188

de Kruif C.G., Weinbreck F., de Vries R. (2004) Complex coacervation of proteins and anionic polysaccharides. *Current opinion in Colloids & Interface Science* **9:**340-349

de Kruif C.G.; Tromp R.H. (2008) Interaction of pectin with casein. *Foods & Food Ingredients Journal of Japan* **213**(3):281-285

Dickinson E., Semenova M.G., Antipova A.S. (1998) Salt stability of casein emulsions. *Food Hydrocolloids* **12**:227–235

Dickinson E. (2006) Colloid science of mixed ingredients. *Soft Matter* **2**:642-652

Donato L, Alexander M, Dalgleish D.G. (2007) Acid gelation in heated and unheated milks: Interactions between serum protein complexes and the surfaces of casein micelles. *Journal of agricultural and food* **55**(10):4160-4168

Einhorn-Stoll U., Salazar T., Jaafar B., Kunzek H. (2001) Thermodynamic compatibility of sodium caseinate with different pectins. Influence of the milieu conditions and pectin modifications. *Nahrung Food* **45**(5):332-337

Fagan C.C., O'Donnell C.P., Cullen P.J., Brennan C.S. (2006) The effect of dietary fibre inclusion on milk coagulation kinetics. *Journal of food engineering* **77**(2):261-268

Flutti L. (2003) Pectin: Properties and determination. In Caballero B. (Eds.). *Encyclopedia of Food Sciences and Nutrition*, Oxford: Academic Press, 4440-4449

Fox P.F., Kelly A.L. (2004) The caseins In Yada R.Y (Eds.). *Proteins in food processing,* Cambridge: Woodhead publishing limited

Gastaldi E., Lagaude A., Tarodo de la Fuente B. (1996) Micellar transition state in casein between pH 5.5 and 5.0. *Journal of food science* **61**:59-64

Gardel M.L., Valentine M.T., and Weitz D. A. (2005) Microrheology. In K. Breuer (Eds.). *Microscale Diagnostic Techniques*, Germany: Springer Verlag

Girard M., Turgeon S.L., Gauthier S.F. (2002) Interbiopolymer complexing between β-lactoglobulin and low- or high-methoxyl pectin measured by potentiometric titration and ultrafitration. *Food Hydrocolloids* **16**:585-591

Glahn P.E. (1982) Hydrocolloid stabilisation of protein suspensions at low pH. *Programmes in Food Nutrition Science* **6**:171–177

Glahn P.E. and Rolin C. (1994). Casein–pectin interactions in sour milk beverages. *Food Ingredients European Conference Proceedings* 252–258

Glahn P.E., Rolin C.E.D., Phillips G.O.; Williams P.A.; Wedlock D.J. (1996) Properties and food uses of pectin fractions. In Phillips G.O., Williams P.A., Wedlock D.J. (Eds.). *Gums and Stabilisers for the Food Industry* 8th International Conference, Oxford: Oxford University Press, 393-402

Goubet F., Ström A., Dupree P., Williams M.A.K. (2005) An investigation of pectin methylesterification patterns by two independent methods: capillary electrophoresis and polysaccharide analysis during carbohydrate gel electrophoresis. *Carbohydrate research* **340**:1193-1199

Guillotin S.E., Bakx E.J., Boulenger P., Schols H.A., Voragen A.G.J. (2006) Determination of the degree of substitution, degree of amidation and degree of blockiness of commercial pectin by using capillary electrophoresis. *Food hydrocolloids* **21***:*441-457

Hansen S., Bauer R., Lomholt S.B., Quist K.B., Pedersen J.S., Mortensen K. (1996) Structure of casein micelles studied by small-angle neutron scattering. *European Biophysics Journal with Biophysics* **24**(3):143-147

Harte F.M., Montes C., Adams M., San Martin-Gonzalez M.F. (2007) Solubilised micellar calcium induced low methoxyl-pectin aggregation during milk acidification. *Journal of Dairy Science* **90**:2705-2709

Hemar Y., Singh H., Horne D.S. (2004) Determination of early stages of rennet-induced aggregation of casein micelles by diffusing wave spectroscopy and rheological measurements. *Current applied physics* **4**:362-365

Hotchkiss A.T., Savary B.J., Cameron R.G., Luzio G.A., Chau H.K., Fishman M.L. (2002) Enzymatic modification of pectin to increase its calcium sensitivity while preserving its molecular weight.. *Journal of Agricultural and. Food Chemistry* **50:**2931-2937

Holt C. (1975) The stability of casein micelles. In Wolfram E. (Eds.). Proceedings of international conference on colloid and surface science, Budapest: Akademia Kiado, (**1**) 641-664

Holt C (1992) Structure and stability of the bovine casein micelle. *Advances in Protein Chemistry* **43:**63-151

Horne D.S. and Davidson C. M. (1993) Influence of heat treatment on gel formation in acidified milks. In: *Protein and fat globule modifications by heat treatment, homogenization and other technological means for high quality dairy products*, Brussels: International Dairy Federation, 267-276

Horne D.S. (1998) Casein interactions: Casting light on the black boxes, the structure in dairy products. *International dairy journal* **8**(3):171-177

Horne D.S. (1999) Formation and structure of acidified milk gels. *International Dairy Journal* **9**:261-268

Horne D.S. (2001) Factors influencing acid-induced gelation of skim milk. In Dickinson E. and Miller R. (Eds.). *Food colloids – Fundamentals of formulation,* Great Britain: Royal Society of chemistry special publication, 345-351

Horne D.S. (2002) Caseins, micellar structure. In Roginski R., Fox P.F., Fuquay J.W. (Eds.). *Encyclopedia of dairy sciences.* New York: Academic Press, 1902-1909

Horne D.S. (2003) Casein micelles as hard spheres: limitations of the model in acidified gel formation. *Colloids and Surfaces A: Physicochem. Eng. Aspects* **213**:255-263

Horne D.S. (2006) Casein micelle structure: Models and muddles. *Current Opinion in Colloid & Interface Science* **11***:*148-153

Hunt J.J., Cameron R., Williams M.A.K. (2006) On the simulation of enzymatic digest patterns: The fragmentation of oligomeric and polymeric galacturonides by endo-polygalacturonase II. *Biochimica et Biophysica Acta* **1760**:1696-1703

Inngjerdingen K.T., Patel T.R., Chen X., Kenne L., Allen S., Morris G.A.,Harding S.E., Matsumoto T., Diallo D., Yamada H., Michaelsen T.E. (2007) Immunological and structural properties of a pecticpolymer from Glinus oppositifolius. *Glycobiology* **17**:1299-1310

Israels R., Leermakers F.A.M., Fleer G.J., Zhulina E.B. (1994) Charged Polymeric Brushes: Structure and Scaling. *Macromolecules* **27**:3249-3261

Jackson C.L., Dreaden T.M., Theobald L.K., Tran N.M., Beal T.L., Eid M., Gao M.Y., Shirley R.B., Stoffel M.T., Kumar M.V., Mohnen D. (2007) Pectin induces apoptosis in human prostate cancer cells: correlation of apoptotic function with pectin structure. *Glycobiology* **17**:805-819

Jenness R., Keeney M., Marth E. H. (2001) In *Fundamentals of dairy chemistry* India: CBS publishers, 81-169

Kaláb M., Allan-Wojtas P., Phipps-Todd B.E. (1983) Development of microstructure in set-style non fat yoghurt - A review. *Food Microstructure* **2**:51-66

Kester H.C.M., Magaud D., Roy C., Anker D., Doutcheau A., Shevchik V., Hugouvieux-Cotte-Pattat N., Benen J.A.E., Visser J. (1999) Performance of selected microbial pectinases on synthetic monomethyl-esterified Di- and trigalacturonates. *The journal of biological chemistry* **274**:37053–37059

Keys A., Anderson J.T., Grande F. (1961) Fiber and pectin in diet and serum cholesterol concentration in man. *Proceeding of the society for experimental biology and medicine* **106**(3):555-558

Kim Y., Teng, Q., Wicker L. (2005) Action pattern of Valencia orange PME de-esterification of high methoxyl pectin and characterization of modified pectins. *Carbohydrate research* **340**(17):2620-2629

Kohn R. (1975) Ion Binding on polyuronates-alginate and pectin. *Pure and applied chemistry* **42**(3):371-397

Kravtchenko T.P., Parker A., Trespoey A. (1995) Colloidal stability and sedimentation of pectin-stabilised acid milk drinks. In: Dickinson E. and Lorient D. (Eds.). *Food macromolecules and colloids*, Cambridge: The Royal Society of Chemistry, 349–355

Laurent M.A., Boulenguer P. (2003) Stabilization mechanism of acid dairy drinks (ADD) induced by pectin. *Food Hydrocolloid* **17**(4):445-454

Leskauskaité D., Liutkevichius A., Valantinaité A. (1998) Influence of the level of pectin on the process of protein stabilisation in an acidified milk system. *Milchwissenschaft* **53**:144–151

Limberg G., Korner R., Bucholt H.S., Christensen T., Roepstorff P., Mikkelsen J.D. (2000) Analysis of different de-esterification mechanisms for pectin by enzymatic fingerprinting using endopectin lyase and endopolygalacturonase II from *A. Niger. Carbohydrate research* **327**:293-307

Liners F., Thibault J.F., Vancustem P. (1992) Influence of the degree of polymerization of oligogalacturonates and of esterification pattern of pectin on their recognition by monoclonal-antibodies. *Plant Physiology* **99**:1099-1104

Liu J.R., Nakamura A., Corredig M. (2006) Addition of pectin and soy soluble polysaccharide affects the particle size distribution of casein suspensions prepared from acidified skim milk. *Journal of Agricultural and. Food chemistry* **54**:6241-6246

Lucey J.A., Singh H. (1997) Formation and physical properties of acid milk gels: a review. *Food Research International* **30**(7):529-542

Lucey J.A., van Vliet T., Grolle K., Geurts T., Walstra P. (1997) Properties of acid casein gels made by acidification with glucono-delta-lactone. 1. Rheological properties. *International dairy journal* **7**(6-7):381-388

Lucey J.A., van Vliet T., Grolle K., Geurts T., Walstra P. (1997) Properties of acid casein gels made by acidification with glucono-delta-lactone. 2. Syneresis, permeability and microstructural properties. *International dairy journal* **7**(6-7):389-397

Lucey J.A., Tamehana M., Singh H., Munro P.A. (1998) A comparison of the formation, rheological properties and microstructure of acid skim milk gels made with a bacterial culture or glucono-[delta]-lactone. *Food Research International* **31**(2):147-155.

Lucey J.A., Tamehana M., Singh H., Munro P.A. (1999) Stability of model acid milk beverage: Effect of pectin concentration, storage temperature and milk heat treatment. *Journal of texture studies* **30**(3):305-318

Lucey J.A. (2002) Formation and physical properties of milk protein gels. *Journal of dairy science* **85**(2):281-294

Marles R. (1995) Antidiabetic plants and their active constituents. *Phytomedicine* **2**(2):137-189

Maroziene A., de Kruif C.G. (2000) Interaction of pectin and casein micelles. *Food hydrocolloids* **14**:391-394

Marry M., Roberts K., Jopson S.J., Huxham I.M., Jarvis M.C., Corsar J. , Robertson E. and McCann M.(2006) Cell-cell adhesion in fresh sugar-beet root parenchyma requires both pectin esters and calcium cross-links. *Physiologia Plantarum* **126**:243-256

Matia-Merino L., Lau K., Dickinson E. (2004) Effects of low-methoxyl amidated pectin and ionic calcium on rheology and microstructure of acid-induced sodium caseinate gels. *Food hydrocolloids* **18:**271-281

Mellema M., Walstra P., van Opheusden J.H.J. & van Vliet T. (2002) Effects of structural rearrangements on the rheology of rennet-induced casein particle gel. *Advances in Colloid and Interface Science* **98**(1):25-50

Mezzenga T., Schurtenberger P., Burbidge A., Michel M. (2005) Understanding food as soft materials. *Nature Material* **4**:729-749

Micheli F. (2001) Pectin methylesterases: cell wall enzymes with important roles in plant physiology. *Trends in plant science* **6**:414-419

Mohnen D. (1999).Biosynthesis of pectins and galactomannans. In B.M. Pinto (Eds.). *Comprehensive Natural Products Chemistry **3** Carbohydrates and their Derivatives Including Tannins, Cellulose, and Related Lignins*, Oxford: Elsevier, 497–527

Morris E.R., Gidley M.J., Murray E.J., Powell D.A., Rees D.A. (1980) Characterisation of pectin gelation under conditions of low water activity, by circular dichroism, competitive inhibition and mechanical properties. *International Journal of Biological Macromolecules* **2**:327-330

Morris E.R., Powell D.A., Gidley M.J., Rees D.A. (1982) Conformations and Interactions of Pectins: II Influence of residue sequence on chain association in calcium pectate gels. *Journal of Molecular Biology* **155**:517-531

Moschakis T., Murray B.S., Dickinson E. (2006) Particle tracking using confocal microscopy to probe the microrheology in a phase-separating emulsion containing nonadsorbing polysaccharide. *Langmuir* **22**:4710-4719

Nakamura A., Yoshida R., Maeda H., Corredig M. (2005) The stabilizing behaviour of soybean soluble polysaccharide and pectin in acidified milk beverages. *International dairy journal* **16**: 361-369

Nussinovitch A. (1997) Pectin. In: Chapman and Hall (Eds.). *Hydrocolloid Applications: Gum technology in the food and other industries*, London: Blackie Academics and Professional, 83-104

Oppong F.K., Rubatat L., Bailey A.E., Frisken B.J., de Bruyn J.R. (2006) Microrheology and structure of a polymer gel. *Physical Review E* **73**:041405

Parker A., Boulenguer P., Kravtchenko T.P. (1994) Effect of the addition of high methoxyl pectin on the rheology and colloidal stability of acid milk drinks. In Nishinari K., Doi E.

(Eds.). *Food hydrocolloids: Structure, properties and functions*, New York: Plenum Press, 307–312

Pereyra R., Schmidt K.A., Wicker L. (1997) Interaction and stabilization o acidified casein dispersions with low and high methoxyl pectins. *Journal of Agricultural and. Food chemistry* **45**: 3448-3451

Perez S., Mazeau K., Herve du Penhoat C. (2000) The three-dimensional structures of the pectic polysaccharides *Plant Physiology Biochem*istry **38**:37-55

Pilgrim G.W., Walter R.H., Oakenfull D.G. (1991) Jams and jellies and preserves. In Walter R.H. (Eds.). *The chemistry and technology of pectin*, New York: Academic Press Inc., 23-50

Powell D.A., Morris E.R., Gidley M.J., Rees D.A. (1982) Conformations and interactions of pectins 2. Influence of residue sequence on chain association in calcium pectate gels. *Journal of molecular biology* **155**:517-531

Ralet M.-C., Dronnet V., Buchholt H.C. and Thibault J.F. (2001) Enzymatically and chemically de-esterified lime pectins: characterisation, polyelectrolyte behaviour and calcium binding properties. *Carbohydrate Research.* **336**:117-125

Rediguieri C.F., de Freitas O., Lettinga M.P., Tuinier R. (2007) Thermodynamic incompatibility and complex formation in pectin/caseinate mixtures. *Biomacromolecules* **8**(11):3345-3354

Renard C.M.G.C, Thibault J-F (1996) Degradation of pectins in alkaline conditions: kinetics of demethylation. *Carbohydrate Research* **286**:139-150

Ridley B.L., O'Neil M.A, Mohnen D. (2001) Pectins: structure, biosynthesis, and oligogalacturonide-related signalling. *Phytochemistry* **57**:926-967

Rees D.A. (1975) Biochemistry of Carbohydrates. In Whelan W.J. (Eds.). *International Review of Science, Biochemistry Series 1 vol 5*, London: Butterworth

Roefs S.P.F.M. and van Vliet T. (1990) Structure of acid casein gels. 2. Dynamic measurements and type of interaction forces. *Colloids and Surfaces* **50**:161-175

Sajjaanatakul T. and Pitifer L.A. (1991) Pectinesterase. In Walter R. (Eds.). *The Chemistry and Technology of Pectin,* New York: Academic Press, 135.164

Savary B.J., Hotchkiss A.T., Cameron R.G. (2002) Characterization of a Salt-Independent Pectin Methylesterase Purified from Valencia Orange Peel. *Journal of Agricultural and food chemistry* **50**:3553-3558

Schmelter T., Wientjes R., Vreeker R., Klaffke W. (2002) Enzymatic modifications of pectins and the impact on their rheological properties. *Carbohydrate polymers* **47**: 99-108

Schmitt C., Sanchez C., Desobry-Banon S., Hardy, J. (1998) Structure and technofunctional properties of protein–polysaccharide complexes: A review. *Critical Reviews in Food Science and Nutrition*. **38**(8):689–753

Schurtenberger P., Stradner A., Romer S., Urban C., Scheffold F. (2001) Aggregation and Gel Formation in Biopolymer Solutions. *CHIMIA Journal of International Chemistry* **55**:155-159

Sejersen M.T., Salomonsen T., Ipsen R., Clark R., Rolin C., Engelsen S.B. (2006) Zeta potential of pectin-stabilised casein aggregates in acidified milk drinks. *International Dairy Journal* **17**: 302-307

Singh S.A., Rao A.G.A (2002) A simple fractionation protocol for, and a comprehensive study of the molecular properties of, two major endopolygalacturonases from *Aspergillus niger. Biotechnology Applied Biochemistry* **35:** 115-123

Stokke B.T., Draget K.I., Smidsrød O., Yuguchi Y., Urakawa H., Kajiwara, K. (2000) Small-angle X-ray scattering and rheological characterization of alginate gels. 1. Ca-alginate gels. M*acromolecules* **33**:1853-1863

Ström A., Williams M.A.K. (2003) Controlled calcium release in the absence and presence of an ion-binding polymer. *Journal of physical chemistry B* **107**(40):10995-10999

Ström A. and Williams M.A.K. (2004) On the separation, detection and quantification of pectin derived oligosaccharides by capillary electrophoresis. *Carbohydrate research* **339***:*1711-1716

Ström A., Ralet M.C., Thilbault J.F., Williams M.A.K. (2005) Capillary electrophoresis of homogeneous pectin fractions. *Carbohydrate polymers* **60**:467-473

Ström A. (2006) Characterisation of pectin fine-structure and its effect on supramolecular properties University College Cork

Ström A., Ribelles P., Lundin L., Norton I., Morris E.R., Williams M.A.K. (2007) Influence of pectin fine structure on the mechanical properties of calcium-pectin and acid-pectin gels. *Biomacromolecules* **8**(9):2668-2674

Surh J., Decker E.A., McClements D.J. (2006) Influence of pH and pectin type on properties and stability of sodium-caseinate stabilized oil-in-water emulsions. *Food Hydrocolloid*s **20**(5):607-618

Swaisgood H.E. (1996) Characteristics of milk In Fennema O.R. (Eds.). *Food chemistry,* New York: Marcel Dekker, 841-878

Tan Y.L., Ye A., Hemar Y., Singh, H. (2007) Effect of biopolymer addition on the dynamic rheology and microstructure of renneted skim milk systems. *Journal of texture studies* **38**(3):404-422

Taylor A.J. (1982) Intramolecular distribution of carboxyl groups in low methoxyl pectins- a review. *Carbohydrate polymers* **2**:9-17

Thebaudin J.Y., Lefebvre A.C., Harrington M., Bourgeois C.M. (1997) Dietary fibres: Nutritional and technological interest. *Trends in Food Science & Technology* **8:**41-48

Tolztoguzov V.B. (1991) Functional properties of food protein and role of protein−polysaccharide interaction. *Food Hydrocolloids* **4**(6):429−468.

Tolztoguzov V. (2001) Some thermodynamic considerations in food formulation. *Food Hydrocolloids* **17**: 1-23

Tromp R.H., De Kruif C.G., van Eijk M., Rolin C. (2004) On the mechanism of stabilisation of acidified milk drinks by pectin. *Food hydrocolloids* **18**: 565-572

Tuinier R., Rolin C., de Kruif C.G. (2002) Electrosorption of pectin onto casein micelles. *Biomacromolecules* **3:**632-639

Turgeon S.L., Beaulieu M., Schmitt C., Sanchez C. (2003) Protein−polysaccharide interactions: Phase-ordering kinetics, thermodynamic and structural aspects. *Current Opinion. in Colloid & Interface Science* **8**(4−5):401−414

van Vliet T., Lucey J.A., Grolle K., Walstra P. (1997) Rearrangements in Acid-Induced Casein Gels during and after Gel Formation. In: Dickinson E., Bergenstahl B. (Eds.). *Food Colloids: Proteins, Lipids and Polysaccharides*, Cambridge: Royal Society of Chemistry

Valentine M.T., Perlman Z.E., Gardel M.L., Shin J.H., Matsudaira P., Mitchison T.J., Weitz D.A. (2004) Colloid surface chemistry critically affects multiple particle tracking measurements of biomaterials. *Biophysical Journal* **86**(6): 4004-4014

Varnam A.H., Sutherland J.P. (1994) In *Milk and milk products: technology, chemistry and microbiology,* New York: Chapman & Hall, 8-27

Vincent R.R., Pinder D.N., Hemar Y., Williams M.A.K. (2007) Microrheological studies reveal semiflexible networks in gels of a ubiquitous cell wall polysaccharide. *Physical review E* **76**(3):63-70

Vincent R.R.R (2008) Microrheology investigation of biopolymer networks. Thesis

Vincent R., Cucheval A., Hemar Y., Williams M. (2009) Bio-inspired network optimization in soft materials – Insights from the plant cell wall. *European Physical Journal E* **28**(1):79-87

Walkinshaw M.D. and Arnott S. (1981) Conformations and interactions of pectins: II. Models for junction zones in pectinic acid and calcium pectate gels. *Journal of Molecular Biology* **153**:1075-1085.

Waugh D.F. (1971) Formation and structure of casein micelles. In McKenzie H.A. (Eds.). *Milk proteins: Chemistry and molecular biology (Vol. II),* New York: Academic Press, 3–85

Weinbreck F., de Vries R., Schrooyen P., de Kruit C.G. (2003) Complex coacervation of whey proteins and gum Arabic. *Biomacromolecules* **4**:293-303

Weitz D.A., Pine D.J., Brown W. (1993) Diffusing-wave spectroscopy. In W. Brown (Eds.). *Dynamic Light Scattering: The Method and Some Applications,* Oxford: Oxford University Press, 652-720

Williams M.A.K, Buffet G.M.C, Norton I.T. (2001) Simulation of endo-PG digest patterns and implications for the determination of pectin fine structure. *Carbohydrate research* **334**:243-250

Williams M.A.K., Vincent R.R., Pinder D.N., Hemar Y. (2008) Microrheological studies offer insights into polysaccharide gels. *Journal of non-Newtonian fluid* **149**(1-3):63-70

Willats W.G.T., Orfila C., Limberg G., Buchholt H.C., van Alebeek G.J.W.M., Voragen A.G.J., Marcus S.E., Christensen T.M.I.E., Mikkelsen J.D., Murray B.S., Knox, J.P. (2001) Modulation of the degree and pattern of methyl-esterification of pectic homogalacturonan in

plant cell walls - Implications for pectin methyl esterase action, matrix properties, and cell adhesion. *Journal of biological chemistry* **276**:19404-19413

Willats W.G.T., Knox P., Mikkelsen J.D. (2006) Pectin: new insights into an old polymer are starting to gel. *Trends in Food Science & Technology* **17:**97-104

Wong I.Y., Gardel M.L., Reichman D.R., Weeks E.R., Valentine M.T., Bausch A.R. and Weitz D.A. (2004) Anomalous Diffusion Probes Microstructure Dynamics of Entangled F-actin Networks. *Physical Review Letters* **92**:178101

Xu J., Palmer A., Wirtz D. (1998) Rheology and microrheology of semi-flexible polymer solutions: Actin filament networks. *Macromolecules* **31**:6486-6492

Zhong Z.H., Williams M.A.K., Goodall D.M., Hansen M.E. (1998) Capillary electrophoresis studies of pectins. *Carbohydrate research* **308**:1-8

Zhong Z.H., Williams M.A.K., Keenan R.D., Goodall D.M., Rolin C. (1997) Separation and quantification of pectins using capillary electrophoresis: a preliminary study. *Carbohydrate polymers* **32**:27-32

Chapter 2

Pectin fine structure: measurements of the intermolecular charge distributions for pectin with random and blocky patterns of methylesterification

Results on intermolecular distributions for randomly demethylesterified and monodisperse homogalacturonans are in press in *Biomacromolecules*: **'Electrophoretic behaviour of co-polymeric galacturonans including comments on the information content of the intermolecular charge**

distribution' Martin A.K. Williams, Aurélie Cucheval, Anna Ström, Marie-Christine Ralet

1 Introduction

Pectin, a ubiquitous polysaccharide in the cell walls of all land plants plays a major role both in plant physiology and in controlling mechanical properties in-vivo. The polymers by interacting with calcium can form networks with different mechanical behaviours and strengths (Vincent *et al.*, 2007 & 2009). Pectins are polymolecular and polydispersed, exhibiting significant heterogeneity with respect to both chemical structure and molecular mass (Perez *et al.*, 2000). Their structure is, in vivo and in vitro, complex but simplified by the extraction process. Indeed commercial pectin samples are essentially composed of a linear heteropolysaccharide consisting mainly of polymerized, partly methyl-esterified (1-4)-linked α-D-galacturonic acid with a small fraction of rhamnose (→4)- α-D-GalA-(1→2)- α-L- rha-(1→) and small side chains formed by other sugars (Morris *et al.*, 1982, Willats *et al.*, 2006).

The interaction of the polymer with other molecules, its affinity to calcium (Ralet *et al.*, 2001) and thus its ability to form a network is strongly dependent on the number of negative charges on its backbone (or number of unmethylesterified galacturonic acid residues), and of the intermolecular and intramolecular distribution of these charges (Vincent *et al.*, 2007).

While the degree of methylesterification has been determined by diverse methods (Maness *et al.*, 1990, Massiot *et al.*, 1997, Synytsya *et al.*, 2003, Rosenbohm *et al.*, 2003) including capillary electrophoresis (CE), the intermolecular methylester distribution however can only be obtained by ion exchange chromatography (Daas *et al.*, 1998 & 1999) and CE (Zhong *et al.*, 1997 & 1998, Williams *et al.*, 2003, Ström and Williams, 2004, Ström *et al.*, 2005). The intramolecular distribution is still not literally resolved (Goubet *et al.*, 2005). Two main approaches have been pursued to determine this intramolecular distribution. By Nuclear Magnetic Resonance (NMR), the frequencies of the

possible triad sequences of residues within the chain are measured (Neiss *et al.*, 1999, Lee *et al.*, 2008). The other pathway is to fragment the polymer with an enzyme e.g. endo-polygalacturonase II (endoPGII) which has high substrate specificity and to examine the liberated fragments (Ström and Williams, 2004). Capillary electrophoresis allows analyzing the digest pattern of pectin by endoPGII as well as the intermolecular charge distribution. Indeed, if the degree of polymerisation (DP) is smaller than ¬25, the electrophoretic mobility depends on the DP and DM of the pectin chain. The DP and DM of the different fragments of the sample analysed are calculated by reference to standard samples (Ström and Williams, 2004). If the DP is higher than ~25, the electrophoretic mobility doesn't depend anymore on the DP but only on the pectin DM in same CE experimental conditions. Traditionally, the pectin DM can be then determined by CE by comparison with standard samples which have a known DM.

Pectin with different and controlled degrees of methylesterification can be designed by the action of an enzyme, pectin methylesterase (PME) or chemically by the addition of alkali or acid. These treatments allow tailoring the charge distribution on the pectin backbone. Indeed, chemical treatment leads to a random distribution of the unmethylesterified group on the backbone and PME (from plant origin) to a blocky distribution. Recently, it has been shown that it is possible to play on the length of these blocks by modifying the polymer in presence of calcium (Vincent *et al.*, 2009).

A signature of this deesterifying treatment (alkali or plant PME) seems to be observed in the intermolecular charge distribution measured by capillary electrophoresis. The pectin samples treated with plant PME have shown broader DM distributions than those produced with fungal PME or alkali treatment (Ström *et al.*, 2005). However, the link between the intermolecular distribution and the intramolecular distribution hasn't been explicitly investigated and, thus they have been treated rather separately. Furthermore, the evolution of the intermolecular and intramolecular distributions during the time course of such demethylesterification processes hasn't been investigated.

In this chapter, pectin fine structure is investigated; especially the intermolecular charge distribution is studied using measurements of the electrophoretic behaviour of the polymer by capillary electrophoresis. First, the

methodology applied to the determination of the intermolecular charge distribution is assessed. Then, with co-polymeric galacturonan chains, the intermolecular distribution is shown to match theory for random processes. Therefore the intramolecular distribution, for these homogalacturonan with a random distribution of charge, is fully determined. The intermolecular distribution thus contains information about the intramolecular charge distribution. Having obtained confidence that the intermolecular charge distribution is as predicted for randomly deesterified substrates, the intermolecular and intramolecular distributions of pectin samples with blocky charge distributions were also investigated.

2 Experimental Section

2.1 Samples

Homogalacturonans (HG) were isolated from commercial citrus pectin and analysed by High Performance Size-exclusion Chromatography combined with multiple-angle laser light-scattering detection by Dr MC Ralet. Rhamnoglacturonan from *Arabidopsis thaliana* seeds was a gift from Dr MC Ralet. The chemical and macromolecular characteristics of the HG and RGI samples used in this study are given in table 1.

All pectin samples used in the section 3.3 of this study were obtained by demethylesterification of the same high methoxyl pectin (apple pectin from Fluka, DM78%, galacturonic content of ~ 90% and molecular weight 30-100 000 g.mol-1). The mother pectin (concentration 1%w/w) was demethylesterified with plant pectin methylesterase (PME, 0.5 mg per gram of pectin) purchased from Sigma Aldrich at pH 7 and 30ºC. The pH was maintained constant during the enzyme action by addition of NaOH (0.1M). This allowed the control of the final degree of methylesterification by quenching the reaction after the addition of known amount of NaOH. The reaction was stopped by addition of HCl (in order to have final pH of 4) and by a temperature treatment (90ºC, 3min).

The digestion of pectin samples was catalyzed by a polygalacturonase, endoPGII provided by Jacques Benen from the University of Wageningen. It is a pure endo-PG II isoform from *Aspergillus niger* (Ström and Williams, 2003) which required unesterified sugar residues in the active site to catalyze the reaction. The degradation pattern on the methylester-sequence is thus dependent on the pectin fine structure. The digestion was carried out in 50mM acetate buffer (pH 4.2) at 30ºC for 12 hours with 20 μL of enzyme solution (0.094mg/ml protein) for 1 mL of pectin substrate (concentration 0.5%w/w). The reaction was stopped by denaturation of the enzyme by a temperature treatment: 90 ◦C for 3min.

In addition to collecting data on pectin samples from the literature a number of samples were also run in this work; and in addition previously unpublished data from PhD thesis work of Dr Anna Ström and experiments carried out at Unilever research have also been included. These samples are detailed in Table 2. While some of these samples may have formed part of previously reported studies re-running some of these samples and including further experimental data permits a better assessment of the reproducibility across laboratories. "Homemade" refers to standard base-catalysed demethylesterification as amply described in literature cited herein. With the exception of two calcium-sensitive samples, all the pectins in Table 2 are believed to have close to random distributions of methylesterification, being generated either by a fungal pectinmethylesterase (f-PME) or by base saponification. Molecular weights of all these samples are between 40 and 120 kDa.

	HG 93	HG-B82	HG-B69	HG-B57	HG-B40	HG-B20	RGI
GalA (mol%)	> 99	> 99	> 99	> 99	> 99	> 99	51
Rha (mol%)	<1	<1	<1	<1	<1	<1	49
DM (%)	93	82	69	57	40	20	0

DP_w	122 ##	80	82	85	87	93 ##	3740

Main population; values from Macquet *et al.*, 2007, ## over-estimated: aggregates

Table 1: The chemical and macromolecular characteristics of the HG and RGI samples used in this study

This Work - Commercial Samples			
Source	DM	AGU	Treatment
Sigma	90	>75%	-
Fluka Biochimica	78	-	-
Copenhagen Pectin	55.8	89.0	f-PME
Copenhagen Pectin	31.1	85.2	f-PME
This Work - Homemade Samples			
Source	DM	AGU	Treatment
CP-Kelco (Initial DM 83%)	60	~85%	Base
	40	~85%	Base
	30	~85%	Base
A Ström Thesis, University of Cork, 2006			
Source	DM	AGU	Treatment
Copenhagen Pectin	77.8	84.5	f-PME
Copenhagen Pectin	65	81.5	f-PME
Copenhagen Pectin	55.8	89.0	f-PME
Copenhagen Pectin	31.1	85.2	f-PME
CP-Kelco (Initial DM 83%)	25	~85%	Base
	20	~85%	Base
	15	~85%	Base
	10	~85%	Base
	5	~85%	Base
Unilever Research			
Source	DM	AGU	Treatment

Copenhagen Pectin	77.8	84.5	f-PME
Copenhagen Pectin	70.3	85.1	f-PME
Copenhagen Pectin	65.0	81.5	f-PME
Copenhagen Pectin	62.2	83.9	f-PME (Ca-sensitive fraction)
Copenhagen Pectin	55.8	89.0	f-PME
Copenhagen Pectin	42.6	85.7	f-PME (Ca-sensitive fraction)
CP-Kelco (LM-12)	35.0	~85%	Base
Copenhagen Pectin	31.1	85.2	f-PME

Table 2: The characteristics of the pectin samples for which previously unreported experimental data is reported.

2.2 Capillary electrophoresis

Experiments carried out in this work used an automated CE system (HP 3D), equipped with a diode array detector. Electrophoresis was carried out in a fused silica capillary of internal diameter 50 μm and a total length of 46.5 cm (40 cm from inlet to detector). The capillary incorporated an extended light-path detection window (150 μm) and was thermostatically controlled at 25 °C, although in reality it is possible that the temperature in the capillary during electrophoresis could exceed this value by several degrees (Levigne *et al.*, 2002). Phosphate buffer at pH 7.0 was used as a CE background electrolyte (BGE) and was prepared by mixing 0.2M Na_2HPO_4 and 0.2M NaH_2PO_4 in appropriate ratios and subsequently reducing the ionic strength to 50 or 90 mM. At pH 7.0 the unmethylated GalA residues are fully charged and while the oligomers are susceptible to base-catalyse β-elimination above pH 4.5, no problems were encountered during the CE runs of some 20 minutes at room temperature. All new capillaries were conditioned by rinsing for 30 minutes with 1 M NaOH, 30 minutes with a 0.1 M NaOH solution, 15 minutes with water and 30 minutes with BGE. Between runs the capillary was washed for 2 minutes with 1 M NaOH, 2 minutes with 0.1 M NaOH, 1 minute with water and 2 minutes with BGE. Detection was carried out using UV absorbance at 191 nm with a bandwidth of 2

nm. Samples were loaded hydrodynamically (various injection times at 5000 Pa, typically giving injection volumes of the order of 10 nL), and typically electrophoresed across a potential difference of 20 kV. All experiments were carried out at normal polarity (inlet anodic) unless otherwise stated. Electrophoretic mobilities, μ, are related to the migration times of the injected samples relative to a neutral marker, t and t_0 respectively, by the equation:

$$\mu = \mu_{obs} - \mu_{eo} = (l\ L\ /V)\ (1/t - 1/t_0) \qquad (1)$$

where L is the total length of the capillary, l is the distance from the inlet to detector, V is the applied voltage, μ_{obs} is the observed mobility and μ_{eo} is the mobility of the electroosmotic flow (EOF) (Weinberger, 2000).

3 Results and Discussion

3.1 Electrophoretic mobility measurement

Figure 1 shows the electrophoretic mobilities measured in this work for HGs, RGI, and a series of pectin samples in 50 mM BGE at 298 K. The fractional charges against which these values are plotted have been measured by at least one other independent (not electrophoretic) method; typically titration, chromatographic assessment of released methanol, or FT-IR, and are estimated to be known to the order of ± 3 %. The mobilities have been calculated as number averages over the CE peaks (after normalization to account for the different lengths of time that species with different electrophoretic velocities spend passing the detection window (Goodall *et al.*, 1991)). The error bars show what are considered as the largest realistic uncertainties. Typical reproducibility is around 2-3%, with the largest uncertainties arising from the estimation of the EOF, typically signalled by a drop in the absorbance signal originating from the refractive index change concurrent with the passage of water from the sample plug moving past the detection window. The occasional use of a UV-absorbing neutral marker did improve the situation somewhat when running experiments with very low charge density samples, where elution was in close proximity to

neutral species. Other uncertainties caused by electromigration dispersion were exacerbated at high charge densities, but could be ameliorated up to a point by modifying the sample concentration and the ionic strength of the BGE.

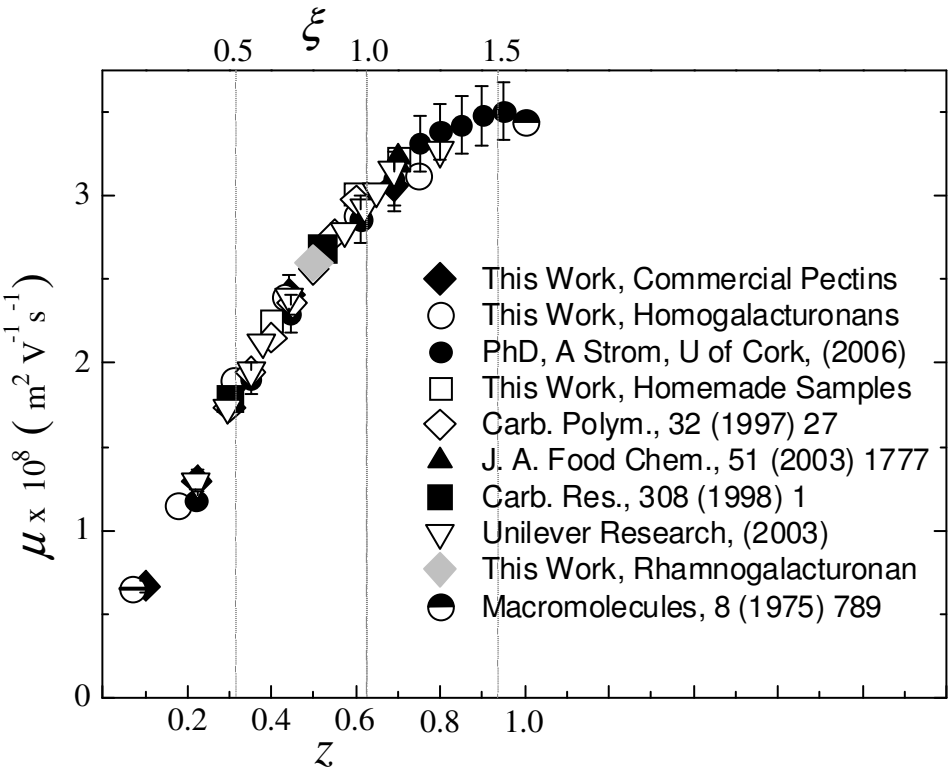

Figure 1: Electrophoretic mobilities, μ, for HGs, RGI, and a number of pectin samples, measured herein or gathered from the literature, as a function of the fraction of the sugar rings charged, z, (50 mM BGE, 298 K, existing data originally measured at different I and/or T has been scaled as described in the main text).

3.1.1 Comparison of mobility measurements with literature

It can be seen that there is, on the whole, excellent agreement in figure 1, not only between the data reported herein, but also when compared with a large amount of further data taken from the existing literature. It should be noted that in the literature data, a small number of the experiments had been carried out in different ionic strength BGE or at a different temperature (i.e. not at 50 mM BGE or at 298 K), and these data have been scaled according to the predictions of theoretical calculations. There is also a data point from the literature for

polygalacturonic acid which it should be noted was made using an alternative experimental set-up to CE, and using sodium chloride as an electrolyte (Tuffile and Ander, 1975).

3.1.2 Mobility of RGI compared with HG

It is also noteworthy that the RGI mobility agrees well with that of a 50 % methylesterified HG; suggesting that, at least in the regime where mobilities are not dependent on DP, that the nature of the linkage between the sugar rings does not have a large impact on the electrophoretic mobility. It also suggests that the overall charge density of the chain is significantly more important than the *intra*molecular arrangement of the charged groups, as the RGI polymeric backbone consists of the strictly alternating dimer: Rha-GalA as described above; while the HG sample has a random placement of the charged groups along the chain. Such an independence of the electrophoretic mobility on *intra*molecular sequence has also previously been found when comparing results obtained from sister pectin samples that had been demethylesterified chemically or by processive enzymes (Williams *et al.*, 2003).

3.1.3 Mobility of HGs compared with pectins

It is also worthy of comment that the data from the pectin samples have had their charge densities calculated from measured DM values without taking account of any neutral sugars that might be present in the molecule. The first study carried out on the CE of pectins also found that the proportion of the pectin sample that was claimed to be GalA didn't seem to be overly important in determining the electrophoretic mobility (Zhong *et al.*, 1997), despite the fact that the addition of neutral sugars attached to the polymeric backbone would be expected to increase the frictional forces acting on the molecule. Certainly it would be expected that the pectin samples would, at the very least, contain a small amount of Rha in the RGI regions that are hypothesized to connect the otherwise fairly monodisperse HG regions (of around DP 100) (Thibault *et al.*, 1993).

Despite this approximation the pectin and HG mobilities shown in figure 1 don't appear different by more than a few percent at most. This effectively limits

the RGI content of the pectins studied to less than around 10%. For example, a pectin consisting of 10% RGI and 90% HG (DM 50) has 95% GalA groups, of which 45% are methylesterified, a DM of 47.4%. Taking this DM value, which might be obtained by say titrametry, neglecting the RGI regions and naively calculating the % of charged residues as 100-%DM, gives 52.6% compared to the real 50%. Even if the RGI backbone carries an equal weight of neutral sugar side chains, then a pectin consisting of 5% RGI in the backbone carrying a further 5% Gal and Ara substituents, and 90% HG (DM 50) has 92.5 % GalA groups, of which 45% are methylesterified, giving a measured DM of 48.6% and a naïve 51.4% charged residues. From these simple considerations it is clear that for typical RGI and neutral sugar contents of extracted pectin samples, the electrophoretic mobility is consistent within experimental uncertainty (a few %) with that predicted simply using the measured DM value in order to calculate the fractional charge; thus explaining the good agreement observed in figure 1. This is certainly reasonable, but does suggest that in commercial samples (typically quoted GalA contents are of the order of 85 % by weight) the weight that is not GalA is not all likely to be sugars covalently attached to the pectic polymer, and does not in fact play a significant role in influencing its electromigration (water, ions and possibly free sugars could account for a large amount of this ~15 %).

3.1.4 Calculation of the dependence of mobility on charge density

It is clear that in the region in which previous work has been carried out, corresponding to z~0.2 to 0.7, there is a well defined consistent relationship wherein simple linear regression analysis based on the mobility of surrounding standards can yield a reasonable estimate of the DM of an unknown sample from its electrophoretic mobility. Indeed, in the region $0<z<0.6$ a single linear regression is a reasonable description of the data. However, it is also abundantly clear from data presented in figure 1 that at lower DM the dependence of electrophoretic mobility on fractional charge is modified. Indeed, above around z=0.8 it is not possible within our experimental uncertainties to confidently assert whether there is any dependence on DM at all, or whether the electrophoretic mobility is constant. With figure 1 in hand, an empirical fit to the data (figure 2)

was carried out in order to obtain an electrophoretic mobility versus fractional charge relationship; yielding:

$$\mu = A + B(1 - \exp(-Cz)) \tag{2}$$

where A=-0.9179x10^{-10}, B=4.6101x10^{-8}, and C=1.719.

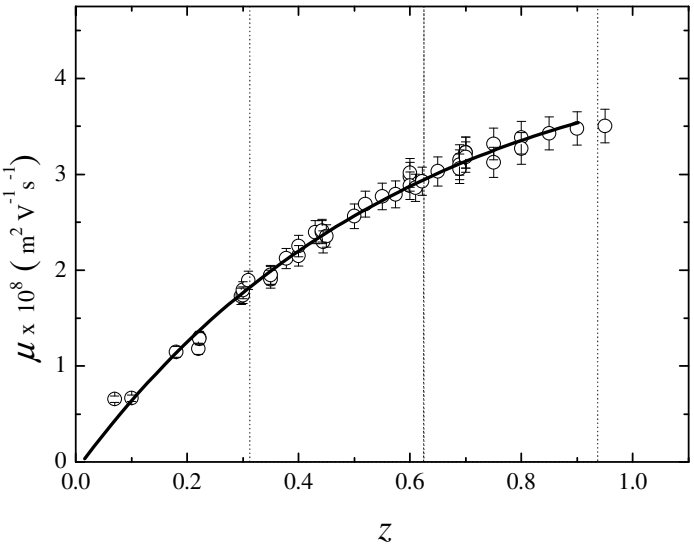

Figure 2: The data from figure 1 compared empirical fit to the data

While this relationship can be confidently used when $0<z<0.8$, at higher charge densities caution should be exercised as the current dataset is unable, within experimental uncertainties, to determine whether there is any variation in this regime. Using such a μ to z mapping it has previously been discussed in some detail how to convert measured electrophoregram into inter*m*olecular distributions of DM. To date, the relationship used to perform this task was a locally linear one, obtained from a calibration run containing three standard samples. By expanding the range of samples previously reported and amalgamating measurements across different laboratories and instruments, a universal electrophoretic mobility versus charge relationship has been derived that might be used without recourse to standards and can be confidently used to generate intermolecular DM distributions.

3.2 Intermolecular Distributions for Randomly Demethylesterified Monodisperse Homogalacturonans

Having confidently measured a relationship between electrophoretic mobility and charge (or for HGs equivalently DM), it is trivial, at least for chains with DMs above 25-30 %, to convert an experimentally measured electrophoregram into a full *inter*molecular DM distribution. With this in mind the expected nature of such a distribution for randomly demethylesterified HG samples was considered. Under the assumption that the charged residues are indeed distributed randomly along the backbone of the polysaccharide then the binomial theorem predicts that the distribution of the number of chains containing different numbers of charged residues is Gaussian. Furthermore, the full width at half height of these distributions (in DM %) can be calculated as $235.5\times\sqrt{((1-p)\ p\ /\ n)}$, where p is the probability of the residue being methylesterified and n is the DP of the chain. (Just as the likelihood of achieving an equal number of heads or tails in classical coin-tossing depends on the number of trials, so the chances that an individual chain will have the sample average DM depends on its DP). This demonstrates that far from simply being a complicating factor to be taken into account in interpreting results from other experimental methodologies designed to infer the *intra*molecular distribution of charges, the *inter*molecular distribution itself contains information regarding the statistical properties of the process that generated charged residues. Furthermore it is our contention that, on the whole, the *inter*molecular DM distribution is easier to measure experimentally. In particular, as described above, if the process that generated the charged sites is entirely random then the resultant *inter*molecular charge distributions should be Gaussian. Figure 4 (a) shows the predicted full width at half height of a 50% methylesterified sample as a function of its DP and figure 4 (b) the fraction by which this width would be reduced as DM increases or decreases either side of 50%.

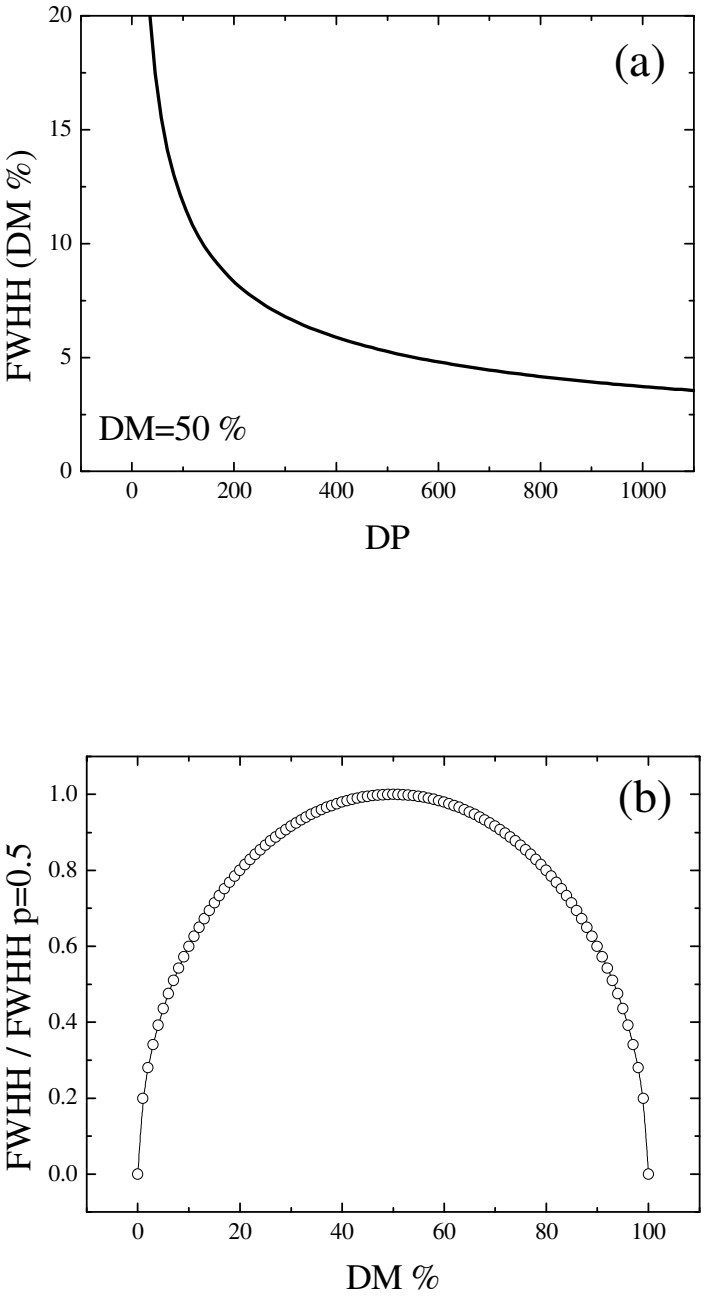

Figure 4: (a) The predicted full width at half height of the intermolecular DM distribution of a 50% methylesterified sample as a function of its degree of polymerization (DP); (b) the fraction by which the width given in (a) will be reduced as degree of methylesterification increases or decreases either side of 50%.

It is clear from figure 4 (b) why most experimentally measured distributions (of pectins with *random* methylester distributions) look similar; samples with DM

values between 30 and 70 % are predicted to have widths less than 10% different from one another. Unfortunately the nature of the relationship between electrophoretic mobility and charge density at high fractional charge, as discussed above, means that for samples below around 25% DM, the interpretation becomes more complex and precludes us from confidently measuring the widths in this region. The electropherograms of these samples clearly show that the observed peaks are narrower but at present a sufficiently precise relationship does not exist in this area to tease out how much of that reduction is due to the fact that the resolution itself is decreasing rather than originating from actual changes in the statistical width. These low DM samples reach a width of a couple of DM units, similar to that found for RGI, and represents the chromatographically obtainable limit.

At the high DM limit where the DM distributions are again predicted to become substantially narrower, experiments are limited by the number of available samples in this region (methylesterifying samples to close to 100% is potentially possible but not trivial); and the fact that (for pectins) the effects of charged residues in the RGI regions becomes more important. However, using reasonably monodisperse, well-characterized HG samples of known DP and DM, as described in this work, provides an excellent test for the proposed hypotheses.

Figure 5 (a) shows the comparisons of the calculated (Gaussian distributions with FWHH values given by the theory displayed in figures 4 (a) and (b), assuming DP=80) and the experimentally measured distributions for a set of HG samples obtained as described in the experimental section, and the agreement can be seen to be good.

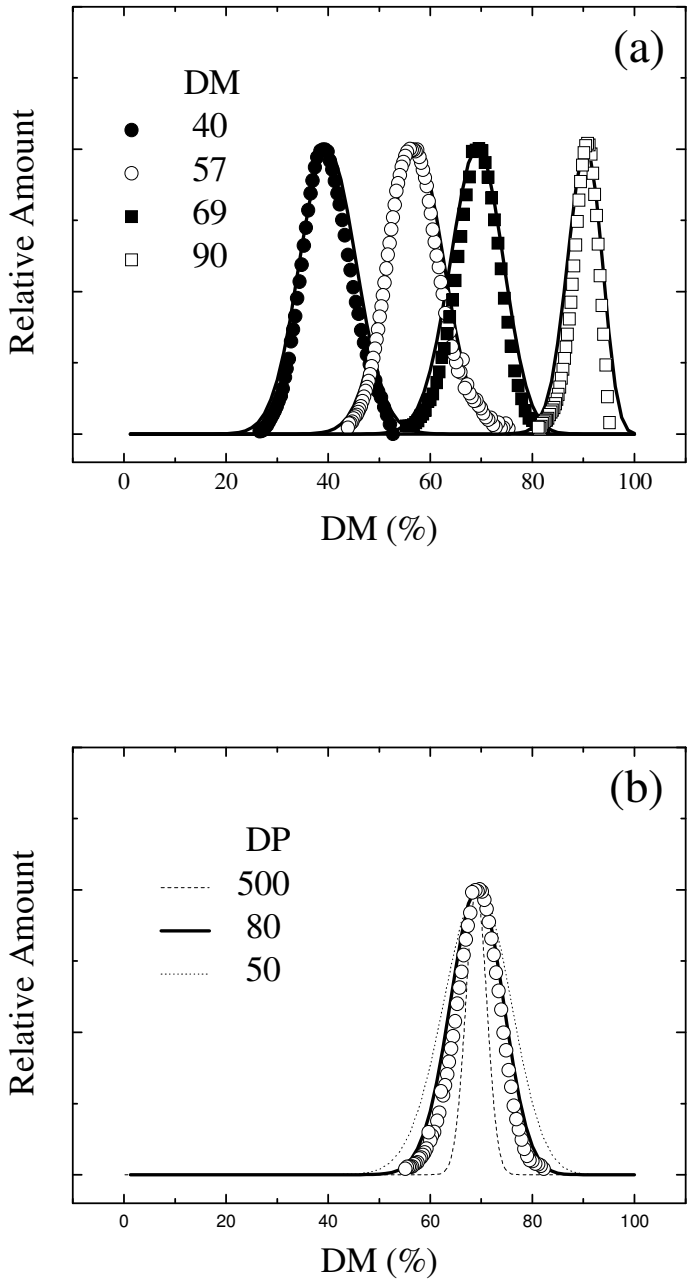

Figure 5(a): Calculated (Gaussian distributions with FWHH values given by the theory displayed in figures 4 (a) and (b), assuming DP=80) and the experimentally measured distributions for a set of HG samples. (b) the calculation obtained for a variety of degrees of polymerization for the DM 69 % sample compared with the experimental data.

It is particularly noteworthy that the sample with the highest DM does indeed possess a narrower intermolecular DM distribution as predicted. For reasonably

monodisperse samples with a fairly low DP figure 4 (a) suggests that the DP dependence of the width of the intermolecular distribution should be strong enough to give a reasonable estimate of the molecular weight of the sample. In figure 5 (b) we explicitly demonstrate the sensitivity in this region by plotting the experimental distribution obtained versus the calculation obtained for a variety of DP for the DM 69 % sample, and the agreement with the prediction based on the independently measured DP=80 can indeed be seen to be reasonable. Simply taking the experimentally measured width and using figure 4 to obtain a DP gives around (120±10).

For real pectin samples the DPs are likely to be higher than those of the HGs, so that the sensitivity of the intermolecular DM distribution width to molecular weight will be reduced somewhat (figure 4(a)), and additionally there is likely to be a degree of polydispersity. However, such measurements might still provide a reasonable average molecular weight estimate for pectin samples that could be of interest. Although techniques such as HPSEC-MALLS are routinely exploited to obtain molecular weight distributions for biopolymers these experiments are by no means trivial (Berth *et al.*, 2008) and having a secondary independent estimate could be advantageous.

Having established the link between the intermolecular and intramolecular distribution and shown it for homogalacturonan polymers with a controlled degree of polymerisation and random distribution of charge, the next part will focus on the fine structure of pectin made by enzymatic processes in particular polymers with a blocky repartition of charges. It is of interest to observe how similar or otherwise the intermolecular distribution is if the pattern of charges is not random.

3.3 Intermolecular and intramolecular distributions for blocky pectin

The deesterification of pectin by plant PME is one way to design polymers with longer blocks of free carboxyl groups and thereby to obtain blocky charges distributions. As previously noted, another effect of modifying pectin by plant PME is the increase of the broadness and the change of shape of the intermolecular methylester distribution (Ström, 2006). It makes sense in the

context that it is the average DM which is monitored during enzymatic processing and determines when the reaction is stopped, but when an average DM is reached it doesn't necessary mean that every pectin chain as been modified similarly. It is worth mentioning at the outset that these DM distributions are not Gaussian which provides good evidence that the pattern is not random, referring to the previous section on homogalacturonan.

However, even if these enzymatically modified pectins are expected to have a blocky pattern and a broader charge distribution than the mother pectin, the evolution of the intermolecular and intramolecular distributions as the enzyme is processing hasn't been assessed yet and will be the object of this work. Furthermore, the effect of the fine structure of the mother or substrate pectin on the final blockiness of the PME treated pectin will be studied.

3.3.1 Influence of the DM decrease on the methylester group intermolecular distribution

In this part, we studied the influence of the DM decrease on the shape of the DM distribution to obtain information on the enzyme mechanism and thereby on the intramolecular distribution. Figure 6 shows the DM distribution for pectins modified by PME treatment from the same mother pectin (apple pectin DM 78%). It is clear from this figure that the methylester intermolecular distribution gets broader as PME action proceeds up to a DM of 62%, however by further processing (DM53%), the distribution became narrower. Furthermore, it appears that it is not just the width which is affected but the form of the distribution is evolving as PME action proceeds. Indeed, the shape seems to rapidly (after a deesterification of around 4%) diverge from a Gaussian which indicates the loss of the random distribution, if we refer to what we have shown previously using homogalacturonan in this chapter. This trend is reinforced as the enzyme proceeds until the DM reaches 53% for which the DM distribution looks to start to diverge less from a Gaussian shape once more. It is also worth noting that as the enzyme proceeds, the DM distribution seems to be comprised of not only one 'population'. When the DM decreases between 79% and 71%, the 'peak summit' shifts to lower DM: from 79% to 71%, the peak loses its symmetrical shape by creation of a small population of pectin between 40-60% DM. This population

becomes more important when the DM decreases to 62% and gets predominant at a DE of 53%.

To highlight the effect of the PME action on the broadness of the DM distribution, the width at half height of the DM distribution peak is plotted versus the average DM distribution in figure 7. By decreasing the DM by about 17% (from 78% to 62%), the peak width at half height is almost multiplied by two. But by decreasing the DM further to 51%, the width at half height decreases from 21% to 15%. This evolution of the DM broadness could be explained by the PME mechanism. All the pectin chains are not modified at the same speed and at the same moment. Some pectin chains seem 'left behind' at the beginning. It would be interesting to do a pectin modification with a higher enzyme concentration to see if the broadness evolution would be less important. This evolution of the DM distribution with PME modification is really different of the random modification obtained by alkali deesterification in which the peak distribution was staying symmetrical and Gaussian and the evolution of the broadness of the distribution was restricted (see section 3.2 of this chapter). The fact that they clearly are different suggests modeling these distributions should form part of future work, as discussed at the end of the thesis

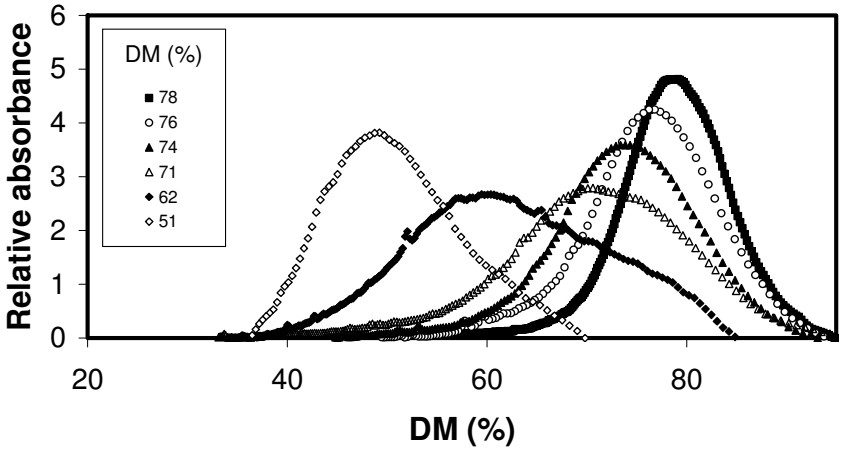

Figure 6: Methylester intermolecular distribution of pectin made by enzymatic (PME) treatment of the same mother pectin (apple pectin DM 77.8%)

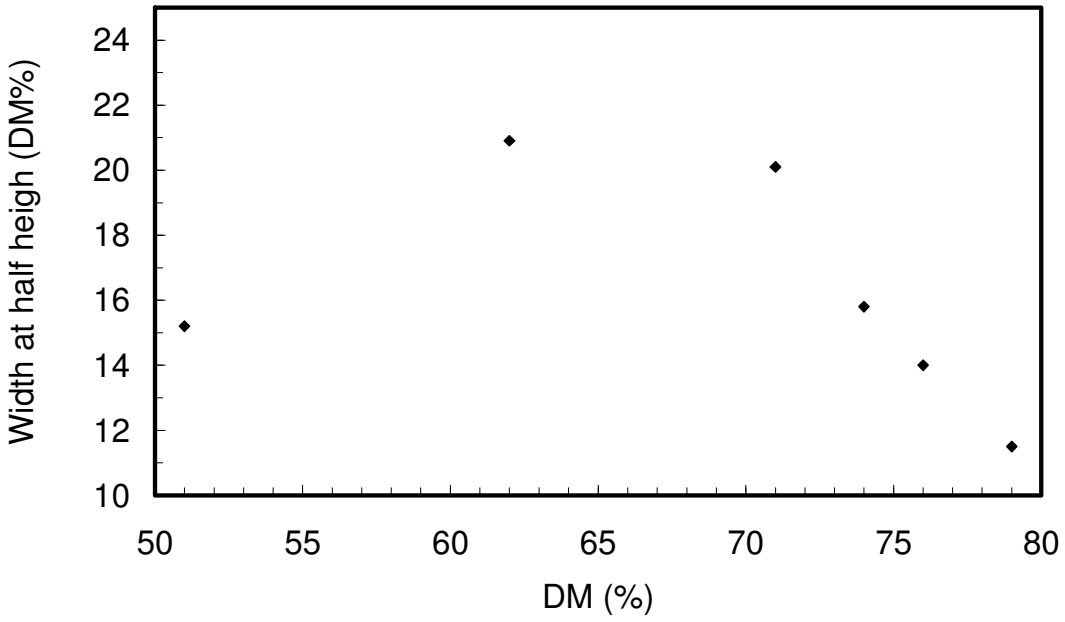

Figure 7: Effect of the PME action on the broadness of the DM distribution

3.3.2 Digest pattern by PGII

The digest pattern of the PME deesterified substrates obtained by PGII digestion for each DM distribution analysed in 3.3.1 is shown in figure 8. Four main peaks are observed in every electrophoregram. As peak identification has been previously achieved on electrophoregrams of pectin having undergone the same type of treatment (Ström, 2006), these 4 peaks were identifiable by analogies. The peak at ~3.5 min corresponds to the pectin residues that were not digestible by PME, the 3 other ones are the oligomers, (by time of migration): mono-, di- and tri-galacturonic acid (1^0, 2^0, 3^0). This digest pattern, in particular the lack of partially oligomers liberated, suggests the presence of unmethylesterified blocks, long enough for undisturbed PGII action and thus is characteristic of blocky pectins (Ström, 2006), which is what it is expected for a PME treatment.

When the DM decreases, the proportion of the non-digestible pectin residues versus the amount of 1^0, 2^0, 3^0 decreases. This shows that the pectin becomes

more blocky when the DM decreases which again could be explained by a stepwise mechanism of the PME enzyme.

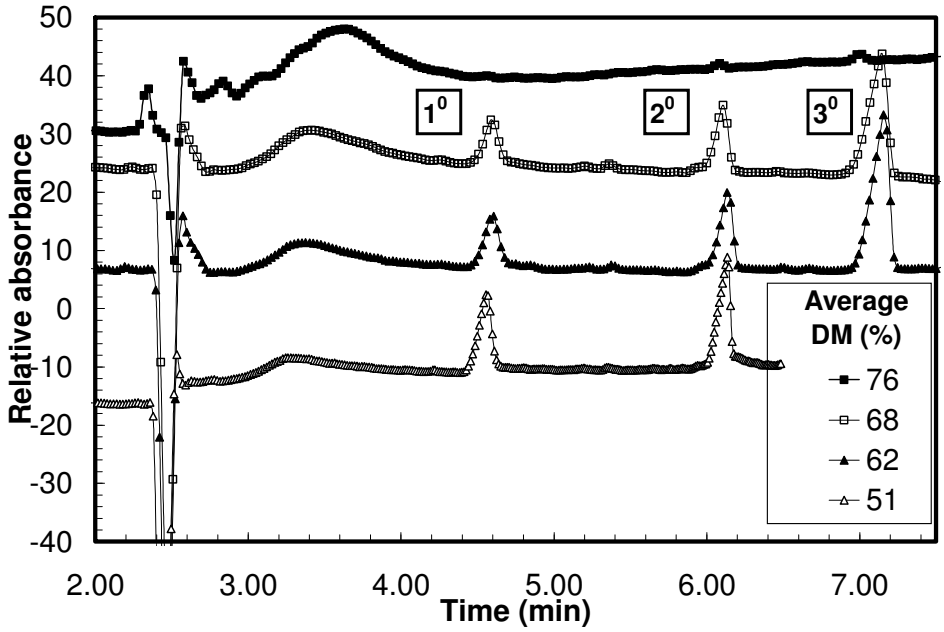

Figure 8: Electrophoregram of the pectin digest by PGII

3.3.3 PGII digestibility of the substrates as a function of the DM decrease induced by PME

In this part, the DM distribution of pectin made by PME treatment (which will be referred to as treatment 1 or T1) is compared with the distribution of any remaining non-digestible polymeric chains after PGII digestion (which will be referred to as treatment 2 or T2) (Schematic 1).

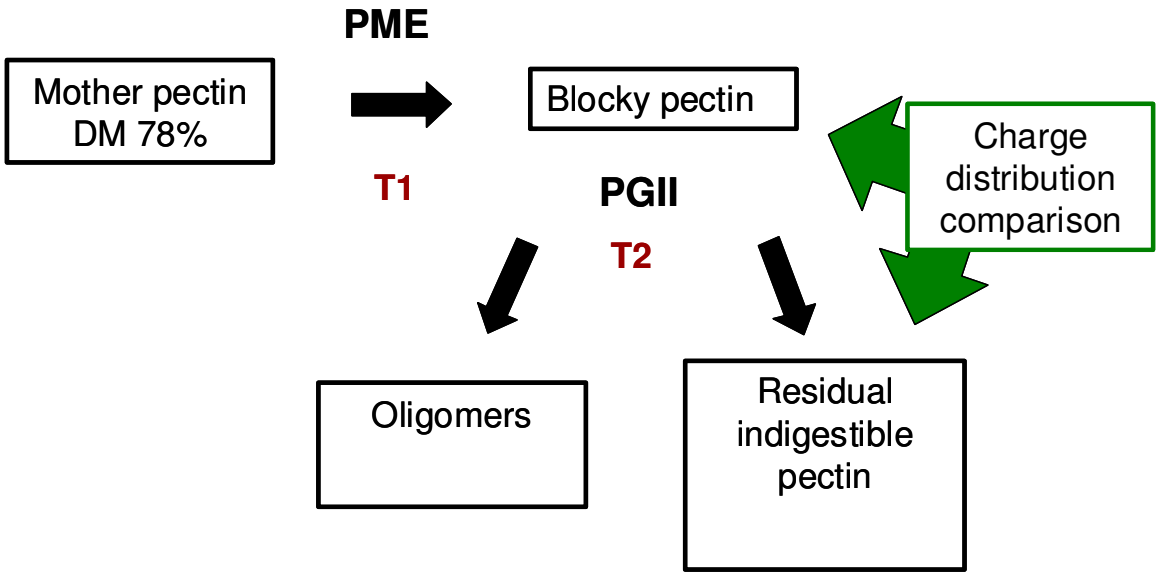

Schematic 1: Principle for the comparison of the distribution of the pectin modified by PME and the remaining non-digestible pectin fraction after PGII treatment. T1 and T2 stand for treatment 1 and 2.

It is the breaking of the scaling symmetry between charge and hydrodynamic friction as described previously in chapter 1 (section 4.1) that allows both products of T2: enzyme liberated fragments (oligomers) and remaining undigested substrate to be visualised in the same technique, unique to CE.

Figure 9 shows the DM distribution before (starting pectin) and after PGII digestion (indigestible pectin fraction) of a pectin having a DM 53% after PME treatment (T1) from the mother pectin (DM 78%). The DM distribution of the pectin chains remaining after PGII treatment is narrow and symmetrical with a shape approximately Gaussian i.e. a distribution characteristic of a random distribution and could be only be explained if the action of PME during T1 has been limited or non existent on this fraction. Furthermore, the distribution of the indigestible pectin after PGII digestion (T2) is similar to the distribution of the mother pectin consistent with this idea. This suggests all regions introduced by PME during T1 seem to be fully digestible and hence the indigestible regions still reflect the mother substrate- see schematic 2.

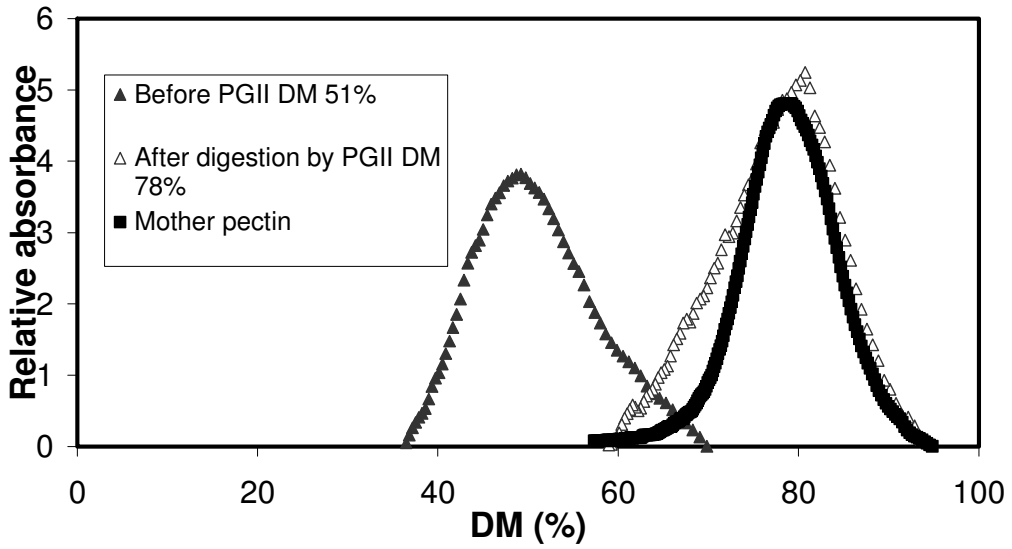

Figure 9: DM distribution before and after digestion by PGII for pectin with different initial DM

Table 3 shows the average DM for a set of pectins which have been deesterified by PME (T1) to different degrees compared to the DM of the corresponding residual fraction after PGII digestion (T2). The DM of residual indigestible portions after treatment with PGII (T2) is found in all cases to be similar (between 75 and 80%) for every fine pectin structure digested. Thus shows that the non-digestible fragment DM is not dependant on the DM of the PME deesterified but on the starting DM of the mother pectin substrate in the range tested.

DM after modification with PME Pectin (%, +/- 3)	DM of residual indigestible portions after digestion by PGII Pectin (%,+/- 3)
76	80
68	75
62	78
51	77

Table 3: Comparison of the DM of pectin (after T1) and indigestible pectin (after T2)

It is also worth noting that what was previously observed for pectin T1 with a DM 51% is applicable to all the pectins in the DM range tested: the indigestible fraction has a DM distribution similar to the mother pectin, giving further evidences of the blockiness of the pectin after PME treatment and showing that the action of PME seems to be extremely blockwise on part of the chain while other parts seem to be untouched as shown in schematic 2.

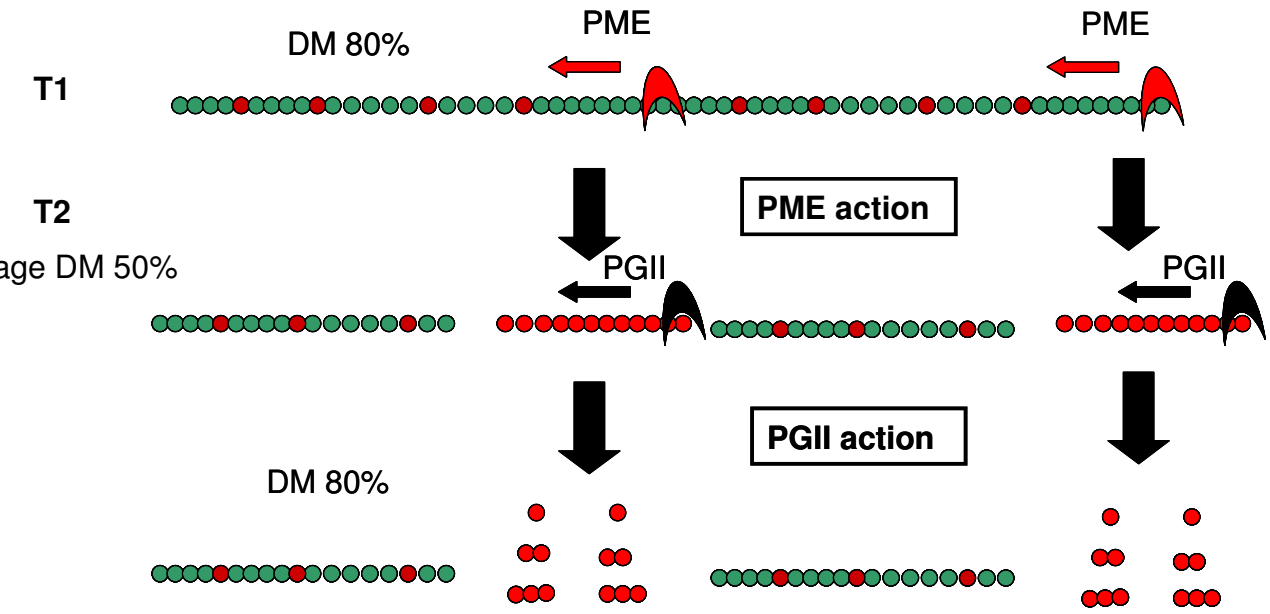

Schematic 2: The action of PME on the pectin fine structure (red circle: acid galacturonic, green circle: methylester acid galacturonic, DM: degree of methylesterification, PME: pectin methylesterase, PGII: polygalacturonase II, T1 and T2: treatment 1 and 2)

To obtain further evidence of the blocky action of PME on parts of the chain while other parts are more or less untouched, the DM of the mother pectin (before PME treatment) was modified prior to action of the PME by alkali treatment (T0) which leads to random pectin with a lower DM: 69%. The process is described in the following schematic.

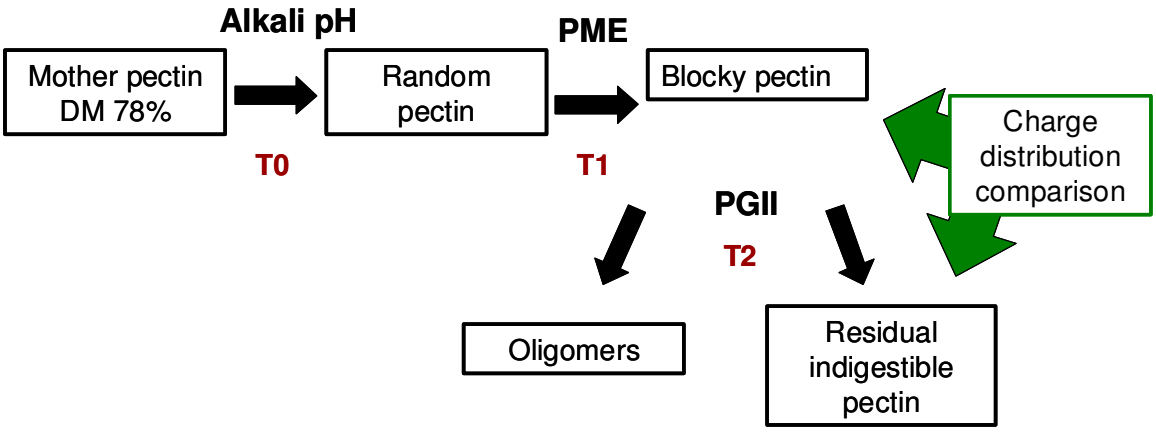

Schematic 3: Principle for the comparison of the distribution of the pectin modified by alkali and PME treatment and the remaining non-digestible pectin after PGII treatment. T0, T1 and T2 stand for treatment 0, 1 and 2.

DM after modification with PME Pectin (%, +/- 3)	DM of residual indigestible portions after digestion by PGII Pectin (%,+/- 3)
63	70
60	68
56	66
52	65

Table 4: Comparison of the DM of pectin after T1 and T0 and indigestible pectin after T2

Table 4 shows the average DM for the pectins which have been deesterified by alkali treatment to DM 69% (T0) and then by PME (T1) treatment to different degrees compared to the corresponding residual fraction after PGII digestion (T2). As observed previously when the PME treatment was carried out on a pectin with a higher DM (78%), the DM of residual indigestible pectin portions after PGII treatment (T2) is not influenced by the DM of the PME generated pectin substrate and has a value (between 65% and 70%), close to the alkali modified pectin (T0, DM 69%) that formed the starting point of the PME processing instead. Thus, if the PME pectin substrate is deesterified by alkali treatment (leading to a random charge distribution) by 10%, the action of PME is not significantly influenced: relatively long blocks on the chains are almost completely deesterified while other

regions are untouched. This provides further evidence of a stepwise action of PME on the pectin backbone leading to blocky repartition of the charges.

4 Conclusion

In conclusion, by comparison of data taken from the literature and measured in this work, the reliability and accuracy of the CE method has been further increased and a relation between electrophoretic mobility and DM has been etablished.

The intermolecular charge distribution of alkali demethylesterified homogalacturonan has been shown to be as expected for a random processes using calculations based on the binomial theorem and thus to contain information on the intramolecular distribution described by the same statistical process.

The action of PME changes the width and the shape of the intermolecular charge distribution which seems to be linked to the stepwise action of the enzyme: parts of chains are modified while other sections remain almost untouched. Furthermore, the indigestible pectin fractions after successive PME and PGII treatments have a DM values and distributions similar to the starting pectin substrates highlighting the blockiness of the PME modified pectin, as shown in Schematic 3.

Pectin deesterified by the enzyme clearly has a distribution which diverges from a Gaussian, characteristic of a random pattern, and thus modelling on this distribution would be able to give further information on their fine structure and the PME mechanism.

References

Berth G., Vukovic J., Lechner M.D. (2008) Physicochemical characterization of carrageenans - A critical reinvestigation. *Journal of Applied Polymer Science* **110**(6):3508-3524

Daas P.J.H., Arisz P.W., Schols H.A., DeRuiter G.A., Voragen A.G.J. (1998) Analysis of partially methyl-esterified galacturonic acid oligomers by high-performance anion-exchange chromatography and matrix-assisted laser desorption/ionization time-of-flight mass spectrometry. *Analytical. Biochemistry* **257**:195-202

Daas P.J., Meyer-Hansen K., Schols H.A., De Ruiter G.A., Voragen A.G.J (1999) Investigation of the non-esterified galacturonic acid distribution in pectin with endo-polygalacturonase. *Carbohydrate Research* **318:**135-145

Goodall D.M., Williams S.J., Lloyd D.K. (1991) Quantitative aspects of capillary electrophoresis. *Trends in Analytical Chemistry* **10**:272-279

Goubet F., Ström A., Dupree P., Williams M.A.K. (2005) An investigation of pectin methylesterification patterns by two independent methods: capillary electrophoresis and polysaccharide analysis during carbohydrate gel elctrophoresis. *Carbohydrate research* **340**: 1193-1199

Lee H., Rivner, J., Urbauer J.L., Garti N., Wicker L. (2008) De-esterification pattern of Valencia orange pectinmethylesterases and characterization of modified pectin. *Journal of the Science of Food and Agriculture* **88(**12):2102-2110

Levigne S., Thomas M., Ralet M.-C., Quemener B., Thibault J.-F. (2002) Determination of the degrees of methylation and acetylation of pectins using a C18 column and internal standards. *Food Hydrocolloids* **16:**547-550

Macquet A., Ralet M.-C., Kronenberger J., Marion-Poll A., North H.M. (2007) In situ, Chemical and Macromolecular Study of the Composition of *Arabidopsis thaliana* Seed Coat Mucilage. *Plant & Cell Physiology* **48**(7):984-999

.

Maness N.O., Ryan J.D., Mort A.J. (1990) Determination of the degree of methyl esterification of pectins in small samples by selective reduction of esterified galacturonic acid to galactose. *Analytical Biochemistry*. **185***(2)*:346-352.

Massiot P., Perron V., Baron A., Drilleau J.F. (1997) Release of methanol and depolymerization of highly methyl esterified apple pectin with an endopolygalacturonase from Aspergillus niger and pectin methylesterases from A-niger or from orange. *Food Science and Technology-Lebensmittel-Wissenschaft & Technologie* **30**(7):697-702

Morris E.R., Gidley M.J., Murray E.J., Powell D.A., Rees D.A. (1980) Characterisation of pectin gelation under conditions of low water activity, by circular dichroism, competitive inhibition and mechanical properties. *International Journal of Biological Macromolecules* **2**:327-330

Neiss T.G., Cheng H.N., Daas P.J.H., Schols H.A. (1999) Compositional heterogeneity in pectic polysaccharides: NMR studies and statistical analysis. *Macromolecular Symposia* **140**:165-178

Perez S., Mazeau K., Herve du Penhoat C. (2000) The three-dimensional structures of the pectic polysaccharides. *Plant Physiol. Biochem*istry **38**:37-55

Ralet M.C., Dronnet V., Buchholt H.C. and Thibault J.F. (2001) Enzymatically and chemically de-esterified lime pectins: characterisation, polyelectrolyte behaviour and calcium binding properties. *Carbohydrate Reearch.* **336**:117-125

Rosenbohm C., Lundt I., Christensen T.M.I.E., Young N.W.G. (2003) Chemically methylated and reduced pectins: preparation, characterisation by H-1 NMR spectroscopy, enzymatic degradation, and gelling properties. *Carbohydrate Research* **338**:637-649.

Ström A., Williams M.A.K. (2003) Controlled calcium release in the absence and presence of an ion-binding polymer. *Journal of physical chemistry B* **107**(40):10995-10999

Ström A., Ralet M.C., Thilbault J.F., Williams M.A.K. (2005) Capillary electrophoresis of homogeneous pectin fractions. *Carbohydrate polymers* **60**:467-473

Ström A., Williams M.A.K. (2004) On the separation, detection and quantification of pectin derived oligosaccharides by capillary electrophoresis. *Carbohydrate research* **339***:*1711-1716

Ström A. (2006) Characterisation of pectin fine-structure and its effect on supramolecular properties University College Cork

Synytsya A., Copikova, J., Matejka P., Machovic V. (2003) Fourier transform Raman and infrared spectroscopy of pectins. *Carbohydrate Polymers* **54**(1):97-106

Thibault J.-F., Renard C.M.G.C., Axelos M.A.V., Roger P., Crépeau M.-J. (1993) Studies of the length of homogalacturonanic regions in pectins by acid hydrolysis. *Carbohydrate Research* **238**:271-286.

Tuffile F.M., Ander P. (1975) Electric transport for aqueous solutions of sodium alginate and sodium polygalacturonate. *Macromolecules* **8**:789-792

Vincent R., Cucheval A., Hemar Y., Williams M. (2009) Bio-inspired network optimization in soft materials – Insights from the plant cell wall. *European Physical Journal E* **28**(1):79-87

Vincent R.R., Pinder D.N., Hemar Y., Williams M.A.K. (2007) Microrheological studies reveal semiflexible networks in gels of a ubiquitous cell wall polysaccharide. *Physical review E* **76**(3):63-70

Weinberger R. (2000) In *Practical Capillary Electrophoresis*, San Diego: Academic Press, 2nd Edition

Willats W.G.T., Orfila C., Limberg G., Buchholt H.C., vanAlebeek G.J.W.M., Voragen A.G.J., Marcus S.E., Christensen T.M.I.E., Mikkelson J.D., Murray B.S., Knox J.P. (2001) Modulation of the Degree and Pattern of Methyl-esterification of Pectic Homogalacturonan in Plant Cell Walls: IMPLICATIONS FOR PECTIN METHYL ESTERASE ACTION, MATRIX PROPERTIES, AND CELL ADHESION. *Journal of Biological Chemistry* ***276****(22)*:19404-19413

Williams M.A.K., Foster T.J., Schols H.A. (2003) Elucidation of pectin methylester distributions by capillary electrophoresis. *Journal of Agricultural and Food Chemistry* **51**(7):1777-1782

Williams M.A.K, Buffet G.M.C, Norton I.T. (2001) Simulation of endo-PG digest patterns and implications for the determination of pectin fine structure. *Carbohydrate research* **334:**243-250

Zhong Z.H., Williams M.A.K., Goodall D.M., Hansen M.E. (1998) Capillary electrophoresis studies of pectins. *Carbohydrate research* **308**:1-8

Zhong Z.H., Williams M.A.K., Keenan R.D., Goodall D.M., Rolin C. (1997) Separation and quantification of pectins using capillary electrophoresis: a preliminary study. *Carbohydrate polymers* **32**:27-32

Chapter 3

Diffusing Wave Spectroscopy investigations of acid milk gels containing pectin

As published in *Colloid and polymer science* (in press)

A. Cucheval, R. R. Vincent, Y. Hemar, D. Otter, M. A. K. Williams

Abstract

The influence of the polysaccharide pectin on the gelation of acidified milk is studied in concentrated, undiluted, quiescent systems, primarily using Diffusing Wave Spectroscopy (DWS). For pectins with a low degree of methylesterification (DM), interactions with milk-serum calcium yielded precipitated polysaccharide aggregates, even without acidification, that subsequently did not interact with casein micelles. However, high DM fine structures do not interact significantly with serum-calcium and absorb onto casein micelles as the pH is reduced below 5. A limited surface coverage of high DM pectin facilitates efficient bridging which enhances the rate of micelle aggregation and subsequent gelation, and produces a clear signature in the shape of the measured MSD. The work highlights the fact that the behaviour of pectin in milk systems depends not only on the interaction of different polymeric fine structures with casein micelles, but also to a large extent on the interactions with calcium.

Keywords*: milk, casein micelles, pectin, diffusing wave spectroscopy*

1 Introduction

Casein moieties in milk are assembled into micelles during biosynthesis and despite the fact that the detailed arrangement of the protein variants is complex, it is well established that these entities are stabilised in solution by κ-casein molecules forming an entropy rich steric barrier at their surface (de Kruif and Zhulina, 1996). Enzymatic cleavage or electrostatic collapse of this barrier destabilises the micelles and triggers assembly, yielding the formation of networks that consist primarily of aggregated casein micelles. While the micellar integrity depends in detail upon the nature of the environmental conditions employed in destabilisation, these systems nevertheless tend to exhibit the microstructural appearance of particulate networks - a fact that has not escaped the attention of physicists interested in colloidal assembly *per-se* (Schurtenberger *et al.*, 2001, Mezzenga *et al.*, 2005). Thus, acid milk gels (those triggered by the

collapse of the stabilising protein layer owing to changes in the polymeric charge brought about by lowering the pH) are built of a three dimensional network of chains and clusters of milk proteins, that at a smaller scale retain some of the integrity of the particulate micellar form (Kaláb *et al.*, 1983). They do however form a heterogeneous and complex system. The heterogeneity manifests at two levels: in the network itself and in the presence of voids in the colloidal system. Acid milk gels have been extensively studied by bulk rheology (Lucey and Singh, 1998) and more recently by microrheological techniques (Schurtenberger *et al.*, 2001, Hemar *et al.*, 2004, Alexander and Dalgleish, 2004, Alexander *et al.* 2008, Donato *et al.*, 2007). In particular Diffusing Wave Spectroscopy (DWS), a non-invasive multiple scattering technique, has found considerable utility in studying the underlying dynamics of these systems. Here, autocorrelation functions resulting from the intensity fluctuations of light that has been multiply scattered by the sample are analysed and information on the dynamics of the scatterers is thus extrated.In these systems, the scattering are dominated by casein micelles and protein aggregates, so that the introduction of probe particles, common in such microrheology experiments is not required. Via DWS, rheological behaviours at high frequency can be obtained, that contain information additional to that obtainable with conventional rheology, with the potential to give insights into the network structure.

Pectin, an ionic polysaccharide extracted from the plant cell wall, is commonly added to acid milk preparations in order to stabilize them as the pH is reduced. Indeed for acid milk drinks, which have low solids content (2-5% w/w), pectin is able to inhibit casein micelles coagulation, yielding a macroscopically-homogeneous viscous solution at pH values below 5, in contrast to the precipitation of milk proteins that is observed in its absence. Pectin is composed of 3 pectic polysaccharides (Willats *et al.*, 2006): homogalacturonan (HG), rhamnogalacturonan I (RGI) and rhamnogalacturonan II (RGII). HG is a linear polymer of (1-4)-linked α-D-galacturonic acid and its methylesterified counterpart with the ratio of uncharged methylesterified residues to the total galacturonic acid content (the degree of methylesterification or DM) playing a major role in determining the polymers functionality. RGI has a backbone consisting of the repeating disaccharide rhamnose-galacturonic acid, where the rhamnose residues

provide potential sites for the attachment of glycan side-chains. RGII has a backbone of (1-4)-linked α-D-galacturonic acid but with many conserved complex sugar side chains. Typical extraction processes modify the in-vivo pectin fine structure, (which is still a matter of debate to some extent), notably by decreasing the number of side-chains, and commercially available pectins are routinely found to consist of primarily linear chain homogalacturonan (around 90%).

The interaction between pectin and casein micelles has been widely studied by dynamic light scattering (DLS) *in diluted systems* (Maroziene and de Kruif, 2000, Liu *et al.*, 2006, Nakamura *et al.*, 2006), and by rheology and microscopy (Matia-Merino *et al.*, 2004, Matia-Merino and Singh 2007, Fagan *et al.*, 2006). It has been suggested that, at sufficient concentrations, pectin can interfere with the aggregation of milk upon acidification by two mechanisms. Firstly, DLS studies have shown that below pH 5, certain pectin fine structures can adsorb onto casein micelles via electrostatic interactions (Tuinier *et al.*, 2002). These pectin layers increase the steric repulsion between casein micelles (Kravtchenko *et al.*, 1995), replacing the stabilizing effect that was produced by the κ-casein at higher pH, and limiting their sedimentation at low protein concentration e.g. in acid milk drink. It has also been suggested that pectin may play a role in forming a weak gel in the voids of the micellar particulate network (Boulenguer and Laurent, 2003) and indeed confocal microscopy studies using Fluorescence Recovery After photobleaching (FRAP) have provided evidence for a reduced pectin mobility in these systems, although the removal of the "serum pectin" by centrifugation did not affect the stability of the system (Tromp *et al.*, 2004). Other studies with systems of lower pectin concentration (0.12 %w/w) located pectin in stabilised systems by using a monoclonal pectin antibody (Arltoft *et al.*, 2007) and found it to be present predominantly in, or at the surface of, the protein aggregates - rather than in the voids of the network. Pectin fine structure, notably the DM (and also the distribution of the methylester group on the backbone) will strongly influence not only the polymers interaction with calcium, as it is well-known, but also with casein. Indeed, high DM pectins have been shown to stabilize casein dispersions more effectively than those of low DM (Pereyra *et al.*, 1997, Laurent and Boulenguer, 2003, Liu *et al.*, 2006).

In this work we were interested in the following questions: 1) if indeed, in the course of acidification, pectin adsorbs around the casein micelles prior to significant micellar aggregation even in more highly concentrated quiescent systems, then how would such a polymer coating effect the mechanical properties of the resultant gel? 2) would such a structural modification to the network composition reveal a characteristic microrheological signature of the polymer adsorption that could be used as an indication of the extent of interaction in the concentrated state, circumventing the current requirements of dilution and 3) what understanding of the interaction might be gained by carrying out these experiments with a judicious choice of polysaccharide fine structures?

2 Materials and methods

2.1 Materials

2.1.1 Acid milk gel preparation

Low heat skim milk powder (NZMP, New Zealand) was used to prepare reconstituted skim milk with 20% w/w milk solids. Sodium azide (0.02% w/v) was added to the reconstituted skim milk to avoid bacterial growth. With a low heat milk powder, only the caseins will be part of the network (in contrast to that which has undergone a more severe heat treatment in which the whey proteins can also play a significant role). A 0.2 % w/w pectin solution was prepared in parallel. Pectins with different fine structures were used, the degree of methylesterification, molecular weight and origin of which are reported in table 1.

	DM / %	Mw / g.mol^{-1}	Origin and treatment
R77.8	77.8	120 000	Copenhagen Pectin fungal PME
R78	78	30000-100000	Fluka Biochemica, Switzerland
R31.1	31.1	120 000	Copenhagen Pectin fungal PME
R30	30	44 000	Homemade by alkali treatment *
E30	30	44 000	Homemade by treatment with a processive enzyme (PME) *

Table 1: Characteristics of pectin samples used in this study.

*: Williams M A K, Foster T J, Schols H A (2003) Elucidation of Pectin Methylester Distributions by Capillary Electrophoresis. J Agric Food chem 51:1777-1781

The two dispersions were stirred overnight at 4 °C to ensure full hydration. Subsequently, pectin and skim milk powder solutions were mixed in equal quantities to obtain a system with a final concentration of 10% w/w milks solids and 0.005-0.1% w/w pectin and sheared for one hour with a magnetic stirrer before any analysis. Acidification of the final sample was achieved by the addition of between 1 - 2.3 %w/w glucono-δ-lactone (GDL) at 20 °C. For all samples studied, the pH was measured every 5 minutes during the acidification process.

2.2 Methods

2.2.1 Diffusing wave spectroscopy

Diffusing wave spectroscopy (DWS) is a light scattering method that is designed to be used with turbid samples, where each photon encounters multiple scattering events between entering the sample cell and being detected. In such systems the photons path can be considered a random walk and, as such, the decay of the autocorrelation function of the scattered light owing to the motion of the scatterers can be calculated from the solution to a well-known diffusion problem. Owing to the multiple scattering nature of the technique each individual scattering particle need only move a small amount in order to generate significant de-

phasing effects when summed over the entire photon trajectory. Thus DWS can measure motions at high frequency, and the technique has found great utility in studying the motion of tracer particles added to systems to probe their microrheological properties over a broad frequency range. In this work the casein micelles themselves act as the probes with the evolution of the correlation function during gelation primarily reflecting changes in their dynamics. The measured temporal autocorrelation of intensity fluctuations of the scattered light was measured as:

$$g_1(t) \equiv \frac{1}{\beta}\left(\frac{\langle I(t)I(0)\rangle}{\langle I\rangle^2} - 1\right) \qquad (1)$$

where β is a constant, characteristic of the optics, and $I(0)$ and $I(t)$ the intensity of the detected light at the time zero and t. While DWS can be carried out in transmission or backscattering modes, transmission is preferred here owing to the increased simplicity of the boundary conditions: each detected photon has clearly traversed a distance equivalent to the width of the sample cell. Under these conditions the calculated temporal autocorrelation function for the transmitted light can be written as (Weitz *et al.*, 1993):

$$g_1(t) = \frac{\frac{L/l^* + 4/3}{z_0/l^* + 2/3}\left\{\sinh\left[\frac{z_0}{l^*}\sqrt{k_0^2\langle\Delta r^2(\tau)\rangle}\right] + \frac{2}{3}\sqrt{k_0^2\langle\Delta r^2(\tau)\rangle}\cosh\left[\frac{z_0}{l^*}\sqrt{k_0^2\langle\Delta r^2(\tau)\rangle}\right]\right\}}{\left(1 + \frac{8t}{3\tau}\right)\sinh\left[\frac{L}{l^*}\sqrt{k_0^2\langle\Delta r^2(\tau)\rangle}\right] + \frac{4}{3}\sqrt{k_0^2\langle\Delta r^2(\tau)\rangle}\cosh\left[\frac{L}{l^*}\sqrt{k_0^2\langle\Delta r^2(\tau)\rangle}\right]} \qquad (2)$$

where l^* is the transport mean free path, z_0 the penetration depth (considered equal at l^* in these experiments), L thickness of the sample (4 mm), $k_o = 2\pi n/\lambda$, the wave vector of the light and $\langle\Delta r^2(t)\rangle$ is the mean square displacement (MSD) of the particle. Hence, when l^* is known, the experimentally determined correlation function can be turned into a plot of MSD versus lag time, by inverting equation 2 with a zero-crossing routine.

l^* is obtained by performing an experiment on a water sample using latex beads, and fitting l^* using the accepted viscosity. Subsequently l^* for future samples is obtained by scaling the value obtained for water, based on the change in transmitted intensity when the sample is introduced, compared to the water experiment. It is known that for non-absorbing slabs of thickness L, the

transmitted intensity is directly proportional to $(5l^*/3L)/(1+4l^*/3L)$, so that by measuring the change in transmittance, the change in l^* can be calculated.

The experimental set up has been fully described elsewhere (Hemar and Pinder, 2006, Williams *et al.*, 2008). Briefly, laser light with a wavelength of 633 nm (35 mW He Ne Melles Griot laser) diffused through the sample, contained in a plastic cuvette of 10 mm width, 50 mm height and 4 mm path length. The transmitted scattered light was collected using a single optical fibre (P1-3223-PC-5, Thorlabs Inc., Germany) and was detected with a photomultiplier tube module (Hamamatsu HC120-08). The auto-correlation analysis was performed using a Malvern 7132 correlator. Tests were run for 3 minutes to ensure low noise intensity autocorrelation functions.

2.2.2 Bulk rheology

The viscoelasticity of the systems was analysed by dynamic oscillatory rheometry using a Paar Physica UDS 200 instrument in the stress-controlled manner. Immediately after the addition of GDL and stirring for 1 minute, the sample was loaded into a measurement cell with a cone geometry. The storage (G') and loss moduli (G'') were recorded during 3 hours at a constant frequency of 1 Hz and a strain of 0.5%. The sample was maintained at 20 °C during all measurements.

2.2.3 Confocal microscopy

A Leica confocal laser scanning microscope (TCS SP5 DM6000B) was used in fluorescence mode with a DPSS 561 laser (excitation wavelength of 561 nm, emission spectrum 565-659 nm) and an oil-immersion objective (×100). The number of pixels per image was 2048×2048. The protein network was dyed with Fast-green prior to acidification by addition of 6µl of dye, from a 0.2 %w/w mother solution, to 1 ml of sample.

2.2.4 ^{31}P NMR

^{31}P NMR experiments were carried on a Bruker 400 Ultrashield spectrometer (^{31}P operating frequency 161.97 MHz) at a temperature of 20 ˚C. Samples were measured in a 5 mm diameter thin wall tube (Wilmad LabGlass, USA). A 1 mm diameter capillary containing phosphoric acid (10 mM) was first inserted into the NMR tube to provide a chemical shift reference (the phosphoric acid peak was set to 0 ppm). The capillary was then removed and spectra (256 scans, 65 000 data points) were recorded for each sample. The glycerophosphoycoline peak which was not affected by the presence of pectin was used as a concentration reference.

3 Results and discussion

3.1 Acid milk gel

Systems containing 10% w/w milk solids non-fat (MSNF), corresponding to around 13% volume fraction of casein micelles (Jeurnink and de Kruif, 1993, Tuinier and de Kruif., 2002) were reconstituted and were acidified at 20° C, using GDL. DWS was used to record the evolution of the correlation function of transmitted multiply-scattered light as described in the experimental section and thereby report on the dynamics of the scatterers; the casein micelles and aggregates thereof formed during gelation. Figure 1(a) shows the light autocorrelation function $g_1(\tau)$ as a function of the time lag τ, as measured by DWS, during the acidification process. The sol-gel transition is clearly reflected in the dynamics of the scatterers. While initially $g_1(\tau)$ is characteristic of a Newtonian fluid, i.e. goes to zero at long times, as acidification proceeds the correlation function does not decay to zero, showing that a high viscosity fluid or visco-elastic gel is formed. At long times, and at low pH values, $g_1(\tau)$ tends to be quite flat corresponding to the presence of a quasi-elastic material. Typically in microrheological studies of soft materials stable scatterers are artificially introduced into the system, l^* is measured, and hence the mean square

displacement of the particles can be obtained by simple inversion of equation 2, with a zero-crossing routine. Such a numerical approach to the extraction of the MSD dispenses with the assumption that MSD=6*Dt*, i.e. that the medium is purely viscous; although in cases where this is known to be the case the substitution of this expression into equation 2 yields an expression to which data can be directly fitted using standard non-linear least squares algorithms. The data in figure 1(a) are analyzed by inversion, although it should be stressed that the integrity and size of these omnipresent scatterers are possible functions of pH.

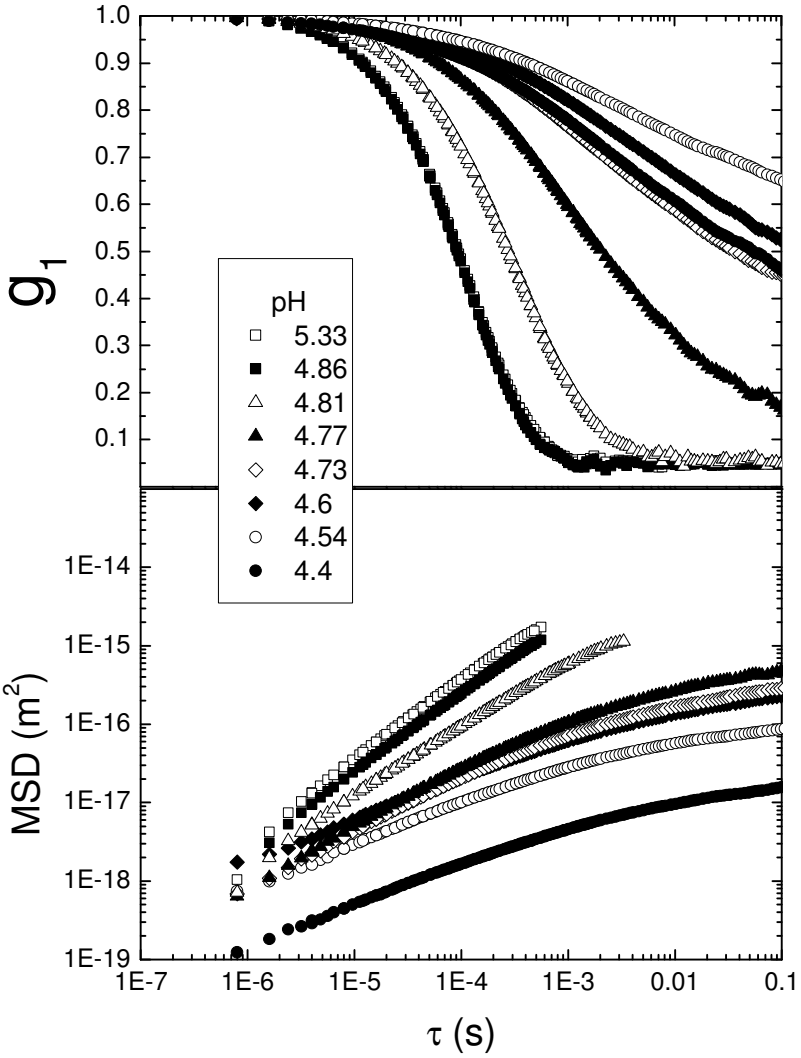

Figure 1(a): Temporal autocorrelation function evolution for milk (10 % w/w MSNF) during acidification and (b) the corresponding evolution of the measured MSDs

Although l^* is re-measured along with each corresponding correlation function this means that the actual MSD values measured after the gelation point should be taken as estimates whose accuracy depends upon the extent of these scatterers modifications. Nevertheless, microscopy evidence suggests that micelles are not completely dissociated and an intact particulate gel is a reasonable model of the system (Kaláb *et al.*, 1983, van Vliet *et al.*, 2004). Furthermore, we still expect the variation of MSD with time lag to capture the essential physics of the gel properties.

Micelle mean square displacements as a function of lag time obtained by inversion of the correlation functions recorded during the acidification process are shown in Figure 1(b). Results from the starting solution yielded a linear dependence of the MSD with time, with a slope of 1 evident from a double logarithmic plot, indicative of a viscous medium. Upon acidification, the slope of the mean square displacement versus time plot retained its power law dependence at high frequency, but the relevant exponent decreased with decreasing pH. As the high frequency behaviour corresponds to small displacements, of the order of 1-10 nm, it predominantly probes the nature of the network's constituent elements. In order to get some information about the nature and the density of the cross-links, the study of the long time behaviour is essential, giving access to the state where large displacements of the beads can significantly strain the network, and indeed the acidification-induced evolution of a gel is clearly reflected at lower frequencies.

As the high frequency behaviour contains fundamental information about the network constitution and had received considerable attention previously focussed on the comparison of the acidified-milk system with other colloidal gels and physical models (Romer *et al.*, 2000, Schurtenberger *et al.*, 2001, Mezzenga *et al.*, 2005, Donato *et al.*, 2007), we initially concentrated on this region. Figure 2 (a) shows the high frequency exponent revealed by the slope of the double logarithmic MSD versus lag time plot, as a function of time during acidification, carried out at different rates as a consequence of different added GDL concentrations.

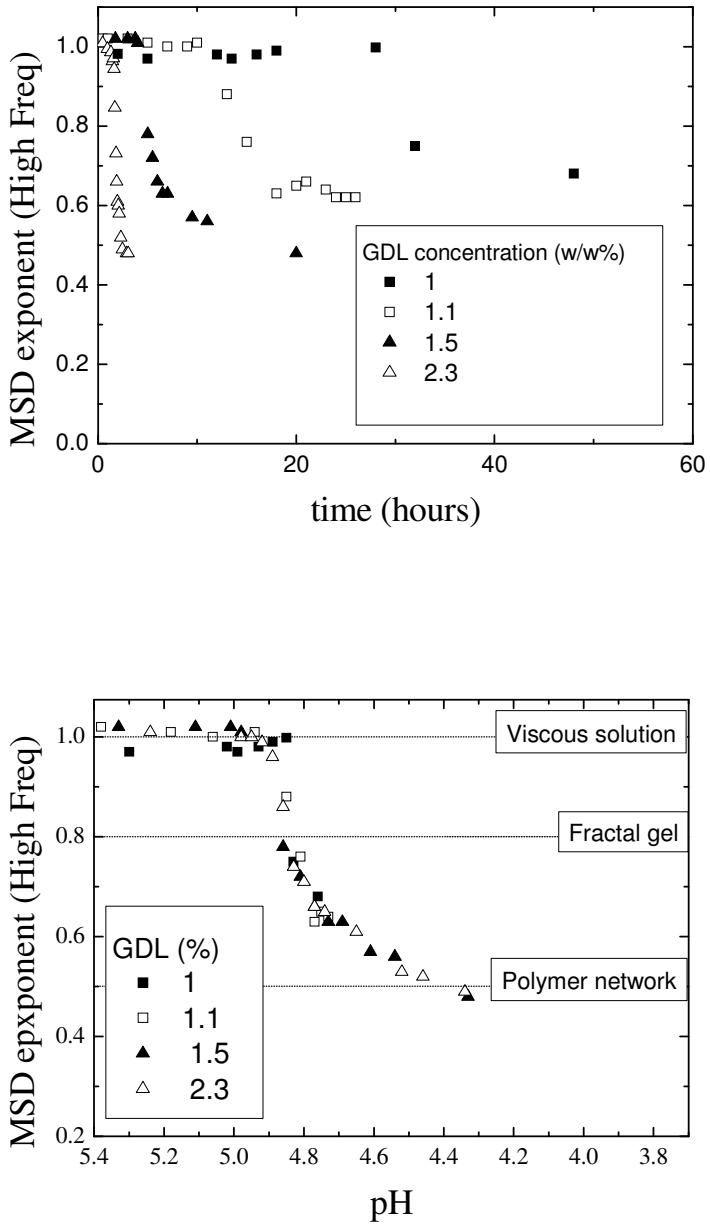

Figure 2(a): High frequency exponent revealed by the slope of double logarithmic MSD versus lag time plot, as a function of time during acidification (carried out at different rates as a consequence of different GDL concentrations) and (b) the data mapped onto pH instead of time, using the varying rates of GDL hydrolysis

By adjusting the concentration of added GDL it was possible to obtain a stable weakly gelled system that exhibited an exponent close to 0.7 at high frequency, as has been found previously (Mezzenga *et al.*, 2005), and attributed to

the percolation of a fractal network. However, in order to achieve this result the terminal pH in this system had to be such that the micelles were just able to interact and percolate *without* their significant disruption. In general when the pH continued to decrease below this value (around 4.8) the slope in the logarithmic MSD plot continued evolving and ultimately achieved a value of around 0.4-0.5; indicating that while the physics of the colloidal fractal network is captured at the point of percolation further evolution of the micellar structure results in a structure that perhaps is more suggestive of the mechanical properties being dominated by a continuous flexible polymer network. While the detailed analysis is complicated by the fact that it is the scatterers themselves that are losing their integrity it is clear at least that, at this temperature, the widely described 0.7 exponent is, in general, fleeting and reports the contact of largely intact micelles beginning to interact, while further changes reflect the loss of micelle integrity. It is possible that in previous work (Donato *et al.*, 2007) such a regime has been more prevalent owing to the fact that many of the prior studies where carried out at 30 °C; where the micelle is known to retain more integrity to lower pH values (Lucey *et al.*, 1997).

In order to achieve a high enough pH in the system at 20 °C so as to capture the fractal regime it was necessary to use a GDL concentration that meant that the actual time-course of acidification was extremely slow; on the order of 48 hours. Using other GDL concentrations ensured different end pH values but also generated different rates of acidification. Nevertheless, when the data were mapped onto a plot showing the slope of the logarithmic MSD plot versus pH, all experiments fell onto the same curve; within experimental uncertainties, as shown in Figure 2 (b). This clearly indicates that our hypothesis is not complicated by kinetic issues and that the same percolated fractal structure (indicated by the 0.7 signature) is reached transiently by systems acidified at all rates used in this study - if the pH is held at around 4.8 then this state persists, but on reducing it further changes to the structure of the micelles are facilitated, and accordingly the high-frequency mechanical properties are modified.

3.2 Addition of pectin

It has previously been clearly shown in systems containing low micelle concentrations compared to those reported here that upon the reduction of pH to around 5, in the presence of the anionic plant polysaccharide pectin, polymers with certain fine structures are able to interact with casein micelles, and that such an adsorption can help to stabilise acidified milk against precipitation of the micelles upon subsequent reduction of pH (Nakamura *et al.*, 2006, Tuinier *et al.*, 2002, Kravtchenko *et al.*, 1995).

Here, two highly methylesterified pectins with random distributions of esterified groups and the same high DM (78%), but different molecular weights, were added at a variety of concentrations to the studied acid-milk system, and the behaviour compared with that found when a pectin containing only (randomly distributed) 31% esterification was used. This low DM sample was of similar molecular weight to one of the high DM pectins used, and indeed was generated from the same mother pectin. In addition, two further pectins with the same low DM value were investigated, both with an identical DM but lower molecular weight; one with a random charge distribution and one with a more blockwise intramolecular charge distribution, generated by the action of a processive demethylating enzyme.

Figure 3 (a) and (b) shows the scatterers mean square displacements as a function of lag time, obtained as described previously, by inversion of the correlation functions, recorded at (a) pH 5.10 and (b) pH 4.40; during the acidification with 1.5 %w/w GDL; of 10 %w/w MSNF systems containing 0.1 %w/w of the examined pectin samples. These samples were all homogeneous one-phase at the starting pH.

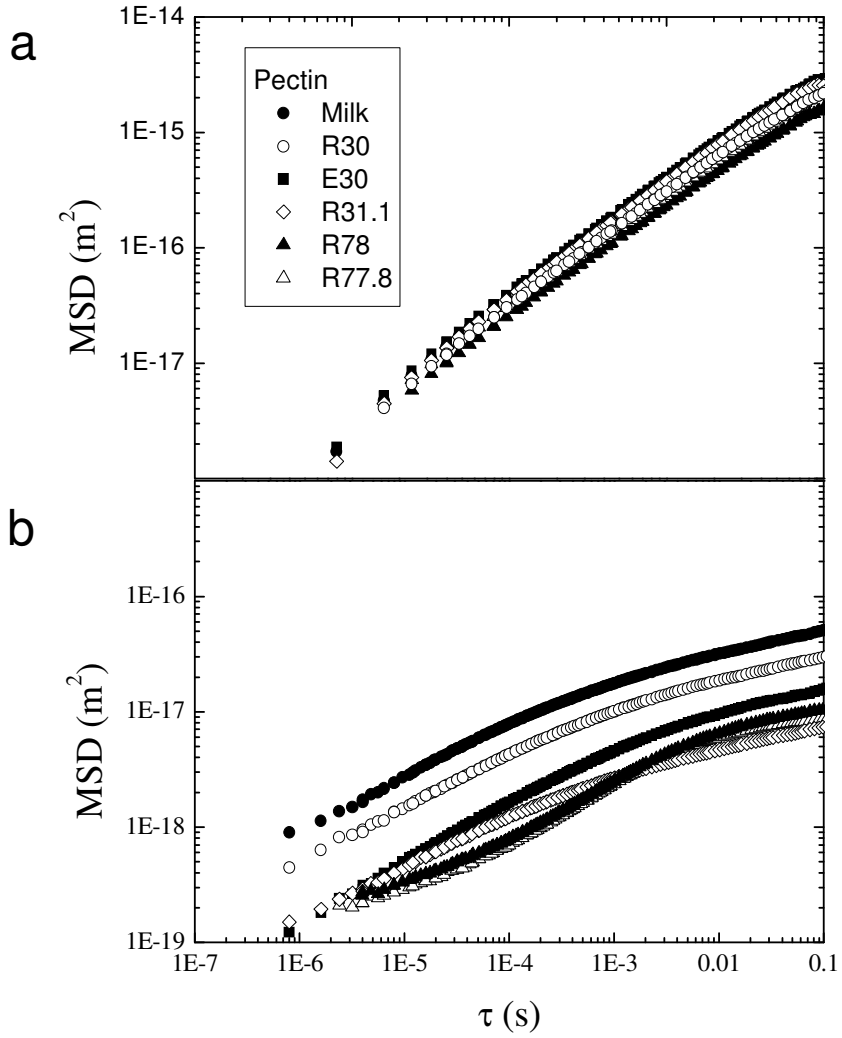

Figure 3: Scatterer mean square displacements as a function of lag time, obtained as described previously, by inversion of the correlation functions, recorded at (a) pH 5.10 and (b) pH 4.40; during the acidification with 1.5 % w/w GDL; of 10% MSNF systems containing 0.1 % w/w of the examined pectin samples

The high DM (78%) pectins both clearly influenced the *shape* of the correlation function after acidification, compared with all the other pectins investigated (including a low DM pectin which was produced from the same mother pectin as one of the 78% samples and had an equivalent molecular weight). We hypothesise then that this change reflects the interaction of this fine structure with the micelles. Exploratory experiments were carried out at 3%

MSNF and indeed only the structures that caused the change of MSD shape in the more concentrated systems studied here were found to stabilise those systems against precipitation upon acidification. For all other samples the MSD versus time followed roughly the same shape as the data recorded during the acid-induced gelation of milk alone. Indeed, taking the high frequency slope of the MSD in a double logarithmic plot and plotting this against pH, the data is indistinguishable (within experimental uncertainties established from three repeat experiments) from the results obtained from milk alone, for all but the 78% samples, as shown in Figure 4.

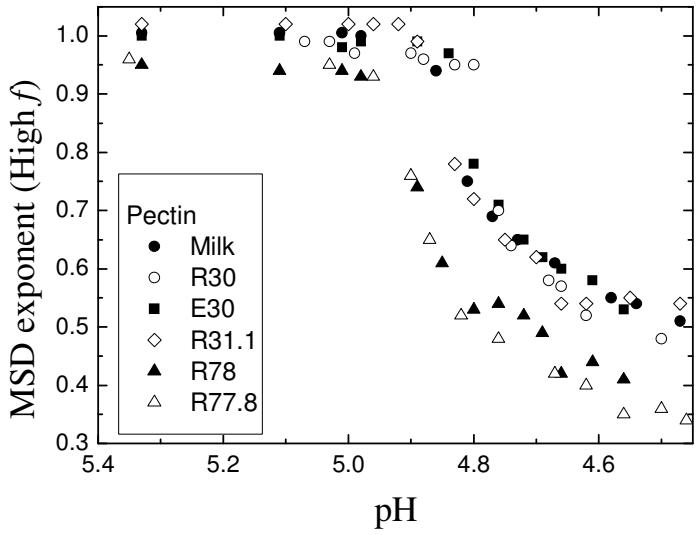

Figure 4: The high frequency exponent revealed by the slope of double logarithmic MSD versus lag time plot, as a function of pH with different pectic polymers added

Figure 4 also shows that for the 78% DM samples, not only is the end slope different in the high frequency region, but additionally an enhanced rate of slowing of the dynamics is observed in time, that persists when the data is mapped onto the variation with pH. Bulk rheological measurements of the gelation of the acidified-milk system with and without 0.1 %w/w 78% DM pectin also demonstrates the rate enhancement in the system with the added pectin, as shown in Figure 5. This suggests that the polymer adsorption, that we suggest is indicated by change of shape of the MSD, also enhances the rate of micellar

aggregation, consistent with the idea of bridging. (Depletion can be ruled out on the basis that; firstly, the adsorption has been shown to be active at pH values above the unperturbed aggregation of the milk so there isn't likely to be significant polymer concentration in solution at the relevant pH, and secondly, that lower DM pectins of the same molecular weight as a DM 78% sample, had no measurable effect). This, in turn, suggests that the surface coverage is incomplete.

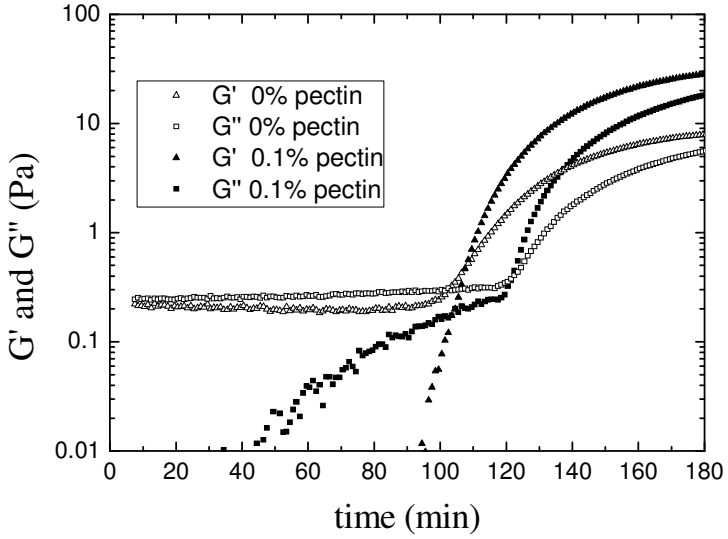

Figure 5: Bulk rheological measurement showing the formation of an acidified milk gel and the repeat experiment in the presence of 0.1 % w/w DM 78 % pectin; i.e. the bulk rheological properties measured at 1 Hz, carried out on the equivalent systems of interest examined by the microrheological analysis.

Taking an approximate radius of 100 nm for a casein micelle and considering a volume fraction of 13 % of casein micelles, we can estimate that one litre of milk contains around $3.1*10^{16}$ casein micelles. The addition of 0.1 %w/w of pectin (R77.8 with a Mw of 120 000 $mol.g^{-1}$) represents therefore around 160 molecules of pectin per micelle or 1 molecule of pectin per $7.8*10^{-16}$ m^2 of the surface of the casein micelle; giving an average pectin molecule an area of around 28 nm by 28 nm of surface to occupy. Since a fully extended pectin molecule is around 350 nm in length and 1 nm diameter, and the most probable conformation has a radius of gyration of the order of 10 nm, the hypothesis of incomplete

coverage certainly seems reasonable. Furthermore, the current estimate of full coverage (Fleer *et al.*, 1993) is 1mg of pectin per m^2 of casein micelle which corresponds to more than twice the pectin concentration used in this study.

In previous work the estimation of the relevant surface coverage of adsorbed polymer has been complicated by the fact that if pectin is added to casein micelles in sufficient concentrations then even prior to acidification depletion flocculation drives the system to phase separate (Einhorn-Stoll *et al.*, 2001). In order to circumvent this problem systems are generally homogenised by shearing devices during acidification (Liu *et al.*, 2006, Kravtchenko *et al.*, 1995) until the evolved visco-elasticity of the system is capable of arresting the demixing (stirred yoghurts). However, in such systems the particulates being stabilised are protein aggregates whose size is determined by the homogenisation process, leaving surface coverage estimates difficult. In addition there is some evidence (Tromp *et al.*, 2004) that suggests that the added polymer has some functionality during this period that does not rely on it being absorbed in the stabilised system (at least not tightly enough that it cannot be removed by centrifugation). In order to avoid the inherent complications in studying such homogenised systems we chose to work at pectin concentrations that were miscible with our chosen micelle concentration. While this limited the concentration range examined it meant that neither demixing nor the role of shear forces had to be considered in the interpretation of the results.

Returning to the fact that the addition of all polysaccharide samples, with the exception of the high DM samples, had a negligible effect on the acidified milk system (Figure 4), we report a crucial observation. It should be noted that on addition of the low DM pectins to the milk systems aggregate / microgel formation was visually apparent in these quiescent systems to varying extents even prior to acidification (being most severe for the PME generated structure).

While it has been clearly demonstrated that the pectin-micelle interaction is largely electrostatic in nature (Pedersen and Jorgensen, 1991, Sejersen *et al.*, 2006), the details of how the polymer charge distribution might influence its adsorption have received relatively scant attention. In the absence of a detailed molecular model of the interaction that could potentially reveal the pectin epitope with the largest binding energy it has tacitly been assumed that unesterified blocks

would fulfil this role more efficiently than those punctuated with methyl groups, although there seems to be minimal experimental evidence of this. It is also worth noting that in terms of the functionality of the adsorbed polymer as a steric barrier the problem is significantly more complex than selection of the polymer with the highest binding, as it is after all the distribution of loops and trains that ultimately generates stabilisation, even if the binding is possibly multilayered. Assuming that the preferential binding epitope is completely unesterified it would seem to be a reasonable hypothesis that indeed a pectin of as high as possible DM interspersed with unesterifed blocks of sufficient length to bind the micelle would provide the idealised fine structure. Unfortunately the value of such a sufficient length is unknown and, although it might possibly be approximated by studying the effect of pectins of very high DM, the only way presently that one might in any case introduce more than the random compliment of a certain blocklength into the chain would be to use enzymatic processing. Such processing may well yield pectins with a greater propensity to bind the micelle but such polymers would also possess a greatly enhanced calcium sensitivity. While a recent study (Harte *et al.*, 2007) has shown that low DM pectins can be gelled with serum extracted from milk at increasing stages of acidification, and hence containing increasing amounts of calcium ions, the possibility of pectins modifying the calcium phosphate equilibrium when present, in an analogous way to EDTA, has not been addressed. In fact we have found in the current study that, even without acidification, calcium induced microgel formation of low DM (or otherwise calcium sensitive) pectins could be observed.

In order to gather further evidence of this phenomena we carried out ^{31}P NMR experiments. High-resolution liquid-state ^{31}P NMR spectroscopy is a non-invasive technique, which has been extensively used to study dairy systems (Belloque and Ramos, 1999). It allows the detection of the resonances from the mobile ^{31}P atoms, such as those of the inorganic phosphorus and the individual phosphoproteins, but not the CCP or the aggregated casein molecules which are not detected due to their low mobility. It is this NMR technique which is used in this work to investigate quantitatively the effects of pectin different fine structures on the inorganic phosphorus and phosphoproteins in milk.

The measured ^{31}P NMR spectra of 10% milk solutions with or without the addition of pectins are reported in figure 6. The spectra show four main peaks, which are assigned in the literature (Belton *et al.*, 1985) as inorganic phosphate (P_i; peak 1), phosphoproteins (SerP; peak 2), glycerophosphoylcoline (Peak 3), glycerophosphorylethanoline (Peak 4). When high DM pectin is added there is no discernable change in the spectrum while with the addition of the low DM sample, the P_i peak increases noticeably, and is slightly shifted. This behaviour is entirely consistent with that observed on the addition of EDTA (Hemar *et al.*, 2008) and is an indication that the low DM pectin indeed removes calcium from the micelle.

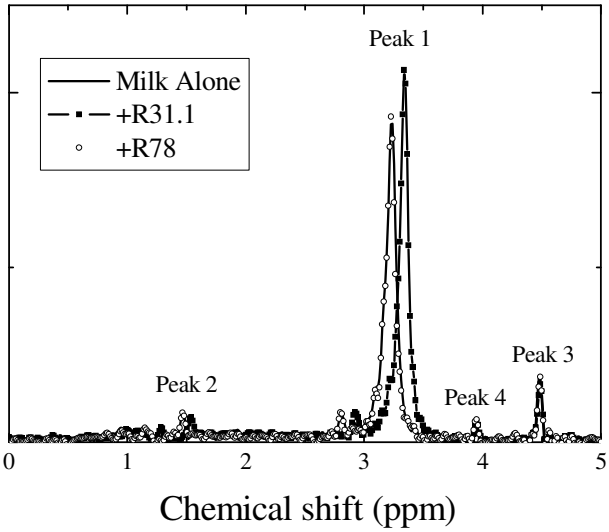

Figure 6: ^{31}P NMR spectra of 10% milk solutions, and with the addition of high (77.8) and low (31.1) DM pectin samples.

To summarise, we suggest our results can be explained in the following way: The ineffective lower DM fine structures (regardless of molecular weights and intramolecular distribution), interact with, and even enhance the concentration of, serum calcium (through the dissociation of the colloidal calcium phosphate present inside the casein micelle), effectively precipitating a substantial fraction of them. Potentially functional residual chains may bind the micelles but at a largely diminished concentration. Indeed, repeat experiments carried out using a reduced amount of even the effective 78% DM polymer, shown in Figure 7, indicate that

any influence on the systems behaviour at this concentration of micelles is negligible below around 0.025%.

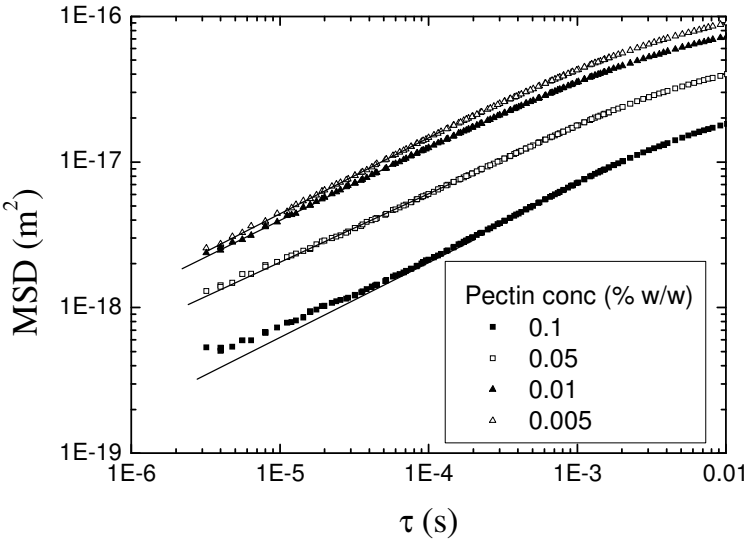

Figure 7: Scatterer mean square displacements as a function of lag time, obtained as described previously, by inversion of the correlation functions, recorded at pH 4.62 as a function of pectin concentration; for high a 78% DM pectin sample and 10% w/w skim milk powder.

In any case, the binding of any residual low DM pectin chains would result in only a small amount of lengthy loops and trains, simply owing to the polymeric fine structure. In contrast, the high DM (random intermolecular distribution) fine structures do not interact significantly with the serum calcium and are more likely to absorb onto the micelles as the pH is reduced below 5. Their limited surface coverage (dictated in this study by the desire to start acidification from a one phase system) leads to efficient bridging which enhances the rate of micelle aggregation and subsequent gelation. While the network appears similar upon visualisation of the resultant milk protein network, as shown in the images displayed in Figure 8, the small amount of absorbed pectin contributes to the high frequency microrheology is a complex manner; providing a change of high frequency slope as a consequence of an observed shape change in the MSD. It is worth noting that similar exponents at high frequency and hints of such a sigmoidal shape have been found previously in studies of colloidal gels embedded

in polymer solutions of varying visco-elasticity (Pashkovski *et al.*, 2003). While these previous studies were carried out at considerably higher polymeric concentrations and focussed on the consideration of how the network and the surrounding medium each contributed to the elastic and viscous components of the system, it could be that in the system studied here the local concentration of the bridging pectin around the micelles is sufficient, even below full coverage, to influence the relaxation modes of the network in a similar manner. It must however be remembered that the colloidal network in our system is itself evolving as the pH is reduced.

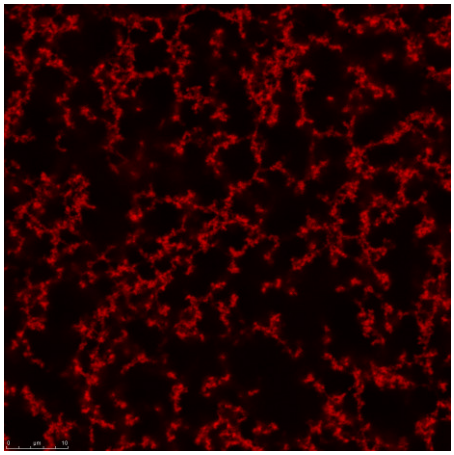

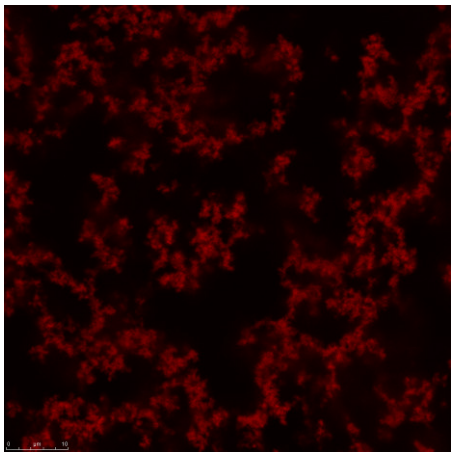

Figure 8: Micrographs showing an acidified milk gel and a gel made in the presence of 0 (figure 8a) and 0.1 % (figure 8b) DM 78 % pectin; i.e. the microstructures pertaining to the systems examined with the bulk rheological measurements in Figure 5.

Thus, for pectic polymers to exhibit in-situ stabilising functionality in acid-milk systems they must be able to adsorb to the micelle surface in a manner providing steric stabilisation upon acidification and be molecularly *available* to do so. For these requirements to be fulfilled at least three factors are crucial: i) at least one micelle binding epitope is available per chain, ii) a significant portion of the chain does not adsorb to the surface of the micelle and iii) the polymer should be sufficiently calcium insensitive not to form microgels pre-acidification. The reasons for the preponderance of high DM and amidated pectins in the industrial stabilisation of acid-milk drinks are then clear. The investigation of whether a more efficient pectin fine structure exists awaits a better molecular model of the adsorption of anionic polysaccharides onto casein micelles that will, among other things, allow the surface coverage to be estimated in a more realistic way, considering the orientation of molecules at the surface. At present all estimates (Tuinier *et al.*, 2002) are order of magnitude estimates based on standard polymer texts (Sejersen *et al.*, 2006).

4 Conclusions

Upon acidification of sufficiently concentrated milk systems a percolated stress -bearing fractal structure, based on associated casein micelles, is transiently established. This state has a high frequency microrheological signature; specifically that the slope of the MSD with lag time follows a power law with an exponent of 0.7; that has been observed in other colloidal systems and discussed theoretically (Mezzenga *et al.*, 2005, Romer *et al.*, 2000). If the pH of this system does not fall significantly below 4.8 then this state is long-lived. However, on reducing the pH further subsequent changes to the structure of the elementary building blocks are facilitated, and accordingly the slope in the logarithmic MSD plot evolves, ultimately achieving a value of around 0.4-0.5; indicating that while the physics of the colloidal fractal network is captured at the point of percolation further evolution of the micellar structure results in a structure in which the mechanical properties are more suggestive of a continuous flexible polymer network.

When pectin was added to such milk systems, at concentrations nominally corresponding to approximately half coverage of the micelles, an interaction of the added anionic polymers with serum calcium was observed visually for all low DM (or otherwise calcium sensitive) pectin fine structures, even without acidification. Further evidence that the appearance of precipitated polysaccharide aggregates was directly linked to interactions with calcium was obtained from phosphorous NMR studies, which clearly showed that changes in the colloidal calcium balance occurred on the addition of such polymers. We hypothesise that this effective precipitation is the reason that the calcium sensitive polymers are found to be ineffectual in interacting with the casein micelles and therefore that the effect of fine structure on the polysaccharide-protein interaction *per-se* is not accessible in experiments of this type. However, high DM (random intermolecular distribution) fine structures do not interact significantly with the serum calcium and absorb onto casein micelles as the pH is reduced below 5. At low casein micelles concentrations such adsorption generates steric stabilisation of the micelles, as the κ–casein brush collapses, and protects the system against precipitation. At higher casein micelles concentrations, but still in thermodynamically compatible systems, the limited surface coverage of the high DM pectins leads to efficient bridging which enhances the rate of micelle aggregation and subsequent gelation, and produces clear signatures in the shape of the measured MSD.

Acknowledgement

The authors acknowledge the financial support from the MacDiarmid Institute (New Zealand) for the PhD scholarship of R.R. Vincent and from Fonterra and FRST for the PhD scholarship of A Cucheval. The authors would also like to thank the Manawatu microscopy centre, in particular Dr Dmitry Sokolov, for his assistance with the confocal microscopy. Dr PJB Edwards is thanked for assistance with the NMR.

References

Alexander M., Dalgleish D.G. (2004) Application of transmission diffusing wave spectroscopy to the study of gelation of milk by acidification and rennet. *Colloids and Surfaces B: Biointerfaces* **38**:83-90

Alexander M., Piska I., Dalgleish D.G. (2008) Investigation of particle dynamics in gels involving casein micelles: A diffusing wave spectroscopy and rheology approach. *Food Hydrocolloids* **22**:1124-1134

Arltoft D., Madsen F., Ipsen R. (2007) Screening of probes for specific localisation of polysaccharides. *Food Hydrocolloids* **21**:1062-1071

Belloque, J., Ramos, M. (1999) Application of NMR spectroscopy to milk and dairy products. *Trends in Food Science & Technology* **10**:447-454

Belton P.S., Lyster R.L.J., Richards C.P. (1985) The 31P nuclear magnetic raisonnance spectrum of cows' milk. *Journal of Dairy Research* **52**:47-54

Boulenguer P., Laurent M.A. (2003) Comparison of the stabilisation mechanism of acid dairy drink (ADD) induced by pectin and soluble soybean polysaccharide (SSP). In: Voragen A.G.J., *et al.* (Eds.). *Advances in pectin and pectinase research*, Dordrecht: Kluwer Academic Publishers, 467-480

De Kruif C.G., Zhulina E.B. (1996) Kappa-casein as a polyelectrolyte brush on the surface of casein micelles. *Colloids and Surfaces A: Physicochemical and Engineering Aspects* **117**:151-159

Donato L., Alexander M., Dalgleish D.G. (2007) Acid gelation in heated and unheated milks: interactions between serum protein complexes and the surfaces of casein micelles. *Journal of Agricultural and Food Chemistry* **55**:4160-4168

Einhorn-Stoll U., Salazar T., Jaafar B., Kunzek H. (2001) Thermodynamic compatibility of sodium caseinate with different pectins. Influence of the milieu conditions and pectin modifications. *Die Nahrung* **45**:332-337

Fagan C.C., O'Donell C.P., Cullen P.J., Brennan C.S. (2006) The effect of dietary fibre inclusion on milk coagulation kinetics. *Journal of Food Engineering* **77**:261-268

Fleer G.J., Cohen Stuart M.A., Schetjems J.M.H.M., Cosgrove T., Vincent B. (1993) In Polymers *at Interfaces*, London: Chapman&Hall

Harte F.M., Montes C., Adams M., San Martin-Gonzalez M.F. (2007) Solubilised micellar calcium induced low methoxyl-pectin aggregation during milk acidification. *Journal of Dairy Science* **90**:2705-2709

Hemar Y., Singh H., Horne D.S. (2004) Determination of early stages of rennet-induced aggregation of casein micelles by diffusing wave spectroscopy and rheological measurements. *Current Applied Physics **4**:362-365*

Hemar Y., Pinder D.N. (2006) DWS microrheology of a linear polysaccharide. *Biomacromolecules* **7**:674-676

Hemar Y., Niere J., McKinnon I., Augustin, M.A. (2008) Manuscript in Preparation

Jeurnink T.J.M., De Kruif K.G. (1993) Changes in milk on heating: Viscosity measurements. *Journal of Dairy Research* **60**:139-150

Kaláb M., Allan-Wojtas P., Phipps-Todd B.E. (1983) Development of microstructure in set-style non fat yoghurt - A review. *Food Microstrusture* **2**:51-66

Kravtchenko T.P., Parker A., Trespoey A. (1995) Colloidal stability and sedimentation of pectin-stabilized acid milk drinks. In: Dickinson E and Lorient D (Eds.). *Food macromolecules and colloids*, Cambridge: Royal Society of Chemistry, 345-351

Laurent M.A., Boulenguer P. (2003) Stabilization mechanism of acid dairy drinks (ADD) induced by pectin. *Food hydrocolloids* **17**:445-454

Liu J.R., Nakamura A., Corredig M. (2006) Addition of pectin and soy soluble polysaccharide affects the particle size distribution of casein suspensions prepared from acidified skim milk. *Journal of Agricultural and Food Chemistry* **54**:6241-6246

Lucey J.A., van Vliet T., Grolle K., Geurts T., Walstra P. (1997) Properties of acid casein gels made by acidification with glucono-delta-lactone. 2. Syneresis, permeability and microstructural properties. *International Dairy Journal* **7**:389-397

Lucey J.A., Singh H. (1998) Formation and physical properties of acid milk gels: a review. *Food Research International* **30**:529-542

Matia-Merino L., Lau K., Dickinson E. (2004) Effects of low-methoxyl amidated pectin and ionic calcium on rheology and microstructure of acid-induced sodium caseinate gels. *Food hydrocolloids* **18**:271-281

Matia-Merino L., Singh H. (2007) Acid-induced gelation of milk protein concentrates with added pectin: Effect of casein micelle dissociation. *Food Hydrocolloids* **21**:765-775

Maroziene A., de Kruif C.G. (2000) Interaction of pectin and casein micelles. *Food hydrocolloids* **14**:391-394

Mezzenga T., Schurtenberger P., Burbidge A., Michel M. (2005) Understanding food as soft materials. *Nature Material* **4**:729-749

Nakamura A., Yoshida R., Maeda H., Corredig M. (2006) The stabilizing behaviour of soybean soluble polysaccharide and pectin in acidified milk beverages. *International Dairy Journal* **16**:361-369

Pashkovski E.E., Masters J.G., Mehreteab A. (2003) Viscoelastic Scaling of Colloidal Gels in Polymer Solutions. *Langmuir* **19**:3589-3595

Pedersen H.C.A., Jorgensen B.B. (1991) Influence of pectin on the stability of casein solutions studied in dependence of varying pH and salt concentration. *Food hydrocolloid* **5**:323-328

Pereyra R., Schmidt K.A., Wicker L. (1997) Interaction and stabilization of acidified casein dispersions with low and high methoxyl pectins. *Journal of Agricultural and Food chemistry* **45**:3448-3451

Romer S., Scheffold F., Schurtenberger P. (2000) Sol-gel transition of concentrated colloidal suspensions. *Physics Review Letter* **25**:4980-4983

Sejersen M.T., Salomonsen T., Ipsen R., Clark R., Rolin C., Engelsen S.B. (2006) Zeta potential of pectin-stabilised casein aggregates in acidified milk drinks. *International Dairy Journal* **17**:302-307

Schurtenberger P., Stradner A., Romer S., Urban C., Scheffold F. (2001) Aggregation and Gel Formation in Biopolymer Solutions. CHIMIA *Journal International for Chemistry* **55**:155-159

Tromp R.H., De Kruif C.G., van Eijk M., Rolin C. (2004) On the mechanism of stabilisation of acidified milk drinks by pectin. *Food hydrocolloids* **18**:565-572

Tuinier R., Rolin C., de Kruif C.G. (2002) Electrosorption of pectin onto casein micelles. *Biomacromolecules* **3**:632-639

Tuinier R, de Kruif C.G. (2002) Stability of casein micelles in milk. *Journal of Chemical Physics* **117**:1290-1295

van Vliet T., Lakemond C.M.M., Visschers R.W. (2004) Rheology and structure of milk protein gels. *Current opinion in colloid & interface science* **9**:298-304

Weitz D.A., Pine D.J., Brown W. (1993) Diffusing-wave spectroscopy. In Brown W. (Eds) *Dynamic Light Scattering: The Method and Some Applications*, Oxford: Oxford University Press, 652-720

Williams M.A.K., Vincent R.R., Pinder D.N., Hemar Y. (2008) Microrheological studies offer insights into polysaccharide gels. *Journal of Non-Newtonian Fluid Mechanics* **149**:63-70

Willats W.G.T., Knox P., Mikkelsen J.D. (2006) Pectin: new insights into an old polymer are starting to gel. *Trends in Food Science and Technologies*. **17**:97-104

Chapter 4

Multiple Particle Tracking investigations of acid milk gels using added tracer particles with designed surface chemistries; and comparisons with diffusing wave spectroscopy studies

As submitted to *Langmuir*

A. Cucheval, R. R. Vincent, Y. Hemar, D. Otter, M. A. K. Williams

Abstract

Multiple Particle Tracking (MPT) is used in an attempt to probe the heterogeneity of acid milk gels, with and without added pectin, by following the distribution of the displacement of added tracer beads, during and after gelation, using the Van Hove distribution. Furthermore, the surface chemistry of the latex beads was modified in an attempt to control their location in the system and probe the rheological properties of the protein network and aqueous phase voids independently. In addition, the mean square displacement (MSD) of the casein micelles / casein aggregates obtained by DWS are compared to the ensemble-averaged MSD calculated from the data obtained by tracking the movement of the added tracer particles, with and without a κ-casein coating.

For the κ-casein coated tracer particles, upon acidification and subsequent gel formation, the MSDs obtained by MPT superimpose well with the MSDs obtained by DWS, despite the fact that one is obtained by tracking the movement of the particle network elements themselves, and the other from directly tracking added tracers. This result has important implications; i) it demonstrates that, although the DWS measurement is intrinsically ensemble-averaged, it really gives insight into the dynamics of the colloidal gel network; ii) it confirms that the κ-casein coated probes used in this MPT experiment are well incorporated throughout the gel network (not just at the void / network interface as was seen with bare latex); and hence iii) that at least in gelled systems κ-casein coated latex probes are an excellent probes which reveal the dynamics of the casein network.

Keywords: Acid milk gels, Pectin, Microrheology, MPT, DWS, Surface-modified tracers.

1 Introduction

Casein micelles in milk are sterically stabilized by a hairy layer of κ-casein present at their surface. Milk gels are formed by the destabilisation of this steric barrier resulting in colloidal aggregation and the formation of a network consisting primarily of aggregated casein micelles. Thus, milk gels are made of a three dimensional network of chains and clusters of milk proteins that retain, at a smaller scale, some of the integrity of the particulate micellar form (Kalab *et al.*, 1983). These milk gels form a heterogeneous and complex system. Heterogeneity can exist at two levels: in the presence of a coarse particulate network within which voids of aqueous phase reside, and in the network itself. Acid milk gels have been extensively studied by microscopy (Kalab *et al.*, 1983), bulk rheology (Lucey and Singh, 1998) and more recently by microrheology using Diffusing Wave Spectroscopy (Hemar *et al.*, 2004, Alexander and Dalgleish, 2004, Mezzenga *et al.*, 2005).

Diffusing Wave Spectroscopy (DWS) is a multiple scattering technique which can be applied to concentrated, turbid samples, in order to measure the dynamics of the scattering entities. These dynamics in turn reflect the viscoelasticity of the surrounding medium and thus, microrheological studies of many soft-matter systems have been carried out with DWS using the addition of tracer particles. The main advantage of DWS is that it allows the measurement of mechanical properties at high frequency, which provides insight into the nature of constituent network elements (Weitz *et al.*, 1993). In the case of acid milk gels, the casein micelles and / or protein aggregates themselves provide the required multiple scattering and the addition of tracer particles is unnecessary. While probing the system at high frequency has proved informative (Mezzenga *et al.*, 2005, Cucheval, in press), DWS clearly only obtains information on the ensemble-averaged motion of the scatterers. Therefore it doesn't allow heterogeneity within the protein network to be probed, or perhaps more importantly report any information regarding the local mechanical properties of the aqueous phase within the voids. Certainly by recording the motion of the casein micelles themselves, there are no complications about how to incorporate added probes into the network and it is clear that it is the rheological properties of

the protein network itself that are being investigated, but the state of the probe is not as well known as that of an added inert particle, with the detailed properties of the casein micelles able to change according to environmental conditions such as pH.

Multiple Particle Tracking (MPT) is a complementary microrheological technique in which the Brownian motion of tracer particles added to the sample (usually fluorescent latex beads), is recorded directly in real space, from which information on the rheological properties of the medium can be obtained. As MPT enables the study the distribution of the motion of single probe particles, it does potentially allow information regarding the heterogeneity of systems to be obtained. For example, Moschakis *et al.* (2006) have used Particle Tracking to probe the microrheology of oil in water emulsion containing a non-absorbing polysaccharide and successfully probed the viscosity of polysaccharide rich regions and that of the oil droplet rich phase independently (Moschakis *et al.*, 2006). Polysaccharides such as pectin can be commonly added to milk gel systems and such an approach using MPT might be promising to measure directly how their presence might modify the rheological properties of aqueous phase voids.

Pectin, an anionic polysaccharide extracted from plants, is widely used in the food industry. Pectin is composed of 3 pectic polysaccharides (Willats *et al.*, 2006): homogalacturonan (HG), rhamnogalacturonan I (RGI) and rhamnogalacturonan II (RGII). HG is a linear polymer of (1-4)-linked α-D-galacturonic acid and its methylesterified counterpart. It is the major (~90%) constituent of commercially available pectins. The ratio of uncharged methylesterified residues to the total galacturonic acid content is the degree of methylesterification (DM). In acid milk drinks, low DM pectin is commonly added and assumed to have the functionality of a thickener, while high DM pectin has been primarily described as a stabilizer (Matia-Merino *et al.*, 2004). Pectin can influence acid milk-gel structure through two mechanisms. Firstly, below pH 5.3 pectin absorbs onto casein micelles through electrostatic interactions (Tuinier *et al.*, 2002) and stericly stabilizes the casein micelles (Kravtchenko *et al.*, 1995) replacing the role of κ-casein, which collapses as the pH is reduced further. It has also been suggested that pectin itself can form a weak gel in the voids of the

micellar network (Boulenguer and Laurent, 2003, Tromp *et al.*, 2004). However, while FRAP measurements indeed seem to show reduced pectin mobility in these regions, there are no direct rheological measurements of the properties of this gel, owing to the difficulty of making spatially resolved measurements.

In this paper, Multiple Particle Tracking is used in an attempt to probe the heterogeneity of the acid milk gels, with and without added pectin, by following the distribution of the displacement of added tracer beads, during and after gelation, using the Van Hove distribution (Wong *et al.*, 2004); described in further detail in the experimental section. Furthermore, the surface chemistry of the latex beads was modified in an attempt to control their location in the system (Valentine *et al.*, 2004) and probe the rheological properties of the protein network and the voids independently. In addition, the mean square displacement (MSD) of the casein micelles / casein aggregates obtained by DWS are compared to the ensemble-averaged MSD calculated from the data obtained by tracking the movement of the added tracer particles, with and without a κ-casein coating.

2 Materials and methods

2.1 Acid milk gel preparation

Low heat skim milk powder (NZMP, New Zealand) was used. The milk powder was dispersed in MilliQ water using a magnetic stirrer, to obtain skim milk solutions of the required concentration (20% w/w). Sodium azide (0.02% w/v) was added to the reconstituted skim milk to avoid bacterial growth. Acidification was achieved by the addition of 2.3 wt% of glucono-δ-lactone (GDL) at 20°C. The pH of each sample was measured every 5 minutes during the acidification process. For the preparation of skim milk and pectin mixtures, a 0.2%w/w stock HM pectin (degree of esterification 78%, Fluka Biochemika, Switzerland) solution was made by dissolving the pectin in water using a magnetic stirrer. The two stock solutions were stirred overnight at 4°C to ensure full hydratation. Pectin and skim milk powder solutions were mixed in equal quantities for one hour with a magnetic stirrer before further analysis to obtain a system with a final concentration of 10% w/w milks solids and 0.1% w/w pectin.

Note that for the MPT experiments, 0.04%w/w of fluorescent latex particles (diameter: 465 nm, Fluoresbrite plain YG, Polyscience Inc., Warrington, PA) or there home-coated versions (2.2.1) were added to the sample prior to acidification.

2.2 Modification of the beads surface chemistry

The latex beads used as tracer particles were used either i) without modification; or with coatings of ii) passively absorbed kappa-casein (Sigma Aldrich, Germany) or iii) amine-terminated methoxyl-poly(ethylene glycol) (n=16, Rapp Polymer, Germany), attached using standard carbodiimide coupling chemistry onto carboxylated beads.

2.2.1 Coatings

(ii)To prepare kappa-coated particles, 1.5 mg of κ-casein was added to 1 mL of mother beads suspension (2.64 %w/w); in the range needed for full surface coverage (3.5 to 5mg/m^2) (Leaver and Horne 1997, Anema, 1997). The excess of κ-casein was removed by discarding the supernatant containing the unbound protein after centrifugation of the κ-casein coated latex dispersion at 13 000 g for 10 min. The centrifuged pellet made of the κ-casein coated latex beads, was redispersed in MilliQ water to the original concentration. Using DWS measurements carried out on the bare starting beads and those κ-casein coated, a size increase of around 10 nm radius was found, suggesting that indeed the κ-casein had absorbed to latex beads. This coating was selected in an attempt to produce beads that would mimic micelles and be incorporated in the interior of the particulate network.

(iii) PEG coated particles were prepared following the protocol proposed by Valentine *et al.* (2004). Carboxylated YG beads (Fluoresbrite Carboxyl YG, Polyscience Inc., Warrington, PA) were used as the starting material. N-hydroxysuccinimide (NHS) and 1-[3-(dimethylamino)propyl]-3-ethylcarbodiimide (EDC) were obtained from Sigma Aldrich (St Louis, MO). While post-coupling size measurement by DLS was suggestive of the beads being coated, it was difficult to determine the size increase for the PEG coated beads

with precision; as the length of the attached molecule was much smaller than that of the κ-casein. Therefore, the success of the coating procedure was also tested indirectly by investigating whether the PEG coated latex beads prevent protein (e.g. BSA) phisisorption (Valentine *et al.*, 2004). To do so, 2 mg of BSA (Sigma Aldrich, St Louis, MO) was added to 1 mL of beads (2.64%w/w) that (a) had undergone the PEG coupling procedure and (b) had not. The mixtures were stirred at around 600 rpm using a magnetic stirrer for 2 h and stored overnight. Subsequently the samples were successively centrifuged (3 times, 13 000 g, 10 min), and after each stage the supernatant, containing unbound protein, was extracted and the beads redispersed in MilliQ water. After the third centrifugation, the beads were then resuspended in SDS (2%w/w) and heated at 95C for 5 minutes, in order to break non-specific interaction between the beads and BSA that was adhered to the latex particles. The sample was then centrifuged at 13 000g for 10 min and the supernatant, containing any protein that had been adsorbed to the beads and subsequently been released by SDS, was extracted and analysed by standard methods. In particular, reducing sodium dodecylsulfate - polyacrylamide gel electrophoresis (SDS-PAGE) with Comassie Blue (CB) detection was carried out on the supernatants, according to the method of Laemmli (1970) (Figure 1).

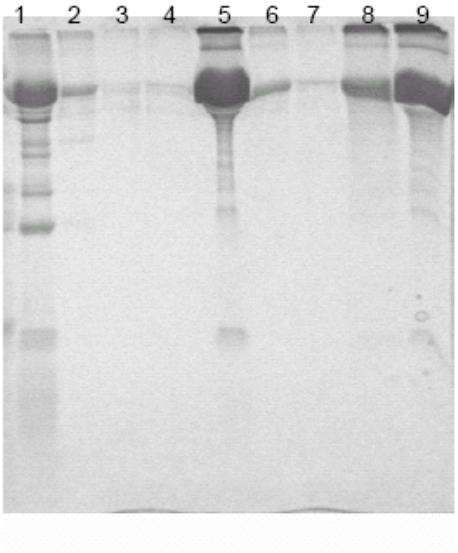

Figure 1: Sodium dodecylsulfate - polyacrylamide gel electrophoresis (SDS-PAGE) with Comassie Blue staining carried out in order to assess the success of the PEG coating of the beads, as described in the text.

The detection of a significant concentration of protein in the supernatant obtained after the SDS treatment for the uncoated beads but not in that obtained from the equivalent beads that had subsequently undergone the PEG coating procedure clearly indicates that the treated particles were indeed well coated and thereby, were able to prevent protein physisorption. This PEG coating was selected in an attempt to produce beads that would have an increased chance of residing in the voids of the colloidal networks.

2.3 Methods

Two methods based on the study of Brownian motion were used to probe the casein and casein / pectin networks. With DWS the casein micelle/ micelle aggregates were the predominant scatterers of light and hence their dynamics was directly studied during the gelation process. In contrast with MPT the motions of added latex beads particles with various surface chemistries were recorded.

2.3.1 DWS

Diffusing wave spectroscopy (DWS) is a light scattering method that is designed to be used with turbid samples, where each photon encounters multiple scattering events between entering the sample cell and being detected. In such systems the photons path can be considered a random walk and, as such, the decay of the autocorrelation function of the scattered light owing to the motion of the scatterers can be calculated from the solution to a well-known diffusion problem (Weitz *et al.*, 1993). Owing to the multiple scattering nature of the technique each individual scattering particle need only move a small amount in order to generate significant de-phasing effects when summed over the entire photon trajectory. Thus DWS can measure motions at high frequency, and the technique has found great utility in studying the motion of tracer particles added to systems to probe their microrheological properties over a broad frequency range. In this work the casein micelles/casein aggregates themselves act as the probes with the evolution of the correlation function during gelation primarily reflecting changes in their dynamics. The measured temporal autocorrelation of intensity fluctuations of the scattered light was measured as:

$$g_1(t) \equiv \frac{1}{\beta}\left(\frac{\langle I(t)I(0)\rangle}{\langle I(0)\rangle^2} - 1\right)^{1/2} \tag{1}$$

where β is a constant, characteristic of the optics, and $I(0)$ and $I(t)$ the intensity of the detected light at the time zero and t. While DWS can be carried out in transmission or backscattering modes, transmission is preferred here owing to the increased simplicity of the boundary conditions: each detected photon has clearly traversed a distance equivalent to the width of the sample cell. Under these conditions the calculated temporal autocorrelation function for the transmitted light can be written as (Weitz *et al.*, 1993):

$$g_1(t) = \frac{\frac{L/l^* + 4/3}{z_0/l^* + 2/3}\left\{\sinh\left[\frac{z_0}{l^*}\sqrt{k_0^2\langle \Delta r^2(\tau)\rangle}\right] + \frac{2}{3}\sqrt{k_0^2\langle \Delta r^2(\tau)\rangle}\cosh\left[\frac{z_0}{l^*}\sqrt{k_0^2\langle \Delta r^2(\tau)\rangle}\right]\right\}}{\left(1 + \frac{8t}{3\tau}\right)\sinh\left[\frac{L}{l^*}\sqrt{k_0^2\langle \Delta r^2(\tau)\rangle}\right] + \frac{4}{3}\sqrt{k_0^2\langle \Delta r^2(\tau)\rangle}\cosh\left[\frac{L}{l^*}\sqrt{k_0^2\langle \Delta r^2(\tau)\rangle}\right]} \tag{2}$$

where l^* is the transport mean free path, z_0 the penetration depth (considered equal at l^* in these experiments), L thickness of the sample (4 mm), $k_o = 2\pi n/\lambda$, the wave

vector of the light and $<\Delta r^2(t)>$ is the mean square displacement (MSD) of the particle. Hence, when l^* is known, the experimentally determined correlation function can lead to the plot of MSD versus lag time, by inverting equation (2) with a zero-crossing routine.

Experimentally, l^* is obtained by performing an experiment on a water sample using latex beads, and fitting l^* using the accepted water viscosity. Subsequently l^* for future samples is obtained by scaling the value obtained for water, based on the change in transmitted intensity when the sample is introduced, compared to the water experiment. It is known that for non-absorbing slabs of thickness L, the transmitted intensity is directly proportional to $(5l^*/ 3L)/(1+ 4l^*/ 3L)$, so that by measuring the change in transmittance, the change in l^* can be calculated.

The experimental set-up used in this study has been fully described elsewhere (Hemar and Pinder, 2006, Williams *et al.*, 2008). Briefly, laser light with a wavelength of 633 nm (35 mW He Ne Melles Griot laser) diffused through the sample, contained in a plastic cuvette of 10 mm width, 50 mm height and 4 mm path length. The transmitted scattered light was collected using a single optical fibre (P1-3223-PC-5, Thorlabs Inc., Germany) and was detected with a photomultiplier tube module (Hamamatsu HC120-08). The auto-correlation analysis was performed using a Malvern 7132 correlator. Tests were run for 3 minutes to ensure low noise intensity autocorrelation functions.

2.3.2 MPT

Trajectories of fluorescent latex beads driven by Brownian motion were recorded using a fluorescence microscope (Olympus OH2) linked to a UP800 CCD camera (Uniqvision, USA). The sample containing 0.04% of fluorescent latex beads was loaded onto a 1cm× 3cm welled microscope slide, with a circular concavity of 1.2-1.3 mm deep, and the objective used was ×100 oil immersion lens. The camera has 1024×772 pixels which allowed recording the motion of beads in a sample area of 102.4 μm × 77.2 μm at a time. Video frames were taken at 45 fps for 20 s. A frame grabber (PCDIG L, Dalsa Coreco, CA) was used to digitize the images and the frames were analysed with tracking software (Image-

Pro Plus, Media-Cybernetics, USA). For each sample, around 30 particle tracks were obtained from at least 300 frames.

The ensemble mean square displacement in two dimensions can be calculated with the following equation:

$$\left\langle \Delta r^2(\tau) \right\rangle = \left\langle \left[r_\alpha(t+\tau) - r_\alpha(t) \right]^2 \right\rangle_{t,\alpha} \quad (3)$$

where the subscript alpha labels the individual particles, and tau, the lag time. The squared displacements are summed over all starting times and all probes. In addition, the probability distribution of particle displacements for a particular time lag can be formed; known as the Van Hove correlation function. The form of this function gives information on the heterogeneity of the system (Wong *et al.*, 2004, Oppong *et al.*, 2006).

2.3.3 Confocal microscopy

A Leica confocal laser scanning microscope (TCS SP5 DM6000B) was used in fluorescence mode with a DPSS 561 laser (excitation wavelength of 561 nm, emission spectrum 565-659 nm) and an oil-immersion objective (×100). The number of pixels per image was 2048×2048. The protein network was dyed with Fast-green prior to acidification by addition of 6µl of dye, from a 0.2 %w/w mother solution, to 1 ml of sample.

3 Results

As mentioned above, MPT has the potential to probe the spatial heterogeneity of the mechanical properties of the system under study; and to follow how this heterogeneity evolves with time, providing, among other things, insights into the kinetics of the gelation. First, the Brownian motions of bare 465 nm fluorescent latex beads added to a sample of milk that was subsequently gelled by acidification were studied.

3.1 MPT carried out in an acid milk gel with uncoated probes

Figure 2 shows the Van Hove correlation function for a lag time of 1s, where the number of occurrences of a particular value of a particles displacement being reached in 1s, is plotted against the displacement. At pH 5.03, the distribution of the beads displacement is approximately Gaussian with large displacements, as is expected for a system that is a homogenous viscous fluid. As the pH decreases further (pH 4.89 and 4.86), the displacement distribution loses its Gaussian shape and appears more like function with two populations manifest as a sharper peak, with broader shoulders, most likely reflecting the presence of at least two populations of probes in the system. The simplest explanation is that the sub-population which has low amplitude motion is probe particles that are entrapped within the forming protein network while the other, large displacement population, represents probe particles that are not yet entrapped in the network. At very low pHs (4.83 & 4), when the acid milk gel has formed, a roughly Gaussian distribution is recovered, corresponding to all probe particles experiencing the identical viscoelastic properties of the gel, with the narrower distribution reflecting the confinement of the tracers within the material.

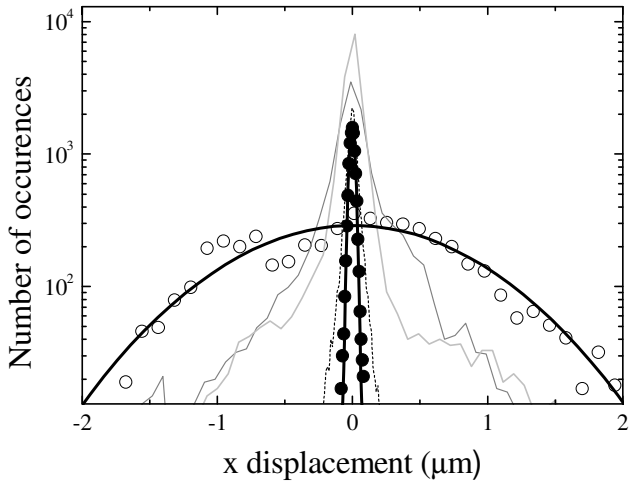

Figure 2: Van Hove distribution of the x-displacement of bare latex tracer particles, at time lag 1s, during acid gelation of milk (10% w/w skim milk powder) at different pHs: 5.03 (○); 4.89 (dark grey line) 4.86, (grey line), 4.83 (dotted line), 4 (●); shown with Gaussian fits to the data at the extreme pHs.

To aid the interpretation and pinpoint the position of the probe particles relative to the protein micellar network, laser scanning confocal microscopy was carried out so that in contrast to our tracking systems, that only observes the florescent tracers, the protein network can be visualised simultaneously, and in addition something of the variation in 3-D could be obtained. The microscopy observation showed that at low pHs, in the formed acid-milk gels, the added bare latex beads were not integrated in the interior of the protein network, nor observed in the voids of the particulate network, but instead all appeared located at the void / protein-network interface (Figure 3). It is possible that these probe particles are driven to the void / protein network interface through a combination of effects. Firstly, the latex beads will be attracted to the void / protein-network interface to a degree through hydrophobic interactions, since the latex particles used are slightly hydrophobic. Secondly it is possible that depletion forces are active, owing to some solubilised proteins being present in the serum, or lastly that that the absorption of the particles at the interface minimizes the interfacial tension in a Pickering type mechanism. These microscopic observations clearly have consequences for the measurement of the micro-rheological behaviour of the system at low pH by MPT, as the recorded dynamics reflect the mobility of the tracers *at the interface* of the void / protein network.

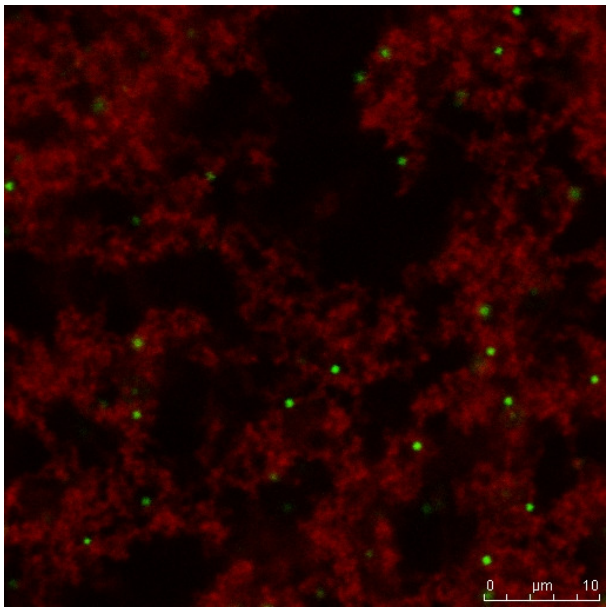

Figure 3: Confocal micrograph of an acid milk gel (10% w/w skim milk protein, 2.3% GDL). The image was captured at the end of the gelation process, as described in the text.

3.2 MPT carried out in an acid milk gel with κ-casein coated probes

Surface modification of the probe particles was performed in an attempt to direct them to be either fully entrapped in the protein network, or, present in the voids, allowing microrheological measurements of these two regions of the acidified milk gels. First, the same acidified-milk-gel system as described in section 3.1 was investigated, once again by MPT, but this time using *κ-casein coated* latex beads.

Figure 4 shows a confocal micrograph of the fully formed acid milk gel containing the κ-casein coated latex beads (0.04% w/w). Contrary to the non-coated beads (Figure 3), the coated latex beads here seem to be more uniformly entrapped in the network. This can be more clearly seen through 3D confocal microscopy imaging (result not shown).

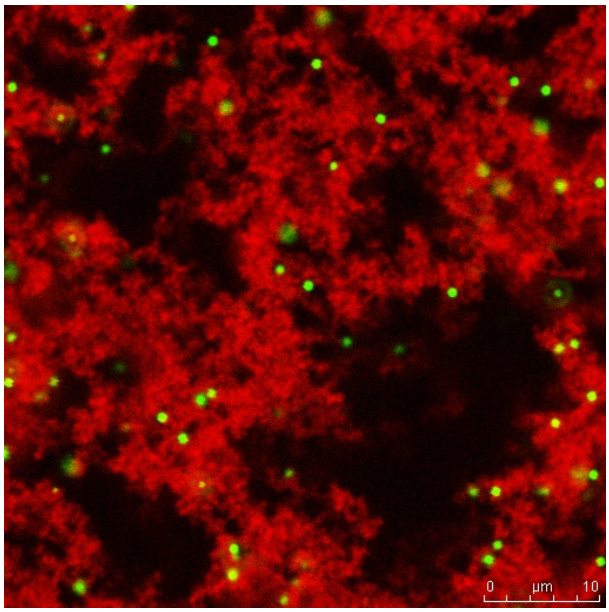

Figure 4: Confocal micrograph of an acid milk gel (10% w/w skim milk protein, 2.3% GDL) with κcasein coated latex beads. The image was captured at the end of the gelation process, as described in the text.

As the latex beads coated by κ- casein are more entrapped within the protein network than their unmodified counterparts, it is possible to assert that the measured microrheological properties should relate more closely to the casein

network. Figure 5 shows the Van Hove distributions, again for the time lag of 1s, probed with κ-casein coated beads. At pH 5.03, the particles displacement distribution is broad and close to Gaussian, confirming a homogenous and viscous system as previously observed when uncoated beads were used (Figure 2). However, as the pH is lowered during gelation, at pH 4.82 and pH 4.89, the distributions show shoulders to a considerably less extent, compared to the case of non-coated latex beads, where different populations of probe particles were clearly observed during the acidification process. This is further evidence that the κ-casein coated beads are homogeneously and fully entrapped within the growing network, as implied by the confocal microscopy. Furthermore at these intermediate pHs, the width at half height of the distribution is considerably narrower than at pH 5.03, indicating that the motion of the probe beads is restricted as the protein network forms, as expected. At pH 4.80, the Gaussian Van Hove distribution become narrower still as the latex bead motions are further restricted. The Gaussian shape of the Van Hove distributions observed at all the different pHs, indicates that at their scale the latex beads actually probe a mechanically homogenous protein network.

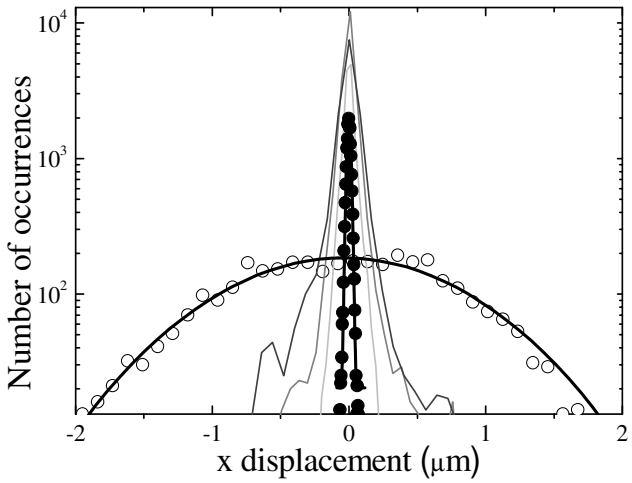

Figure 5: Van Hove distribution of the x-displacement of κcasein coated latex tracer particles, at time lag 1s, during acid gelation of milk (10% w/w skilm milk powder) at different pHs: 5.03 (○); 4.89 (dark grey line) 4.82 (grey line), 4.80 (light grey line), 4.63 (●); shown with Gaussian fits to the data at the extreme pHs.

3.3 Comparison of the MPT measured ensemble-MSDs for bare and κ-casein coated probes

In addition to the differences observed in the confocal micrographs and the Van Hove correlation functions for the system containing κ-casein coated particles versus bare latex; the ensemble mean square displacements of the tracked particles was also calculated directly at all time lags, according to equation 3. These mean square displacements (MSDs) obtained by MPT measurements on a 10 wt% skim milk undergoing acid gelation, and containing κ-casein coated latex beads or non-coated latex particles are reported in Figure 6.

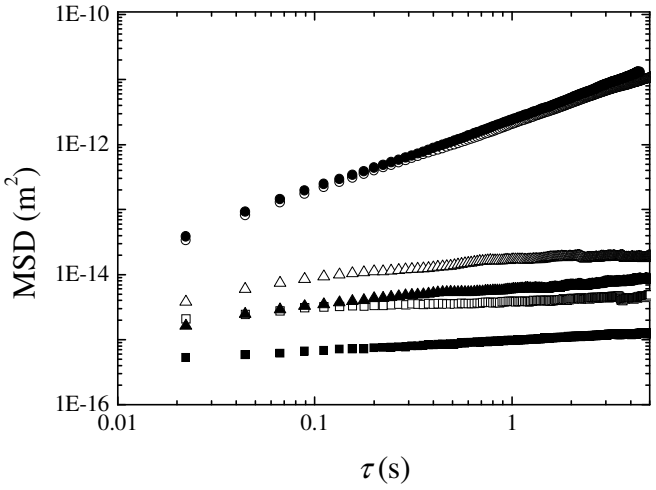

Figure 6: Comparison of the ensemble-averaged MSDs obtained from the κ-casein coated beads (filled symbols) and naked latex probes (unfilled symbols) for the same acid milk gel sample: pH 5.03 (circles); pH 4.80 (triangles); pH 4.63 (squares).

At pH 5.03, prior to network assembly, the MSD displacements of the coated and uncoated beads have very similar values as expected, with a slope of 1 on a double logarithmic plot, demonstrating that the MSD is proportional to time and the system is a Newtonian fluid. However, at pH 4.8 and below, as gel formation proceeds the MSDs of both sets of particles exhibit a substantially smaller dependence on lag time, in particular at low frequencies, characteristic of a viscoelastic system. For the κ-casein coated beads at this pH and below, it is the

microrheology of the protein network that is being probed as demonstrated above. However, for the uncoated probes, the Van Hove distributions and confocal micrographs have argued that the probes are localized at the void / network interface. Correspondingly the MSD of the bare beads at pH 4.8 is found to be some six times higher than found for the κ-casein coated beads for the same system, indicating increased mobility of the probes at the interface in comparison with those embedded in the particulate network. The same trend was observed at pH 4.6, but accentuated further. The difference observed in mobilities could be explained by uncoated probes, trapped at the void / network interface, being in more open and weaker traps in which they are still able to exhibit a larger degree of motion.

3.4 MPT carried out in an acid milk gel with PEG coated probes

In an attempt to probe the microrheological behaviour of the acid milk gel voids independently (with a view in particular to applying such a methodology in the presence of polymeric additives) a set of latex beads were coated with PEG (Valentine *et al.*, 2004), which indeed promisingly was shown in the experimental section of the paper to limit protein adsorption from solution. Unfortunately, upon repeating the acidified milk gel experiment described in sections 3.1 and 3.2 with these beads, it was clearly shown by confocal microscopy (Figure 7) that the PEG-coated latex beads still adsorbed at the void / protein network interface. It did not appear that any of these probe particles could be located in the interstitial voids of the particulate network simply by the application of this probe coating. Although this result indicates that spatially resolved microrheological measurements of the void properties wasn't possible, it provides valuable information regarding the incorporation of probe particles into the system and what strategies might prove more successful in the future.

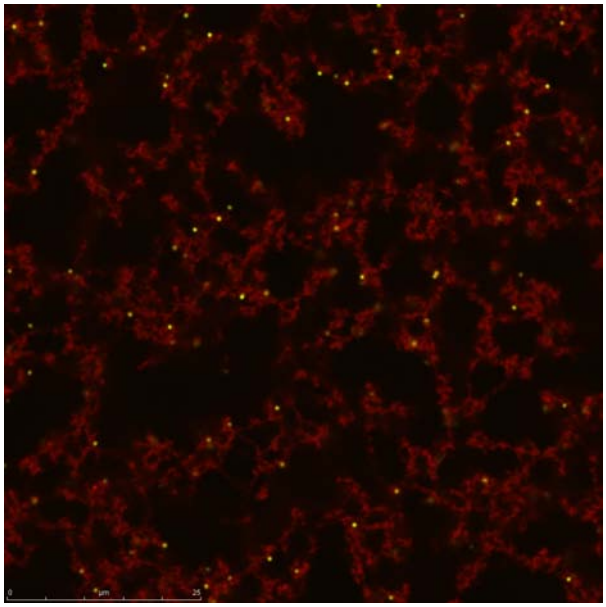

Figure 7: Confocal micrograph of an acid milk gel (10% w/w skim milk protein, 2.3% GDL) containing PEG-coated latex beads. The image was captured at the end of the gelation process.

3.5 Comparison between MPT and DWS methodologies

As stated in the introduction, the use of MPT and DWS in combination presents certain advantages. In particular, DWS allows probing the scatterers dynamics at short times, typically down to (~10^{-6}), while MPT allows probing the spatial heterogeneity of the system, albeit at longer times (>0.01s). Interestingly, in the system at hand, MPT monitors the motion of *added fluorescent probe particles*, while DWS studies the scattering from the *casein micelles themselves and their aggregates,* in the absence of added particles (which in these experiments would severely complicate interpretation). In figure 8, the MSDs from DWS (open symbols) and MPT (solid symbols) measurements performed on acidified milk gels are compared, using the κ-casein coated latex particles as probes in the MPT experiment. The data are presented at three characteristic pH values; pH 5.03, prior to gelation, and pH 4.80 and pH 4.63, at and below the onset of gelation.

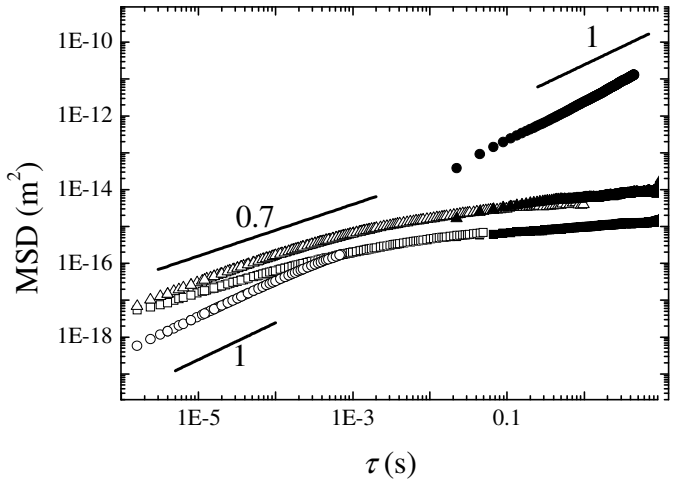

Figure 8: The MSDs obtained by MPT with κ–casein coated latex beads (filled symbols) compared with DWS results (unfilled symbol), obtained on the same acid milk gel before and after gelation, at different pH values pH 5.03 (circles), pH 4.80 (triangles), pH 4.63 (squares).

It can clearly be seen that for the initial milk samples the same exponent in the MSD (MSD~t^1) is found with both techniques, as expected for a Newtonian fluid. However, even upon acidification and subsequent gel formation it is extremely interesting to note that the MSDs obtained by MPT superpose well with the MSDs obtained by DWS, as confirmed by the data where overlap in timescales exists; despite the fact that one is obtained by tracking the movement of the particle network elements themselves, and the other from directly tracking added tracers. This result has important implications; i) it demonstrates that, although the DWS measurement is intrinsically ensemble- averaged, it really gives insight into the dynamics of the colloidal gel network; ii) it confirms that the κ-casein coated probes used in this MPT experiment are well incorporated throughout the gel network (not just at the void / network interface as was seen with bare latex); and hence iii) that at least in gelled systems κ-casein coated latex probes are an excellent dynamical model of the existing casein aggregates.

It is noteworthy that the MSDs for the acidified milk gel at the percolation point, obtained by the combination of DWS and MPT, are typical of that of colloidal gels (Mezzenga *et al.*, 2005, Cucheval, in press). In particular, at pH 4.8,

MSD ~$t^{0.7}$ at very short times and at long time, a "plateau" is observed, characteristic of gel formation.

3.6 Effect of pectin on the casein network

As reported, to-date finding a probe surface coating that ensures the probe particles are localized in the voids of the acid-milk-gel protein network has proved elusive, and as such obtaining unique microrheological information on void aqueous phase mechanical properties has not been possible. Nevertheless, finally, the effect of high methoxyl pectin addition on the microrheological behaviour of acid milk gels is investigated by MPT, using the κ–casein coated beads. Figure 9 shows the Van Hove distribution, for the time lag of 1s, for a system made of acidified 10 wt% skim milk containing 0.1 wt% pectin, prepared as described in detail in the experimental section. Compared to skim milk without pectin addition, at pH 5.00 the beads displacement distribution is slightly less broad in presence of pectin. This is due to the increase in viscosity of the system, and to the adsorption of the pectin to the latex particle through pectin / κ–casein electrostatic interaction, resulting in the decrease in the probe particle motion. (Indeed, microscopy showed, that κ-casein coated latex in higher concentrations of pectin (0.4%) do aggregate due to these pectin-κ-casein interactions – *Manuscript in Preparation*).

As the pH is reduced below 4.93 the Van Hove distributions remain close to Gaussian, indicating that similarly to the acidified milk without pectin, the particles probe a homogenous system. In the presence of pectin, restrictions to the beads motions occurred at slightly higher pH values than those measured for the milk without pectin, in agreement with a previous study by bulk rheology and DWS on the acid gelation of milk containing pectins, which suggested at these low concentrations a major effect of the addition of pectin is in increasing the rate of gelation (Cucheval, in press).

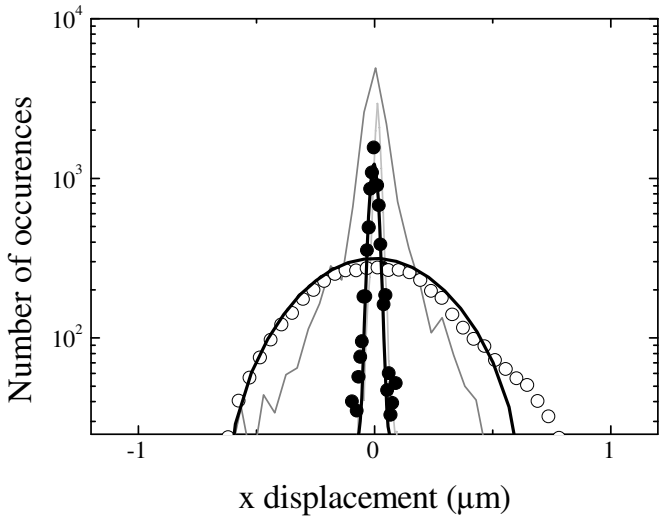

Figure 9: Van Hove distribution of the x-displacement of κcasein coated latex tracer particles, at time lag 1s, during acid gelation of milk (10% w/w skilm milk powder), in presence of pectin (0.1%), at different pHs: 5.00 (○); 4.93 (dark grey line) 4.89 (light grey line), 4 ●); shown with Gaussian fits to the data at the extreme pHs.

Finally, the ensemble averaged MSDs of the κ-casein coated latex particles obtained from equation 3, for all lag times, are shown in figure 10 for acid milk gels with and without pectin addition. Before gelation, as observed with the Van Hove function correlation, the MSD of the probes in the system with pectin is slightly lower than in the milk sample, due as mentioned above to the increase in viscosity and to the adsorption of pectin to the κ-casein coated latex particle. Below pH 4.8, the MSDs of both samples are similar within the experimental uncertainties, since, at these concentrations, the structure and the dynamics of the acidified milk gel with pectin present and absent are expected to be similar (Cucheval, in press).

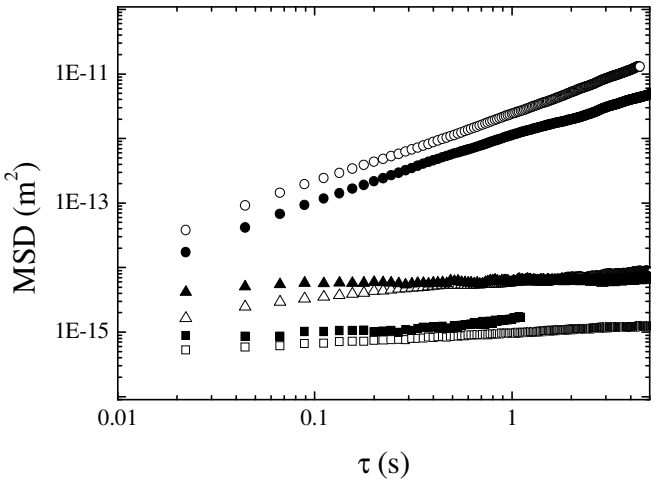

Figure 10: Comparison of the MSDs obtained with κcasein coated latex probe particles, in presence (filled symbol) and absence (unfilled symbol) of 0.1% w/w pectin, for the same acid milk gel sample at different pH values pH 5.03 (circles), pH 4.80 (triangles), pH 4.63 (squares).

4 Conclusions

Multiple Particle Tracking has been used to probe acid milk gels, formed with and without the addition of the polysaccharide pectin, by following the distribution of the displacement of added tracer beads, during and after gelation, using the Van Hove distribution (Wong *et al.*, 2004) and the ensemble-averaged MSD; which was compared with results from DWS. Furthermore, the surface chemistry of the latex beads was modified in an attempt to control their location in the system. The success of the application of these coatings was experimentally validated.

Firstly, a κ-casein coating was selected in an attempt to produce beads that would mimic micelles and be incorporated in the interior of the colloidal proteinaceous network. The study of Van Hove distributions, confocal micrographs and tracer MSDs showed that indeed, in contrast to uncoated probes, which were found to be localized at the void / particulate network interface, these κ-casein coated tracer particles were embedded in the network and reported directly on its microrheology.

Secondly, a PEG coating was selected in an attempt to produce beads that would have an increased chance of residing in the voids of the colloidal network. Unfortunately, it did not appear that any of these probe particles were located in the interstitial voids of the particulate network simply by the application of this probe coating; they were instead localized at the void / network interface, as the uncoated beads.

For the κ-casein coated tracer particles upon acidification and subsequent gel formation, the MSDs obtained by MPT superimpose well with the MSDs obtained by DWS, despite the fact that one is obtained by tracking the movement of the particle network elements themselves, and the other from directly tracking added tracers. This result has important implications; i) it demonstrates that, although the DWS measurement is intrinsically ensemble-averaged, it really gives insight into the dynamics of the colloidal gel network; ii) it confirms that the κ-casein coated probes used in this MPT experiment are well incorporated throughout the gel network (not just at the void / network interface as was seen with bare latex); and hence iii) that at least in gelled systems κ-casein coated latex probes are an excellent probe to reveal the dynamics of the casein network.

Acknowledgments

The authors acknowledge financial support from the MacDiarmid Institute (New Zealand), and from Fonterra and FRST for PhD scholarships of RRV and ASBC respectively. The authors would also like to thank the Manawatu microscopy centre, in particular Dr Dmitry Sokolov, for his assistance with the confocal microscopy, and Medhat Al Ghobashy for his assistance with the polymer adsorption protocol.

References

Alexander M., Dalgleish D.G. (2004) Application of transmission diffusing wave spectroscopy to the study of gelation of milk by acidification and rennet. *Colloids and Surfaces B: Biointerfaces* **38**:83-90

Anema S.G. (1997) The effect of chymosin on [kappa]-casein-coated polystyrene latex particles and bovine casein micelles. *International Dairy Journal* **7**(8-9):553-558

Boulenguer P., Laurent M.A. (2003) Comparison of the stabilisation mechanism of acid dairy drink (ADD) induced by pectin and soluble soybean polysaccharide (SSP). In Voragen A.G.J. et al. (Eds.). *Advances in pectin and pectinase research,* Dordrecht: Kluwer Academic Publishers, 467-480

Cucheval, A.; Vincent, R. R., Hemar, Y.; Otter, D.; Williams, M.A.K. Diffusing Wave Spectroscopy investigations of acid milk gels containing pectin. *Colloid & Polymer Science*, In Press

Hemar Y., Singh H., Horne D.S. (2004) Determination of early stages of rennet- induced aggregation of casein micelles by diffusing wave spectroscopy and rheological measurements. *Current Applied Physics* **4**:362-365

Hemar Y., Pinder D.N. (2006) DWS microrheology of a linear polysaccharide. *Biomacromolecules* **7**:674-676

Kaláb M., Allan-Wojtas P., Phipps-Todd B.E.(1983) Development of microstructure in set-style non fat yoghurt - A review. *Food Microstrusture*. **2**(1):51-66

Kravtchenko T.P., Parker A., Trespoey A. (1995) Colloidal stability and sedimentation of pectin-stabilized acid milk drinks. In E. Dickinson, & D. Lorient (Eds.), *Food macromolecules and colloids* (pp.345-351). Cambridge: Royal Society of Chemistry.

Laemmli U.K. (1970) Cleavage of structural proteins during the assembly of the head of bacteriophage T4. *Nature* **227**(5259):680-685

Leaver J., Horne D.S. (1996) Chymosin-Catalyzed Hydrolysis of Glycosylated and Nonglycosylated Bovine [kappa]-Casein Adsorbed on Latex Particles *Journal of Colloid and Interface Science* **181**(1):220-224

Lucey J.A., Singh H. (1998) Formation and physical properties of acid mlik gels: a review. *Food research international* **30**(7):529-542

Matia-Merino L., Lau K., Dickinson E. (2004) Effects of low-methoxyl amidated pectin and ionic calcium on rheology and microstructure of acid-induced sodium caseinate gels. *Food hydrocolloids* **18**:271-281

Mezzenga T., Schurtenberger P., Burbidge A., Michel M. (2005) Understanding food as soft materials. *Nature Materials* **4**:729-749

Moschakis T., Murray B.S., Dickinson E. (2006) Particle tracking using confocal microscopy to probe the microrheology in a phase-separating emulsion containing nonadsorbing polysaccharide. *Langmuir* **22**:4710-4719

Oppong F.K., Rubatat L., Bailey A.E., Frisken B.J., de Bruyn J.R. (2006) Microrheology and structure of a polymer gel. *Physical Review E* **73**:041405

Tromp R.H., De Kruif C.G., van Eijk M., Rolin C. (2004) On the mechanism of stabilisation of acidified milk drinks by pectin. *Food hydrocolloids* **18**:565-572

Tuinier R., Rolin C., de Kruif C.G. (2002) Electrosorption of pectin onto casein micelles *Biomacromolecules* **3**:632-639

Valentine M.T., Perlman Z.E., Gardel M.L., Shin J.H., Matsudaira P., Mitchison T.J., Weitz D.A. (2004) Colloid surface chemistry critically affects multiple particle tracking measurements of biomaterials. *Biophysical Journal* **86**(6):4004-4014

Weitz D.A., Pine D.J., Brown W. (1993) Diffusing-wave spectroscopy. In Brown W. (Eds) *Dynamic Light Scattering: The Method and Some Applications*, Oxford: Oxford University Press, 652-720

Willats W.G.T., Knox P., Mikkelsen J.D. (2006) Pectin: new insights into an old polymer are starting to gel.. *Trends in Food Science & Technology* **17:** 97-104

Williams M.A.K, Vincent R.R., Pinder D.N., Hemar Y. (2008) Microrheological studies offer insights into polysaccharide gels. *Journal of Non-Newtonian Fluid Mechanics* **149**:63-70

Wong I.Y., Gardel M.L., Reichman D.R., Weeks E.R., Valentine M.T., Bausch A.R. and Weitz D.A. (2004) Anomalous Diffusion Probes Microstructure Dynamics of Entangled F-actin Networks. *Physical Review Letters* **92**:1781

Chapter 5

Direct measurements of interfacial interactions between pectin and κ-casein and implications for the stabilization of calcium-free casein micelle mimics

As submitted to *Journal of colloid and interface science*

A. Cucheval, M. Al-Gobashy, Y. Hemar, D. Otter, M. A. K. Williams

Abstract

Firstly, the effect of the fine structure of the anionic polysaccharide pectin on its interfacial interaction with a κ-casein coated gold surface was investigated, in the pH range 3.5-6.8, by surface plasmon resonance (SPR). The amount of pectin binding onto the κ-casein coated SPR chip was found to be strongly dependant on the pectin fine structure, with the highest SPR signal being observed for pectin with the lowest charge density tested (a degree of methylesterification (DM) around 90%). It is hypothesised that minimising the amount of binding regions available on each pectin chain maximises the amount of possible polymer bound; optimising the efficiency with which the protein-pectin layer can create an entropy rich brush. Secondly, the behaviour of κ-casein-coated latex particles was investigated. These were used in order to provide calcium-free 'model casein micelles'. The Brownian motions of these κ-casein coated particles in pectin solutions were studied using Diffusing Wave Spectroscopy (DWS) and microscopy, and were compared with measurements made on naked latex beads. At every pH value studied (with the exception of 3.5), bridging of the protein-covered probe particles was observed for pectins of both DM 28 and DM 78. However, no aggregated complexes were found in these model casein micelle systems when pectin of an unusually high DM was used, (90%). It was hypothesised that having a limed number of binding regions of a spatially limited extent maximises the number of chains binding to the protein layer, (as found with the SPR measurement), encourages the formation of loops and trains, and additionally limits the potential for destabilisation via bridging.

Keywords: κ-casein, pectin, SPR, DWS, κ-casein coated latex particles, interfacial interaction.

1 Introduction

While the detailed internal structure of the native casein micelle is still a source of controversy to some extent (Horne, 2006), it is well known that κ-casein molecules form an entropy-rich brush at their surface, ensuring the steric stabilisation of these bio-colloids (de Kruif and Zhulina, 1996). The destabilisation of this steric barrier initiates aggregation and depending on the phase volume can cause precipitation or the formation of colloidal-networks consisting primarily of aggregated micelles. Pectin, an anionic polysaccharide extracted from plants is commonly used as a 'stabilizer' in acid milk drinks where it inhibits this precipitation; and as a 'thickener' in other dairy desserts, where it is assumed to form a gel in the serum aqueous phase (Matia-Merino *et al.*, 2004).

Pectin is composed of 3 pectic polysaccharides (Willats *et al.*, 2006): homogalacturonan (HG), rhamnogalacturonan I (RGI) and rhamnogalacturonan II (RGII). HG is a linear polymer of (1-4)-linked α-D-galacturonic acid and its methylesterified counterpart. The ratio of methylesterified galacturonic acid units to the total galacturonic acid content is given by the degree of methylesterification (DM) and determines how the polymer interacts with other molecules. RGI has a backbone consisting of the repeating disaccharide rhamnose-galacturonic acid and carries glycan side chains. RGII has a backbone of (1-4)-linked α-D-galacturonic acid and has many conserved complex sugar side chains. Typical extraction processes modify the in-vivo fine structure of pectin and commercially available samples are routinely found to consist of primarily linear homogalacturonan chains (around 90%).

There is good evidence that in acidified milk systems pectin derives its functionality by absorbing onto casein micelles via electrostatic interactions at pH values less than around 5.3 (Maroziene and de Kruif, 2000), preventing the flocculation that would otherwise be initiated by the pH-induced collapse of the κ-casein layer (Tuinier *et al.*, 2002). In such a scenario, the polysaccharide adsorbs onto the casein micelle via its charged regions, while the other parts of the molecule protrude into solution as loop and tails (Tromp *et al.*, 2004). Knowing more about the details of this interaction might allow pectins with particular DMs and charge distributions to be identified as offering maximal functionality.

In commercial systems, high methoxyl (HM) pectins have empirically been shown to stabilize acid milk drinks more efficiently than those of low DM (Liu *et al.*, 2006, Pereyra *et al.*, 1997). However, the ability of pectin to stabilize a casein micelle dispersion is clearly strongly dependant on its molecular availability, which can be severely compromised by its binding with calcium (Cucheval *et al.*, 2009). Indeed, it has been recently shown that i) the serum calcium liberated in milk systems as they are acidified (Harte *et al.*, 2007) is sufficient to gel low DM pectins; and ii) that simply the presence of low DM pectin in samples of milk at natural pH (6.8) modifies the calcium mineral balance. Susceptible pectin fine structures can then be trapped by calcium and are thus not able to interact with caseins (Cucheval *et al.*, 2009). In other words, the interaction between pectin and the calcium in the serum forbids the direct assessment of the effect of pectin fine structure on the direct interaction of pectin with casein micelles. One of the pathways available to study the interaction in absence of calcium is to use sodium caseinate (Pereyra *et al.*, 1997; Matia-Merino *et al.*, 2004) instead of native micelles. Pereyra *et al.* (1997) compared the efficiency of LM and HM pectin in stabilizing an acidified sodium caseinate dispersion and concluded that, at low pH, higher DM pectins were more effective. However, sodium caseinate exists as small self-assembled protein particles of casein aggregates in equilibrium with free casein molecules (Creamer and Berry, 1975; Chu *et al.*, 1995) and is not found in a form akin to the native casein micelles with a κ-casein layer at its surface.

In this work, the direct interfacial interaction of pectin with κ–casein has been investigated in the absence of calcium. Firstly, the effect of the pectin fine structure on the amount of binding onto a κ-casein layer was studied by surface plasmon resonance (SPR) as a function of pH. κ-casein was covalently attached to the gold surface of an SPR chip by a standard coupling procedure and changes in the resonance angle were monitored while pectin solutions were flowed over the immobilized κ-casein. Three different pectins with distinct degrees of methylesterification (DM 90, 78, 28) were tested. Secondly, we then investigated the interaction of pectin with κ-casein in a system that more closely mimics the casein micelle, but without calcium present. More specifically, κ-casein coated latex particles were used as ‘synthetic casein micelles’ which were mixed into

pectin solutions at low phase volumes. The mean square displacements of the κ-casein coated particles were obtained with Diffusing Wave Spectroscopy (DWS) and compared to those found with naked beads. Additionally, the systems were visualised by microscopy and the results obtained were interpreted within a coherent framework incorporating the results from the SPR study.

2 Materials and methods

2.1 Materials

2.1.1 Control of surface chemistry

Covalent immobilization of κ-casein onto an SPR sensor chip

κ-casein (Sigma, St Louis, USA) was covalently immobilized on the surface of one cell of a CM5 sensor chip by a standard amine coupling procedure (Pharmacia Biosensor, 1994). Such chips contain two cells and are pre-coated by carboxylmethyl dextran. The immobilization reaction involved an amide group of κ-casein, which can be from the N-terminal amino acid or from the side chains of the amino acids lysine, glutamine, aspartame or arginine.

Prior to covalent immobilization, a pH scouting exercise (carried out in acetate buffer 10mM pH 4, 4.5, 5 and 5.5) determined pH 4 as the optimum pH for the immobilization procedure. The dextran surface was first activated with N-hydroxysuccinimide (NHS, Biacore AB) and N-ethyl-N′-(dimethylaminopropyl)-carbodiimide (EDC, Biacore AB) and then κ-casein was flowed over the cell. The binding level was 3000 Resonance Unit (RU). The second cell incorporated on the chip was used as a control, and was activated with the same procedure (NHS and EDC) but subsequently blocked with ethanolamine (Biacore AB). The binding response was calculated by the subtraction of the signal obtained from the sample cell minus that from blocked control cell, in order to correct the response for nonspecific binding. The running buffer used for the immobilization procedure was HBS buffer (10 mM HEPES buffer at pH 7.4 containing 150 mM NaCl, 3

mM EDTA, and 0.005% of the nonionic surfactant polyoxyethylenesorbitan (P20)) (Biacore AB).

Once immobilized on the sensor chip the state of the bound κ-casein was qualitatively compared to that of micellar κ-casein by investigating the action of the enzyme chymosin (a κ-casein cleaving enzyme). Chymosin (at a concentration of 84 Unit, in HEPES buffer pH 6.8 10mM) was flowed, at 25 ºC, over the CM5 chip covered with κ-casein, twice for 540 s at a 1 µl / min, and changes in the baseline were recorded. The availability of the immobilized κ-casein to chymosin provided some insight into the potential effect of the covalent immobilization procedure on the state of the protein itself.

Passive absorption of κ-casein onto the surface of latex beads

Latex beads of diameter 465 nm (2.62% w/v stock solutions) purchased from Polyscience Inc. (Warrington, PA) were used without modification or with a coating of κ-casein (Sigma Aldrich, Germany) produced by passive absorption. More specifically, to create κ-casein coated particles, 1.5 mg of κ-casein was added to 1 mL of the mother beads solution in the range 3.5-5 mg / m^2 needed for full surface coverage (Anema, 1997, Leaver, 1999). The efficiency of the coating was tested by particle size measurements with DWS. The diameter of the treated latex particles increased, by ~20 nm consistent with previous observations.

2.1.2 Sample preparation and interaction study

Pectins with different fine structures were used in this study, the degree of methylesterification, molecular weight and origin of which are reported in Table 1.

For the sample studied by SPR, 0.1% w/w pectin solutions were prepared by stirring overnight at room temperature to insure good dissolution, in 10 mM acetate buffer, at pH 3.5, 4.5 or 5.3 and additionally in HEPES buffer (Sigma, USA) at pH 6.8. The running buffer for the SPR analysis was 10 mM HEPES, pH 7.4 (Sigma, USA). All buffers were filtered and degassed. The temperature was maintained at 25 °C. A large range of pectin concentration (0.001-0.5 %w/w) was tested at pH 4.5 with a high DM pectin (which according to the literature should

present the most favourable conditions for the interaction) in order to determine the most suitable pectin concentration to investigate the effect of pH and pectin fine structure. A pectin concentration of 0.1% w/w was judged optimal in the range tested and was used to study the interaction of pectin with κ–casein using SPR. The experiment was performed with the analyte first being injected (60 s, 10 µl / min), followed by a dissociation phase (30 s) in running buffer and finally a regeneration step (120 s) with glycine pH 2.5 (10 mM). Each experiment was repeated three times, and the mean value recorded (the standard deviation of which was always less than 5%).

	DM / %	**Mw / g.mol^{-1}**	**Origin and treatment**
DM 90	90	31 000	Sigma Aldrich, St Louis, USA
DM 78	78	30 000-100 000	Fluka Biochemica, Switzerland
DM 28	31.1	30 000-100 000	Homemade by alkali deesterification with DM 78 Fluka Biochemica, Switzerland as starting material

Table 1: Characteristics of pectin samples used in this study.

For the sample studied by DWS, 1 or 1.5 % w/w mother pectin solution was prepared by stirring overnight at room temperature to ensure complete dissolution. The pH values of the mother solutions were then adjusted using NaOH (1 and 0.1M) and HCl (1 and 0.1M). Appropriate amounts of pectin and κ-casein coated or bare latex particles were subsequently mixed at ~700 rpm so that the final concentration achieved was 0.8% w/w of latex particles and 0.4 % w/w pectin. The pH was then checked and the sample stored at 20 °C for 30 min before the measurements were taken to allow the temperature to equilibrate.

2.2 Methods

2.2.1 SPR

Surface plasmon resonance is an optical method which allows the visualization of interactions of a flowing analyte with an immobilized ligand in real time. The ligands are bound to a metal surface where surface plasmons (surface electromagnetic waves with a parallel propagation to the metal / solvent interface) are highly sensitive to any change in the refractive index at the metal surface interface which could result, for example, from molecular absorption. While the majority of incident light is totally reflected, an evanescent wave penetrates a distance of the order of one wavelength into the buffer and is able to interact with freely-oscillating electrons at the metal film surface. A photon detector is used to monitor the reflected light intensity as a function of angle, and hence the refractive index of the solution close to the bound ligand.

The SPR analyses were done on a Biacore X100 (Biacore AB, Uppsala, Sweden) with a CM5 sensor chip (Biacore AB, Uppsala, Sweden) which has a gold surface coated with carboxyl methyl dextran. The interaction of κ-casein with pectin was investigated by first immobilizing covalently κ-casein (the ligand) on the sensor chip, as described in section 2.1.1 A pectin sample (the analyte) is then flowed over the κ-casein coated surface in a controlled manner. Any change in the surface properties resulting from the interaction is detected in the reflected light intensity by the photodetector and expressed in resonance units (RU). The change in the resonance angle versus time (the so-called Sensorgramm) gives insight into the interaction of the ligand and analyte, and can be separated into an association and dissociation phase. The surface is regenerated after each interaction analysis with an appropriate solution (glycine, pH 2.5) which doesn't affect the immobilized ligand but strips off all the absorbed species.

2.2.2 DWS

Diffusing Wave Spectroscopy (DWS) is a light scattering method which can be applied to turbid samples. Each photon going through the sample encounters multiple scattering events, such that the photons path can be considered as a

random walk. In this study, the light is scattered by bare latex particles (or κ-casein coated latex beads). The autocorrelation function of the scattered light owing to the motion of the scatters can be calculated from the temporal intensity fluctuation:

$$g_{(1)}(t) \equiv \frac{1}{\beta}\left(\frac{\langle I(t)I(0)\rangle}{\langle I\rangle^2} - 1\right)^{1/2} \quad (1)$$

where β is a constant characteristic of the optical set-up, *I(t)* the intensity of the detected light at the time *t*. DWS has been carried out in transmission mode which allows writing the temporal autocorrelation function as follows (Weitz *et al.*, 1993):

$$g_1(t) = \frac{\frac{L/l^* + 4/3}{z_0/l^* + 2/3}\left\{\sinh\left[\frac{z_0}{l^*}\sqrt{k_0^2\langle\Delta r^2(\tau)\rangle}\right] + \frac{2}{3}\sqrt{k_0^2\langle\Delta r^2(\tau)\rangle}\cosh\left[\frac{z_0}{l^*}\sqrt{k_0^2\langle\Delta r^2(\tau)\rangle}\right]\right\}}{\left(1+\frac{8t}{3\tau}\right)\sinh\left[\frac{L}{l^*}\sqrt{k_0^2\langle\Delta r^2(\tau)\rangle}\right] + \frac{4}{3}\sqrt{k_0^2\langle\Delta r^2(\tau)\rangle}\cosh\left[\frac{L}{l^*}\sqrt{k_0^2\langle\Delta r^2(\tau)\rangle}\right]} \quad (2)$$

where l^* is the transport mean path, z_0 the penetration depth (considered equal to l^* in these experiments), L is the thickness of the sample (4mm), $k_o = 2\pi n/\lambda$ the wave vector of the light and $\langle\Delta r2\ (t)\rangle$ is the mean square displacement (MSD) of the particle. Hence, when l^* is known, the experimentally determined correlation function can be turned into a plot of MSD versus lag time, by inverting equation 2 with a zero-crossing routine. l^* can be calculated by fitting the autocorrelation for a reference sample of known viscosity (water) with the viscous Stokes-Einstein substitution (Weitz *et al.*, 1993). Subsequently l^* for future samples is obtained by scaling the value obtained for water, based on the change in transmitted intensity when the sample is introduced, compared to the water experiment. It is known that for non-absorbing slabs of thickness L, the transmitted intensity is directly proportional to $(5l^*/3L)/(1+4l^*/3L)$, so that by measuring the change in transmittance, the change in l^* can be calculated.

The experimental set up has been fully described elsewhere (Hemar and Pinder, 2006, Williams *et al.*, 2008). Briefly, a laser light source with a wavelength of 633 nm (35 mW He Ne Melles Griot laser) diffused through the sample, contained in a plastic cuvette of 10 mm width, 50 mm height and 4 mm path length. The transmitted scattered light was collected using a single optical

fibre (P1-3223-PC-5, Thorlabs Inc., Germany) and was detected with a photomultiplier tube module (Hamamatsu HC120-08). The auto-correlation analysis was performed using a Malvern 7132 correlator. Tests were run for 3 minutes to ensure low noise intensity autocorrelation functions. The comparison of the motion of the κ-casein coated particles and the bare particles motion in pectin solutions provided information on interactions between biopolymeric components. Indeed, while the Brownian motion of the particles reflects the rheological properties of the surrounding system for both the bare and coated beads; it is also affected for the coated beads by the interaction between the κ-casein coating and the pectic polymers.

2.2.3 Microscopy

Photomicrographs of the κ-casein coated and bare beads in water or pectin solution were obtained in brightfield using a Leica microscope (Leica Microsystems AG, Wetzler, Germany) using a x60 water-immersion objective.

3 Results and discussion

3.1 Interaction of κ-casein with pectin studied by SPR

3.1.1 State of the immobilized κ-casein on the sensor chip surface

Comparison with the conformation on the casein micelle surface

κ-casein was covalently bound to the carboxylmethyl dextran coating of the gold surface of the sensor chip as previously described. The covalent binding involved at least one amide group of the κ-casein from the N-terminal or an amino acid side chain. Being mindful that covalent binding may not be without repercussions on the orientation of the protein on the surface, and thus its interaction with pectin, we aimed to qualitatively compare the state of κ-casein immobilized on the SPR chip to the same molecule as it is manifest on the surface of a casein micelle. Are

the orientation and the conformation of the protein similar? Looking at the amino acid sequence for κ-casein, the amino acids with amid groups in their side chains (glutamine, lysine, aspartame, and arginine) are mostly grouped in the first 100 amino acids but there are also a few in the region, close to the C terminus, which constitute the "hairy" portion sticking out from the casein micelle. To have more insight into the effect of covalent bonding on the state and conformation of κ-casein, we studied the ability of chymosin to hydrolyse the covalently immobilized κ-casein. Chymosin was flowed, in two successive injections; at pH 6.8 over the κ-casein coated and reference cells. The baseline levels were recorded before the first chymosin injection and after the end of each injection. Figure 1 shows the resonance angle (RU) versus time for the signal from the κ-casein cell, once the reference cell data have been subtracted.

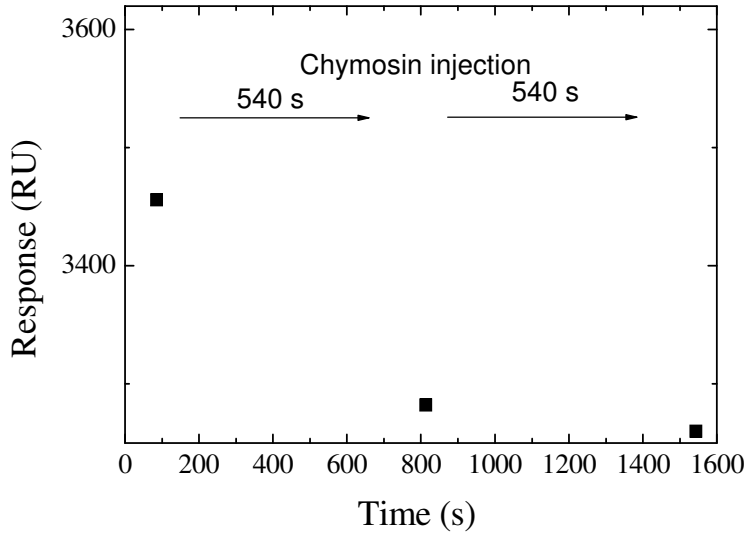

Figure 1: Effect of chymosin on κ-casein immobilized on the SPR chip. Injection of chymosin (84 units) at 1µl/min during 540 s.

The baseline level decreases after each chymosin injection. The enzyme is thus able to interact at least with part of the covalently immobilized protein and to hydrolyse it, reducing the density of polymer in the vicinity of the surface and hence its refractive index. The part of the κ-casein available for hydrolysis was found to be important enough that after the injection of chymosin and regeneration of the surface, the refractive index of the surface had changed. The

decrease of the baseline level was found to be more pronounced following the first injection compared with the second. It seems then, that almost all 'available' κ-casein was hydrolyzed during the first injection. In conclusion, this accessibility of the bound ligand to chymosin is an indication that conformation and orientation of the κ-casein on the sensor chip is likely not significantly different from that found on the surface of the casein micelle.

Effect of pH on the immobilized κ-casein conformation

As the interaction between κ-casein and pectin was studied as a function of pH, the effect of pH on the immobilized ligand itself was first investigated. As reported in the introduction, κ-casein forms a hairy brush layer on the casein micelle surface. Indeed at pH 6.8, it has been reported that the protein protrudes into solution by around 12 nm (Dalgleish *et al.*, 1985); and as expected for a polyelectrolyte, this size has been reported to be pH sensitive. Between pH 6.7 and 5.8, a slight size decrease in the average diameter of around 10 nm has previously been observed by light scattering measurements (De Kruif and Zhulina, 1996, Alexander and Dalgleish, 2004), while an acidification of the system to below pH 5 induces an electrostatic collapse of the κ–casein (Tuinier *et al.*, 2002). One might expect then changes of a similar type in the covalently immobilized κ–casein with pH, and the extent of these was investigated as a prelude to studying the effects of the addition of pectin.

The effect of pH on the immobilized κ-casein conformation was investigated by flowing buffer (10 mM) with different pH values (3.5, 4.5, 5.3 and 6.8) over both the κ-casein coated and reference cells. Changes in the refractive index of the surface close to the sensor chip were recorded via monitoring the resonance angle with SPR. Figure 2 shows the response (RU) as the resonance signal recorded for the κ-casein coated cell after subtraction of the reference cell data, versus pH. A positive response was recorded for every pH change; from the running buffer at pH 7.4, to each pH in the range tested: 3.5-6.8. The response increases as the pH decreases although clearly not linearly: the value measured for pH values of 6.8 and 5.3 are in the same range, whereas further acidification of the κ-casein coated surface to pH values of 4.5 and 3.5 induced significant increases in the recorded

response. We thus observed a net effect of pH on the refractive index of the molecular layer covalently linked to the gold surface that tentatively might be interpreted as the result of the collapse of the κ-casein layer, indeed akin to that which causes micelle destabilisation in milk.

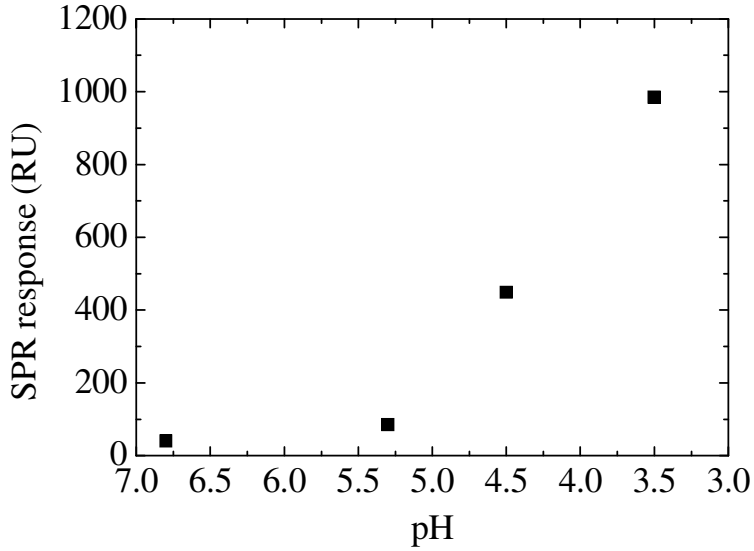

Figure 2: The change in the κ-casein state (response in RU) versus pH.

However, it should be considered that the polymer layer includes the carboxymethyl dextran coating on the gold surface of the CM5 chip which has been used for the coupling reaction in addition of the κ-casein covalently bound by reaction of its amine group to the dextran carboxyl group. The effect of pH on the resonance angle for proteins covalently bonded onto carboxymethyl dextran coated CM5 sensor chips has previously been investigated for dihydrofolate reductase (Sota *et al.*, 1998), myoglobin (Mannen, 2000), and for cytochrome c, concanavalin A, and poly-L-lysine (Paynter and Russell, 2002). Sota *et al.* (1998), by comparison of their SPR data to circular dichroism spectra, concluded that the changes in the SPR signal corresponded to conformational changes of the reductase during acid denaturation. On the other hand, Paynter and Russell (2002) did not observe concurrent changes in dichroism spectra accompanying SPR manifest changes, and suggested that the SPR data might be explained by electrostatic interactions between the immobilized biomolecules and the

carboxylmethyl dextran. Indeed, higher SPR signals were recorded when the immobilized ligand and the carboxylmethyl dextran were of opposite sign. However, in our experiments with immobilized κ-casein the highest SPR signal was obtained at pH 3.5 where κ-casein and carboxylmethyl dextran are both net negatively charged. The simplest explanation would seem to be that changes in the SPR signal versus pH obtained for covalently immobilized κ-casein reflects modifications in the conformation of the ligand itself. As the pH decreases below pH 5.3, the κ-casein layer coils closer to the gold surface increasing the density and the local refractive index. As the pH moves below 4.5, the SPR signal increases significantly as the κ-casein layer collapses further. This interpretation is consistent with what is known about the pH sensitivity of κ-casein as part of a casein micelle; as the pH is lowered, the κ-casein brush collapses on the surface of the micelle. Furthermore, this provides further evidence, in addition to the chymosin sensitivity, that the behaviour of the immobilised κ-casein layer used should not be too far removed from that of the bio-assembled casein micelle coating.

3.1.2 Effect of pectin fine structure on the interaction

As the pH dependant conformation of the ligand is clearly reflected in the SPR signal, as described above, care must be taken to take this into account when interpreting the results of experiments carried out to investigate the interaction of pectin and κ-casein. It has been clearly shown that in acidified milk systems pectin absorbs onto casein micelles by electrostatic interactions (Tuinier *et al.*, 2002, Maroziene and de Kruif, 2000). However, the effect of the amount and distribution of negative charges on the polysaccharide backbone on the interaction with the κ-casein layer on the surface of the casein micelle is still unclear. (Recently such considerations have been addressed regarding the interaction of pectin with β-lactoglobulin (Sperber *et al.*, 2009)). While high methoxyl pectins are generally reported to be more efficient in stabilizing acid milk drinks (Liu *et al.*, 2006) when calcium is present (in serum and additionally leaking from casein micelles), calcium sensitive pectins are trapped preventing a direct assessment of the interaction with the casein protein itself (Cucheval *et al.*, 2009). Here, the

direct interaction of the main casein on the surface of the micelle, κ-casein, and the polysaccharide, was tested, in absence of calcium. Although it might be argued that this is not as directly relevant for milk, it does help in the fundamental understanding of the interaction, particularly in relation to the pectin fine structure. The investigation was carried out using three pectin fine structures: common low (DM 28), and high methoxy pectins (DM 78); and a more unusually high DM sample (DM 90). These were flowed over a κ-casein coated surface in turn and changes in the refractive index of the surface were recorded versus pH by measuring the resonance angle by SPR as described previously herein.

Figure 3 shows the SPR signal at a given pH obtained by subtracting the response recorded when just the buffer was used (3.1.1) from the one recorded with the pectin analytes present. Pectin samples dissolved in buffers (0.1% w/w) at different pH values (6.8, 5.3, 4.5, and 3.5) were flowed over the cell at a low flow rate (10 µl / min) for 60 s, as previously described in the experimental section, and the SPR signal (taken 10 s before the end of the injection) was taken as the binding response.

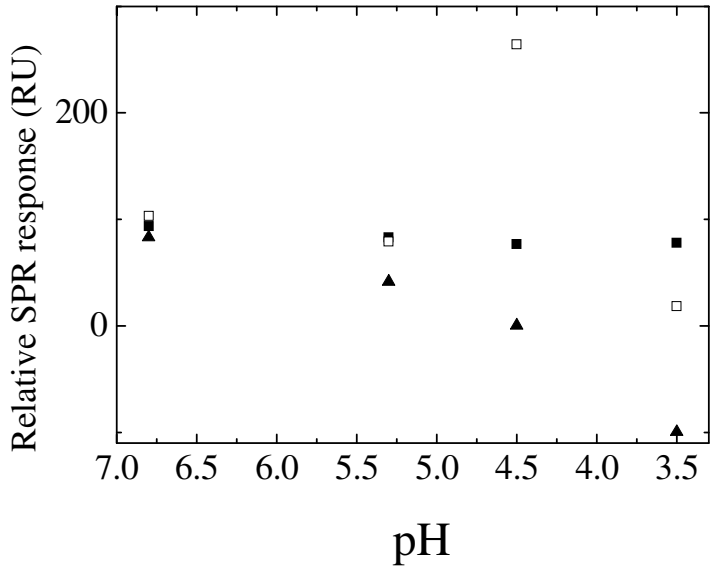

Figure 3: Effect of pectin structure on pectin- κ casein interfacial interaction versus pH: ■ DM 78 □ DM 90 ▲DM 28. Relative response (RU) obtained by subtraction of the response obtained at the same pH for κ-casein alone (figure 2).

At pH 6.8, a small positive SPR response was recorded for every pectin fine structure. This indicates that the presence of the polysaccharide changes the refractive index of the layer on the gold surface, which is most simply explained by the interaction of pectin with the κ-casein immobilized on the sensor chip and by the binding of some of the pectin molecules. At this pH, the net charge for both molecules is negative but at around one pH unit higher than the isoelectric point of κ-casein (5.9), around 10% of the charges on the protein are still positive and pectin seems to be able to bind κ-casein through these positive patches. It should be noted however that it has been clearly shown that at this pH, pectin doesn't adsorb onto casein micelles (Maroziene and de Kruif, 2000). This divergence at pH 6.8 between the interaction with κ-casein on a gold surface or on the outer of a casein micelle could be explained by the lower pI (4.6) of the micelle, resulting from the other proteins present in the interior of the assembled biocolloid.

At pH 6.8, pectins presented a higher binding response in the order DM 90 > DM 78 > DM 28. Higher SPR values are recorded for pectin with more methylesterified backbone e.g. those less negatively charged. By SPR, the variation of refractive index of the layer next to the surface is followed; it is not the strength of the interaction per-se but the amount of polysaccharide binding on the κ-casein coated surface (and in detail the effect of this interaction on the protein conformation) and hence density of material close to the surface which is being probed. At pH 6.8, a pectin molecule with a higher DM has less charged binding sites that can interact with the relatively small number of positive patches on κ-casein, thus leaving more available sites for other chains to bind to. In contrast, in the sample of lower DM, each individual molecule can bind more patches on the protein, essentially saturating the surface at a fewer number of pectin molecules bound. When the pH is decreased to 5.3, the SPR signal for all three pectins decreases; slightly for the HM pectins and in a more pronounced manner for the LM pectin. At this pH, the net charge of the κ-casein is positive, while pectin is still highly negatively charged. Under these conditions, there are more available binding sites on the protein so that one pectin molecule is more likely to bind to multiple sites, restricting the number of chains that might interact with the κ-casein layer. This pH decrease has the greatest effect on the binding of the low DM pectin, which with a large number of negative blocks on the pectin

backbone are most likely to 'lie down' on the surface, essentially blocking many positives sites on the protein and limiting the number of adsorbed chains.

As the pH is reduced further to 4.5, the binding level becomes even more dependent on the pectin DM. Higher SPR responses are registered for pectin with higher DM and the signal for low methoxyl pectin is weak. At this pH, the interaction is likely to be the strongest, as more of 90% of the charges are of opposite sign between the two biopolymers. More positive sites are available on the protein to bind pectin than at pH 5.3 and around the same percentage of negative charges are present on the pectin backbone. It makes sense then that the difference between the amount of polysaccharide chains containing differing amounts of potential binding sites for the same number of binding sites on the protein will be more pronounced. The weak signal observed with LM pectin likely results from a strong interaction of the polysaccharide with the κ-casein on multiple sites of its backbone driving each molecule to 'lay flat' on the κ-casein layer with limited formation of loops and tails; and limiting available sites for further molecules to bind.

Finally at pH 3.5, the binding level is still influenced by the pectin structure. The SPR signal is similar for DM 78 but an important decrease is observed for the DM 90 and DM 28. By decreasing the pH by one unit further, it is the amount of binding sites on the polysaccharide that is primarily affected (as the pKa of the carboxylic group is traversed, while the number of positive sites on the protein increases only slightly). At this pH, considerably less than 50% of the unmethylesterified acid galacturonic residues will be charged and presumably for the DM 90 sample, this only leaves a few percent of the galacturonic acid residues charged which may not be in runs of sufficiently charged patches to take part in binding. For the DM 78 sample, the binding response is similar to that at pH 4.5, showing that this polysaccharide still has enough charged patches to bind successfully. In contrast, a negative signal is observed for the low methoxyl pectin (DM 28). This change in the SPR signal when the pectin is flowed over the protein layer, despite its negative nature, can only be explained by interaction between the polymer and the κ-casein, as the effect of pH on the protein is eliminated by taking it as a reference. Its decreasing nature indicates that the biopolymer layer next to the gold surface is less dense when the low methoxyl

pectin is present than it is for the protein on its own, suggesting that its presence lessens the collapse of the protein at low pHs, as measured in the control experiments described in 3.1.1.

While, to date, the effect of pectin DM on the efficiency of the polysaccharide to stabilize acidified casein micelle systems has mostly been studied with high (DM 60-80) and low methoxyl pectin, our results indicate that 'unusually high' DM pectin should be of particular interest in stabilisation, especially at pH values around 4.5 where the highest pectin binding is observed with this structure. The relatively small percentage of charge on such a highly methylesterified structure implies that for potential binding sites to the protein to be formed small charged regions suffice. The effectiveness of this fine pectin structure give hints about the size of such 'epitopes' needed on the pectin backbone for the interaction. Indeed, even if we consider the pKa of the unmethylesterified groups to be approximately that of galacturonic acid monomers so that more than 90% of the unmethylesterified residues are charged, then for the average degree of polymerisation of the DM 90 sample used herein, each chain would have around 13 occurrences of single negatively charged galacturonic acid residues, one occurrence of a site with 2 consecutive charged residues, and a negligible probability of any runs of three consecutive charges. The effective 'epitope' on the pectin backbone is thus likely to consist of 2 charged residues next to each other.

3.2 Interaction of "model casein micelles" with pectin

Having elucidated the effect of pectin fine structure on the binding of pectin to a κ-casein layer at different pH values in the absence of calcium, the interaction was investigated on an intermediate model system: a 'synthetic casein micelle' without calcium. It might be argued that this model is far from a native casein micelle; however it is an interesting tool to get better understanding of the role of the interfacial interaction. The Brownian motion of these models 'synthetic casein micelles' was recorded by DWS in pectin solutions, and by comparison with their motion in water, the interfacial interaction between the surrounding polymer matrices and the κ-casein coated beads was studied. The state of these model

synthetic micelles was also followed by light microscopy. Specifically, calcium-free model casein micelles were synthesised by surface modification of latex particles, as described in the experimental section. κ-caseins were bound by physisorption to the latex surface, mainly through their hydrophobic residues leaving the hydrophilic residues exposed in the solution (Dalgleish *et al.*, 1985). The coating by κ-casein led to an increase of 20 nm in diameter (measured by DWS) which agrees well with measurement reported previously (Leaver *et al.*, 1994, Anema, 1997). This layer thickness suggests that the κ-casein must form loops and tails on the latex surface (Leaver *et al.*, 1994). In similar experiments to those carried out herein with protein layers, the action of chymosin on κ-casein coated latex particles has been reported previously and was found to be similar to its action on the casein micelle, highlighting that the conformation and orientation of κ-casein in these model systems may not be too dissimilar to when it forms part of the native casein micelle (Anema, 1997, Leaver, 1999). Furthermore, it has been recently shown by the comparison of the motion of casein micelles with κ-casein coated latex beads in acid milk systems that κ-casein coated latex probes can be excellent casein micelle models (Cucheval *et al.*, 2009).

3.2.1 κ-casein coated probes versus naked particles in water

The effect of the κ-casein coating on the Brownian motion of latex beads was first investigated in water. These preliminary experiments serve as controls in the study of the effect of pectin on the motion of coated and naked particles. The behaviour of bare and κ-casein coated latex particles (0.8% w/w) in a low concentration buffer (10 mM) were analyzed versus pH. DWS was used to record the evolution of the autocorrelation function of the transmitted light scattered by the coated and uncoated latex particles respectively. Figure 4 shows the autocorrelation functions, $g_1(\tau)$ as a function of the time lag τ, as measured by DWS at different pHs. For every pH, they decrease to zero at long times for both the bare and the κ-casein coated beads, characteristic of a diffusive motion in a Newtonian fluid. The correlation functions of the bare beads at all pHs between 3.5 to 6.8 (figure 4a) are similar which was expected as the size of the scatterers is constant and there is no significant change in viscosity of water with pH.

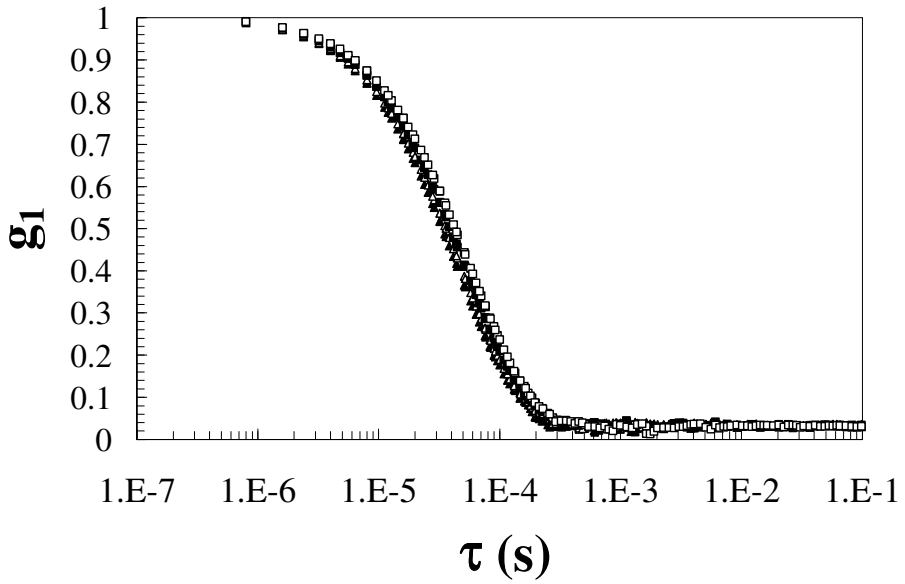

Figure 4a: Temporal autocorrelation function measured by DWS for (a) bare latex beads in 10mM buffer at different pHs (■ 3.5,△ 4.6,▲ 5.3, □ 6.8)

However, for the κ-casein coated beads (figure 4b), the autocorrelation function was not measurable for every pH. Indeed at pH 4.6, the system with κ-casein coated beads in water forms macroscopic precipitates, and an analysis of this bulk phase separated and heterogeneous system with DWS is not relevant. The difference of behaviour for the coated and bare beads at pH 4.6 could be explained by the fact that the layer of κ-casein on the latex beads doesn't only change the size of the particles but also gives the surface a hydrophobic character not possessed by the naked beads. Subsequently when the pH drops and the κ-casein layer collapses (as seen in the SPR experiment) aggregation is induced; the same phenomenology as observed with casein micelles themselves. For the other pH values, where the polymer layer is still able to sterically stabilise the particles (figure 4b), the autocorrelation function was observed to move slightly to higher correlation time when compared with the naked beads, corresponding well with the change in size induced by the coating.

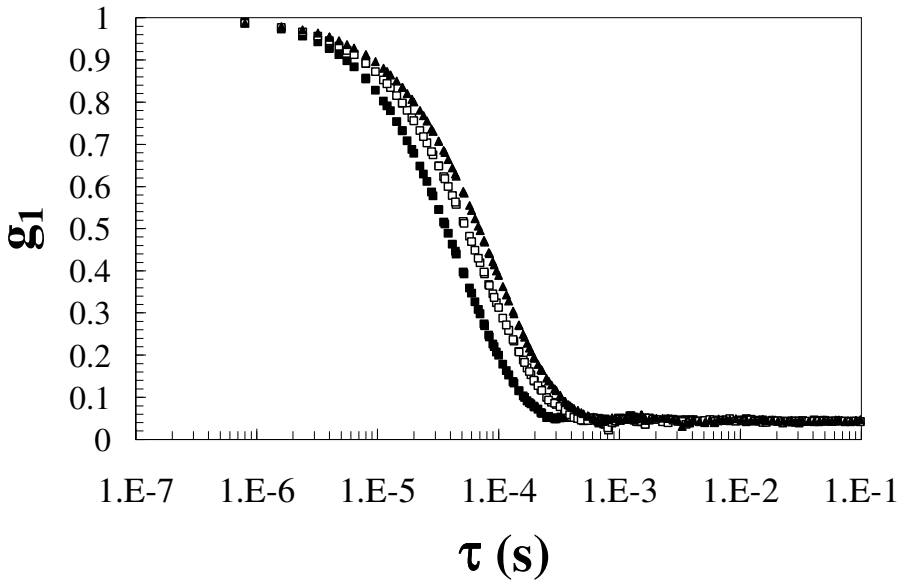

Figure 4b: Temporal autocorrelation function measured by DWS for (b) κ -coated beads, in 10mM buffer at different pHs (■ 3.5, ▲ 5.3, □ 6.8)

Subsequently, the mean square displacements of the scatterers were obtained from the autocorrelation functions by inversion of equation 2, with a zero-crossing routine as previously described in the experimental section and elsewhere (Weitz *et al.*, 1993). Figure 5 shows the corresponding mean square displacements (MSD) for bare and coated latex particles as a function of time lag τ, as measured by DWS at pH: 3.5 (A), 4.6 (B), 5.3 (C) and 6.8 (D) derived from the data shown in figure 4.

The slope of the MSD versus time lag follows the same power law dependency with a slope close to 1, characteristic to diffusive motion in a viscous medium, as expected. The fact that the κ-casein coated particles move slightly less than the bare ones in the same time at each pH and that the intensities observed for both types of particles were similar, is again evident, consistent with the size increase of the coated scatterers.

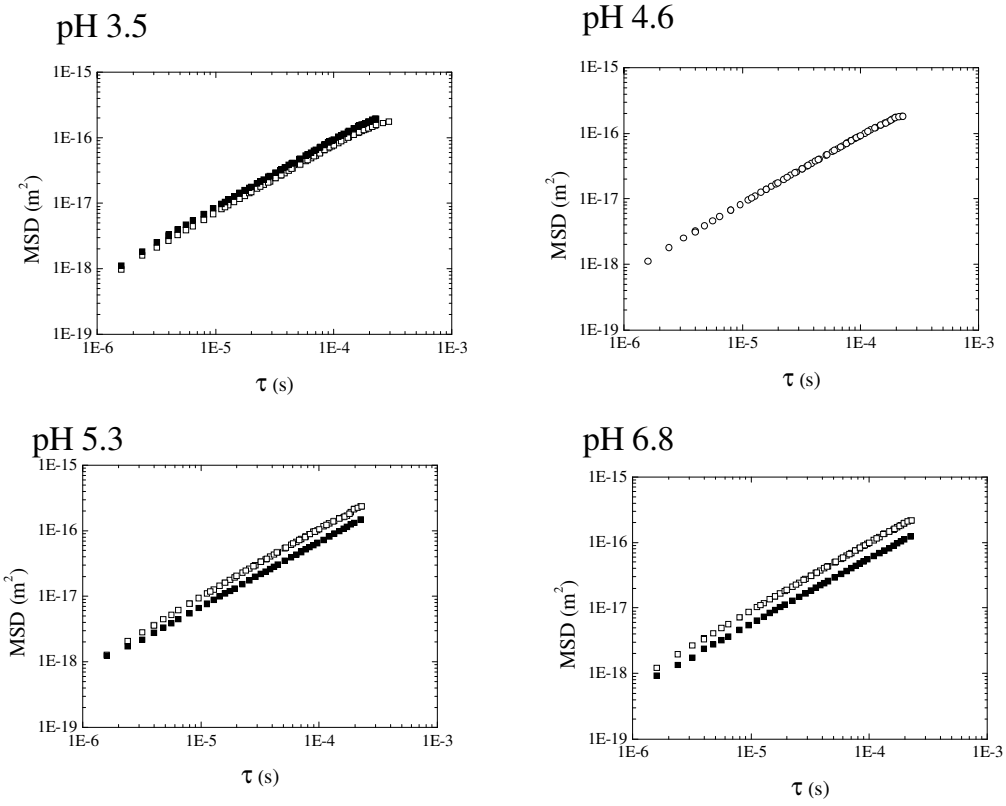

Figure 5: Scatterers mean square displacements as a function of lag time for κ-casein coated and bare latex beads in water, calculated form the data presented in figure 4. ■ κ -casein coated latex beads □ bare latex beads.

3.2.2 κ-casein coated probes versus naked particles in HM pectin solutions

The motion of the same bare and coated particles was probed and compared in HM pectin solution in order to investigate the interaction of pectin with synthetic 'model casein micelles' (without the complication of calcium). While in the system with bare latex particles the dynamics of the scatterers reflects the viscoelastic properties of the medium: i.e. the pectin solution (as in conventional microrheology), in systems containing κ-casein coated particles, the displacement of the probes can also reflect interactions between the particle surface and the surrounding pectin polymers.

Systems containing 0.4 %w/w high methoxypectin (DM 78) and 0.8% w/w κ-casein coated, or, bare latex, particles were adjusted to different pHs between 6.8 and 3.5 and DWS was used to record the fluctuation of the transmitted intensity scattered by the coated or uncoated latex beads. Figure 6 shows the autocorrelation functions, g1(τ), as a function of the time lagτ, measured by DWS at different pHs. For the bare beads system (figure 6a), the g1(τ) values decrease to zero at long times and are extremely similar for every pH, characteristic of Newtonian fluids of similar viscosity. This is expected as the size of these scatterers doesn't change with pH, and pH-induced changes in the viscosity for high DM pectin solutions are limited (owing to the low concentration and limited number of ionizable groups on the polymer). No pectin-induced depletion flocculation was observed either in the DWS experiments or by microscopy, over long time scales (>12 hrs).

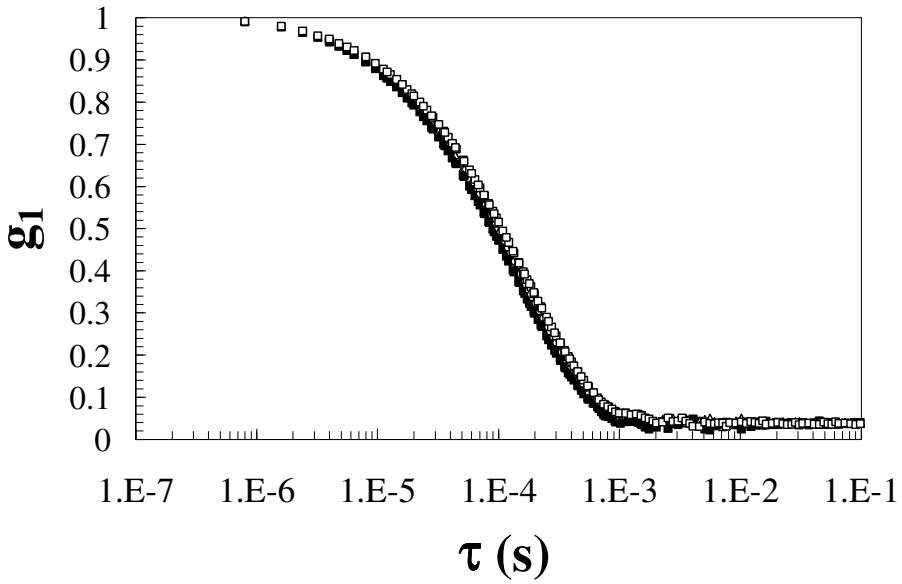

Figure 6a: Temporal autocorrelation functions measured by DWS for (a) bare latex beads at different pH values at different pHs (■ 3.5,▲ 5.3, □ 6.8)

Interestingly, κ-casein coated beads in pectin solution (figure 6b) did not show any bulk precipitation at any pH, including 4.6; whereas in water, bulk phase separation has been evident (3.2.1). It was however evident from the autocorrelation functions of the κ-casein coated beads in pectin solution that the

functional forms had changed in comparison to the experiments with bare beads, especially at pHs 4.6, 5.3, and 6.8. This change in the shape of the autocorrelation function could be explained by the local aggregation of the scatterers themselves, which fits well with the higher intensity observed for the κ-casein coated bead system compared with the naked one for these three pHs.

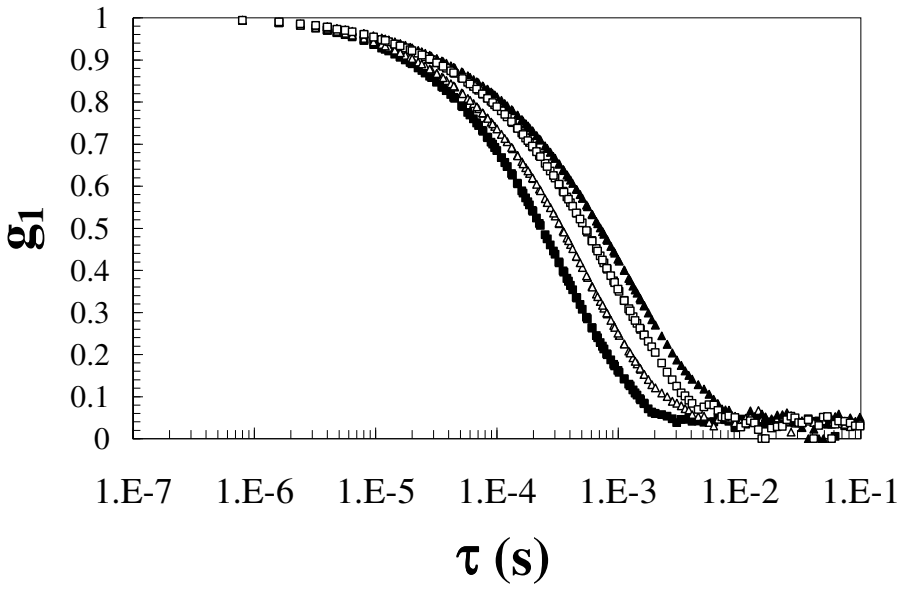

Figure 6b: Temporal autocorrelation functions measured by DWS for κ -coated beads in 0.4 %HM pectin solution, at different pH values at different pHs (■ 3.5,△ 4.6,▲ 5.3, □ 6.8)

This hypothesis was confirmed by microscopy of these systems in a large range of pectin concentration (Figure 7)- (small aggregates of κ-casein coated particles can be visualized at all pH values examined with the exception of 3.5). This limited local aggregation is the result of the presence of pectin in the system: it was not observed at these pH values for the same κ-casein coated beads in water, nor, importantly, did it occur for bare beads in pectin solution: both the protein coating and the polysaccharide solution are required. As such, the bridging of the κ-casein coated micelles by the polysaccharide would seem to offer a natural explanation for the observed phenomena.

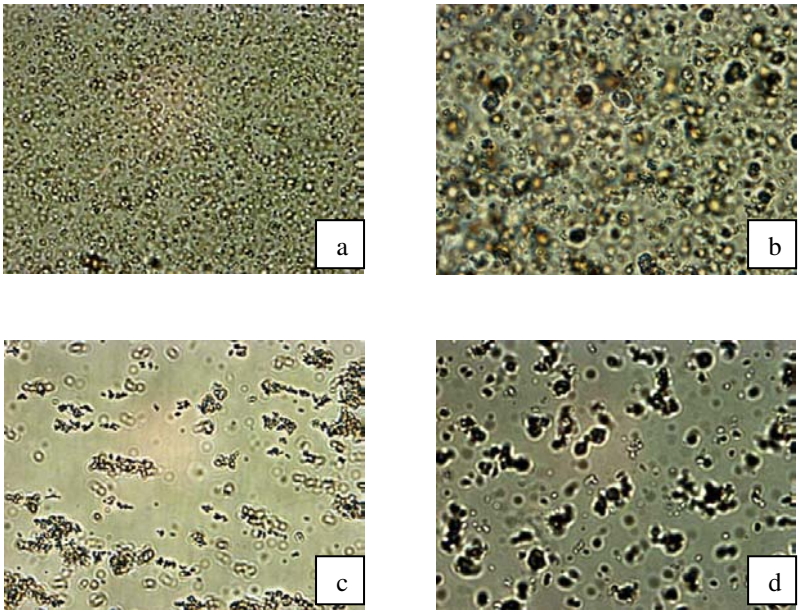

Figure 7: Micrographs showing the system κ-casein coated latex beads and DM 78 pectin (1 % w/w) at different pH values: (a) 3.5, (b) 4.6, (c) 5.3, (d) 6.8.

The MSDs obtained by inversion of the correlation functions were analyzed. Figure 8 shows the MSD versus time lag for the bare beads and their κ-casein coated counterparts in 0.4 % pectin solution for different pH values.

At pH 3.5, the MSD for the κ-casein coated and bare particles are almost identical, as expected where no aggregates were visualized by microscopy. Although pectin and κ-casein do carry opposite charges at this pH, the negative charge on the pectin backbone is low. Even though SPR measurements did show (section 3.1.2) that at this pH, some pectin was binding on the κ-casein (when immobilized on a gold rather than latex surface) it is possible that the rarity of charged binding regions on the high DM polymers at low pH values make bridging less likely and stabilization a more common outcome.

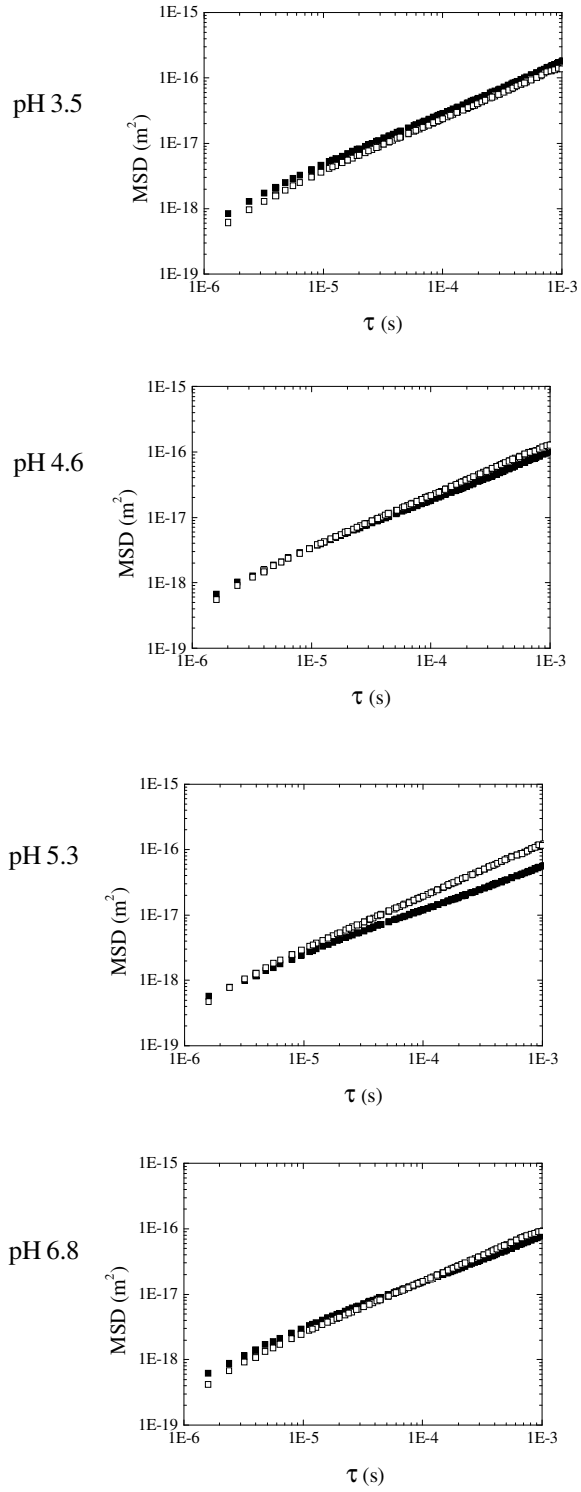

Figure 8: Scatterers mean square displacements as a function of lag time for κ-casein coated and bare latex beads in HM pectin (0.4 %), calculated form the data presented in figure 6. ■ κ -casein coated latex beads □ bare latex beads.

At higher pHs (at pH 3.5 and above) different slopes at high frequency and subtle but distinct differences in the shapes of the MSD are observed, with a change of slope at time lag around 0.1 ms, for the κ-casein coated scatterers. Once again it is important to emphasize that this change of slope has not been observed in any systems investigated without the presence of pectin, or in pectin solution with bare beads. Such MSD shape changes have previously been observed however in acidified skim milk systems (10% w/w solid content) with high methoxypectin (0.1% w/w), and was suggested to provide a signature of the bridging of the casein micelles by pectin (Cucheval *et al.*, 2009). Further, hints of such a sigmoidal shapes have also been found previously in studies of colloidal gels embedded in polymer solutions of varying visco-elasticity (Pashkovski *et al.*, 2003). We hypothesize then that the change of slope and shape in the MSD reflects the same phenomena previously observed with casein micelles: model κ-casein coated micelles are bridged by pectin and the aggregates observed by microscopy are complexes of the synthetic micelles, stabilized by pectin, sterically by non-bridging chains, possibly aided by the viscosity of the solution.

3.2.3 Effect of pectin fine structure on the interaction

In addition to the DM 78% pectin data previously reported (3.2.2), the effect of pectin fine structure on the interaction with synthetic casein micelles was studied. Two other pectin fine structures previously used in the SPR experiments were tested and compared: low methoxypectin (DM 28) and higher methoxypectin (DM 90). Systems with the same concentration of pectin (0.4 %w/w) and κ-casein-coated or bare latex particles (0.8 %w/w) were adjusted to pHs between 6.8 and 3.5. DWS was used to record the fluctuations of the transmitted intensity scattered by the coated or uncoated latex beads. Figure 9 (A, B) shows the MSD versus time lag for bare beads and their κ-casein coated counterparts in 0.4 % LM pectin, and in the previously reported DM 78 pectin, for comparison at different pHs.

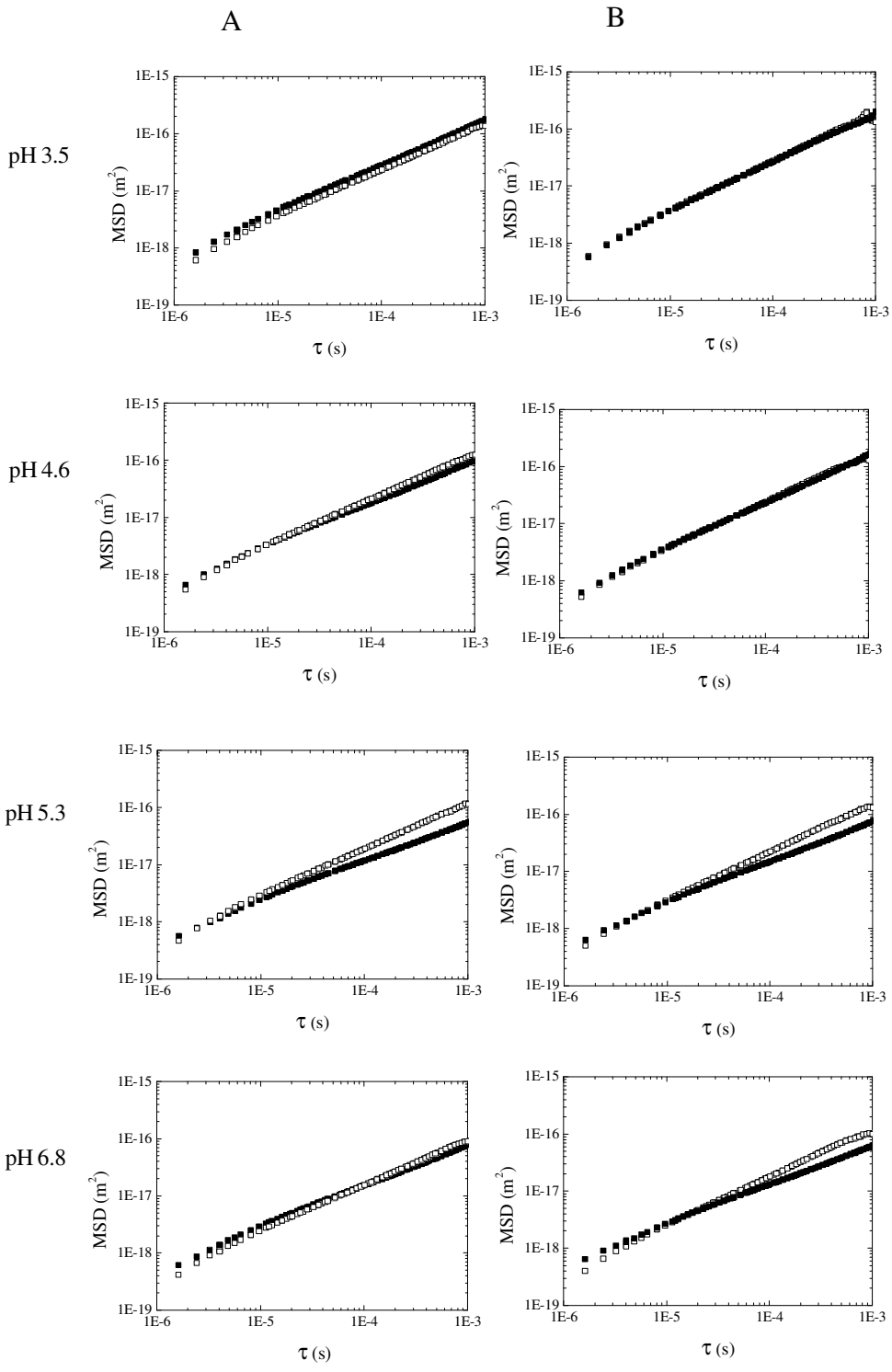

Figure 9: Scatterer mean square displacements as a function of lag time for κ-casein coated and bare latex beads in 0.4%w/w pectin solution A: HM pectin (DM 78%), B: LM (DM 28%) pectin, at different pH. ■ κ -casein coated latex beads □ bare latex beads.

At pH 3.5, the MSDs for the κ-casein coated and bare particles are almost identical for the LM pectin as was observed for the DM 78 pectin while, SPR measurements have shown different behaviour, in terms of the bound density on a gold surface, for these two pectin fine structures. The negative SPR response recorded at this pH for LM pectin was interpreted as a higher effectiveness of the polysaccharide in inhibiting the collapse of the κ-casein layer which might explain the reluctance to induce bridging and stabilization a favoured outcome.

At pH 4.6 and above, the MSDs measured for the κ-casein coated and bare particles are similar for the LM pectin to the corresponding responses observed for the DM 78 sample. Once again the slope at high frequency is slightly different for κ-casein coated and bare particles and the same sigmoid shape reported for the DM 78 pectin solution is observed (3.2). To this extent, it appears that the DM 28 and DM 78 samples both form similar soluble complexes with κ-casein coated particles formed by bridging of the synthetic casein micelles by the polysaccharide that are sterically stabilised by non-bridging chains, possibly aided by the viscosity of the solution.

Finally, the MSDs of κ-casein coated particles and their naked forbears, moving in a solution of 0.4 %w/w of an unusually high, DM 90, pectin sample are shown in figure 10 as well as the micrographs for the coated particles, once more as a function of pH. In stark contrast to the behaviour observed for the other fine structures, here the MSDs measured for the κ-casein coated particles are almost identical to those of their naked counterparts, *for every* pH. This pectin and the κ-casein coated particles did not aggregate in the pH range tested, which was confirmed with microscopy (figure 10).

While pectin with a DM of 90% is only ever going to be weakly negatively charged regardless of the pH, the SPR measurements carried out herein conclusively showed that i) DM 90 does bind onto a κ-casein immobilized layer at every pH tested and ii) owing to its sparing attachment to multiple sites on the protein, the actual amount of bound polymer is higher than for the other fine structures.

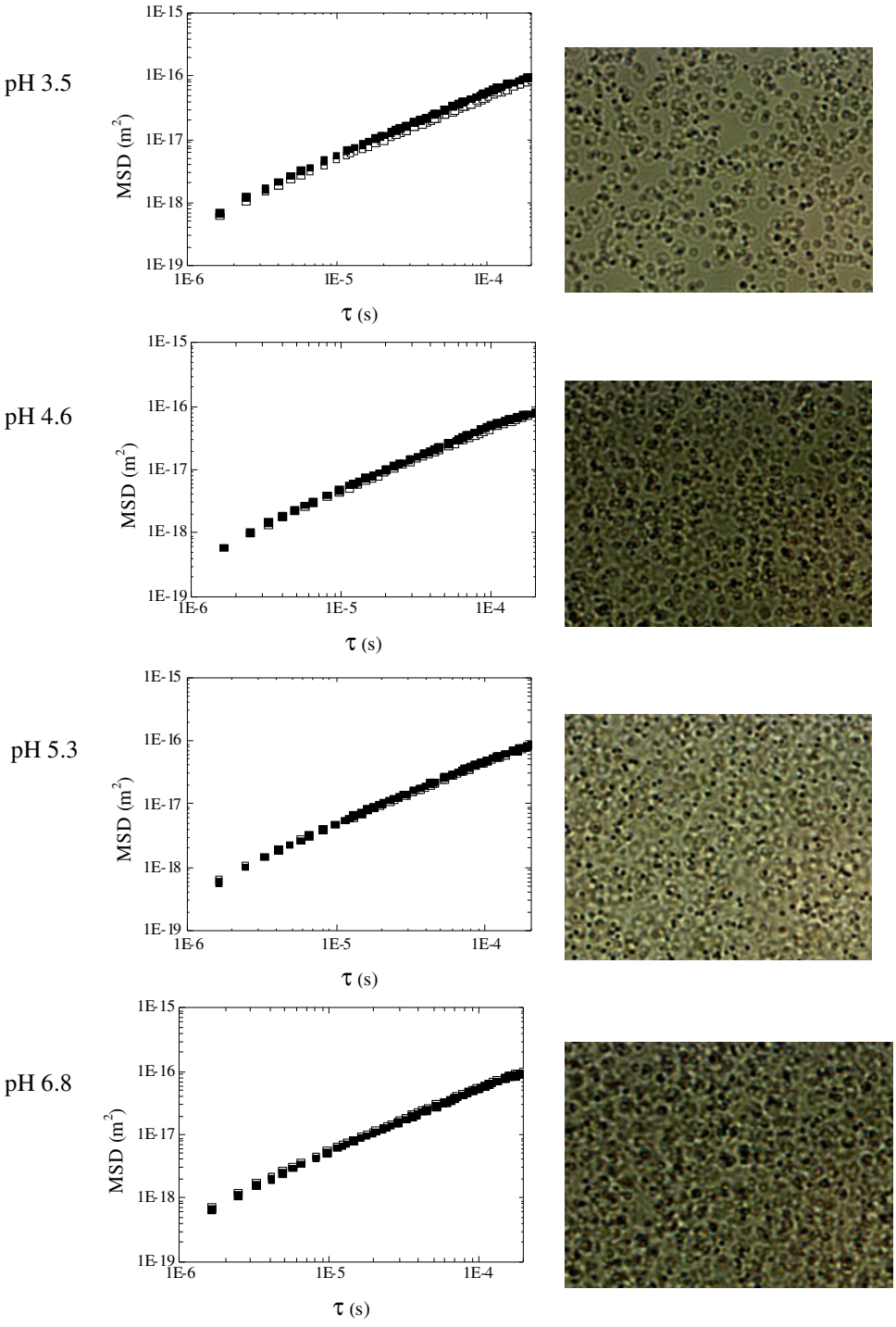

Figure 10: Scatterers mean square displacements as a function of lag time for κ-casein coated and bare latex beads in 0.4%w/w DM 90 pectin solution at different pH. ■ κ -casein coated latex beads □ bare latex beads. Right hand side: micrographs showing the system κ -casein latex beads.

The effectiveness of DM 90 in stabilising the micelle mimics over the pH range tested, while simultaneously avoiding not only macroscopic precipitation, but also local bridging-mediated aggregation, reinforces the hypothesis that ideally stabilising fine structures would be those containing the minimal amount of binding regions per chain.

4 Conclusion

Utilising model casein micelles (in order to avoid the complications of calcium binding) LM and HM pectin samples have been shown to produce similar phenomenology when added to the system at different pHs (6.8-3.5). This includes (i) the stabilisation of κ-casein coated particles at pH 3.5. This is consistent either (for HM samples) with the binding observed in SPR coupled with a lack of multiple binding patches on each chain owing to the low charge, or with the stabilisation of the protein collapse also seen in SPR at low DM. (ii) The formation of bridged soluble complexes at higher pH values, confirmed by microscopy, and reminiscent in their DWS signature of the findings of previous work on bridged micelles in acid milk gels.

Additionally it has been shown that unusually HM pectins (DM 90) do not exhibit the formation of such synthetic casein micelle-pectin complexes over a considerably broader pH range, instead stabilising the dispersion to aggregation. This is corroborated by the SPR study that clearly shows the largest polymer density bound to the κ-casein coated SPR chip for this fine structure; supporting the hypothesis that having a minimal number of binding regions per polymer chain is beneficial; both allowing the protein binding sites to be used more efficiently in harvesting the solution for more stabilising chains, and ensuring that where multiple sites exist large loops, trains and tails can be formed. Figure 11 shows a schematic diagram summarising the proposed interpretation of the experiments reported herein.

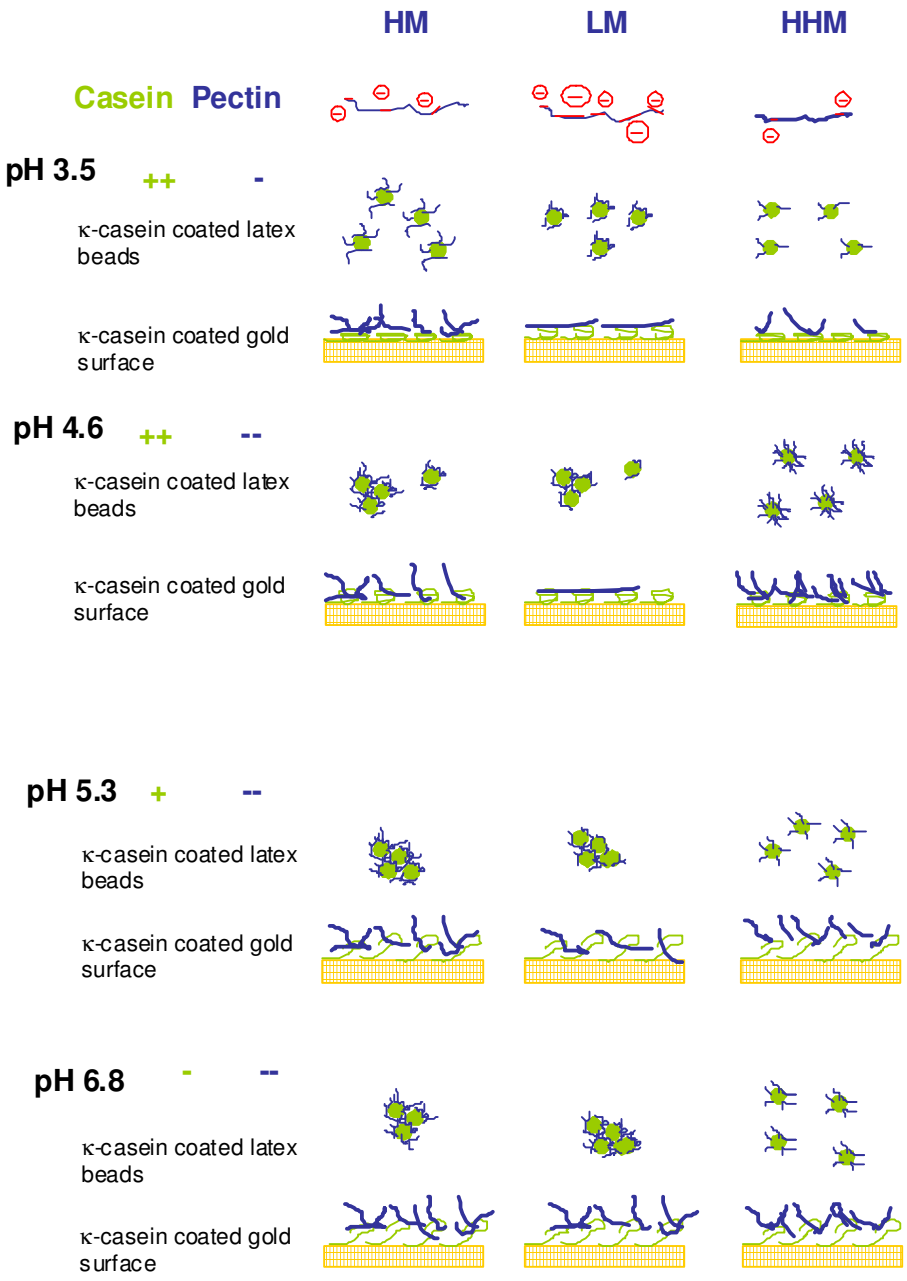

Figure 11: Schematic diagram summarising the proposed interpretation of the experiments reported herein. LM: low methoxy pectin; HM: high methoxy pectin; HHM: unusually high methoxy pectin.

Acknowledgments

The authors acknowledge financial support from Fonterra and FRST for a PhD scholarship for A Cucheval. The authors would also like to thank Dr Ashton Patridge to let them use the Biacore.

References

Alexander M., Dalgleish D.G. (2004) Application of transmission diffusing wave spectroscopy to the study of gelation of milk by acidification and rennet. *Colloids and surfaces B-Biointerfaces* **38**(1-2):83-90

Anema S.G. (1997) The effect of chymosin on κ-casein-coated polystyrene latex particles and bovine casein micelles. *International Dairy Journal* **7**(8-9):553-558

Chu B., Zhou Z., Wu G.W., Farrell H.M. (1995) Laser-Light Scattering of Model Casein Solutions - Effects of High-Temperature. *Journal of Colloid and Interface Science* **170**:102-112.

Creamer K., Berry G.P. (1975) Study of properties of dissociated bovine casein micelles. *Journal of Dairy Research* **42**:169-183

Cucheval A., Vincent, R.R., Hemar Y., Otter D., Williams M.A.K. Diffusing Wave Spectroscopy investigations of acid milk gels containing pectin. *Colloid & Polymer Science*, In Press

Cucheval A., Vincent R.R., Hemar Y., Otter D., Williams M.A.K. Multiple Particle Tracking investigations of acid milk gels using added tracer particles with designed surface chemistries; and comparisons with diffusing wave spectroscopy studies *submitted to Langmuir*

Dalgleish D.G., Dickinson E., Whyman R.H. (1985) Ionic strength effects on the electrophoretic mobility of casein-coated polystyrene latex particles *Journal of colloid and interface science* **108**(1):174-179

De Kruif C.G., Zhulina E.B. (1996) Kappa-casein as a polyelectrolyte brush on the surface of casein micelles. *Colloids* and Surfaces A: *Physicochemical* and *Engineering Aspects* **117**:151-159

Harte F.M., Montes C., Adams M., San Martin-Gonzales (2007) Solubilized micellar calcium induced low methoxyl-pectin aggregation during milk acidification. *Journal of Dairy Science* **90**:2705-2709

Hemar Y., Pinder D.N. (2006) DWS microrheology of a linear polysaccharide. *Biomacromolecules* **7**:674-676

Horne D.S. (2006) Casein micelle structure: Models and muddles. *Current Opinion in Colloid & Interface Science* **11***:*148-153

Leaver J., Brooksbank D.V., Horne D.S. (1994) Influence of glycosylation and surface charge on the binding of kappa-casein to latex particles. *Journal of colloid interface Science* **162**:463-469

Leaver J. (1999) Protein absorption on to latex beads. In Schwarz J.I., Contescu C.I. (Eds.). *Surfaces of Nanoparticles and Porous Materials,* New York: Marcel Dekker

Liu J.R., Nakamura A., Corredig M. (2006) Addition of pectin and soy soluble polysaccharide affects the particle size distribution of casein suspensions prepared from acidified skim milk. *Journal of Agricultural and Food Chemistry* **54**:6241-6246

Maroziene A., de Kruif C.G. (2000) Interaction of pectin and casein micelles. *Food hydrocolloids* **14**:391-394

Matia-Merino L., Lau K., Dickinson E. (2004) Effects of low-methoxyl amidated pectin and ionic calcium on rheology and microstructure of acid-induced sodium caseinate gels. *Food hydrocolloids* **18**:271-281

Pashkovski E.E., Masters J.G., Mehreteab A. (2003) Viscoelastic Scaling of Colloidal Gels in Polymer Solutions. *Langmuir* **19**:3589

Paynter S. and Russell D.A. (2002) Surface plasmon resonance measurement of pH-induced responses of immobilized biomolecules: conformational change or electrostatic interaction effects? *Analytical Biochemistry* **309**:85–95

Pereyra R., Schmidt K.A., Wicker L. (1997) Interaction and stabilization of acidified casein dispersions with low and high methoxyl pectins. *Journal of Agricultural and. Food chemistry* **45**:3448-3451

Sperber B.L.H.M., Schols H.A., Stuart M.A.C., Norde W., Voragen A.G.J. (2009) Influence of the overall charge and local charge density of pectin on the complex formation between pectin and beta-lactoglobulin. *Food Hydrocolloids* **23**(3)765-772

Sota H., Hasegawa Y., Iwakura M. (1998) Detection of conformational changes in an immobilized protein using surface Plasmon resonance. *Analytical Chemistry* **70**:2019–2024

Tromp R.H., De Kruif C.G., van Eijk M., Rolin C. (2004) On the mechanism of stabilisation of acidified milk drinks by pectin. *Food hydrocolloids* **18**:565-572

Tuinier R., Rolin C., de Kruif C.G. (2002) Electrosorption of pectin onto casein micelles. *Biomacromolecules* **3:**632-639

Weitz D.A., Pine D.J., Brown W. (1993) Diffusing-wave spectroscopy. In Brown W. (Eds) *Dynamic Light Scattering: The Method and Some Applications*, Oxford: Oxford University Press, 652-720

Williams M.A.K., Vincent R.R., Pinder D.N., Hemar Y. (2008) Microrheological studies offer insights into polysaccharide gels. *Journal of Non-Newtonian Fluid Mechanic* **149**:63

Willats W.G.T, Knox P., Mikkelsen J.D. (2006) Pectin: new insights into an old polymer are starting to gel.. *Trends in Food Science & Technologie* **17**:97-104

Conclusion and further work

1 Summary

The aim of this thesis was to understand better the interaction between casein micelles and pectin. The behaviour of pectin was investigated in different casein micelle systems and analogues, and using different pectin fine structures and the distribution of the methylester groups. As a prelude to the study of the interaction, the degree of methylation on the pectin fine structure was investigated for pectins with random and blocky distribution of charges. Furthermore, in this work, intermolecular and intramolecular charges distributions were envisaged as two characteristics resulting from the same process and thus intimately linked.

Having thoroughly investigated the fine structure of the polymers, the focus was turned to investigating the interaction between pectin and casein micelles. Firstly, the effect of pectin on acid milk gels for concentrated, quiescent systems was investigated by passive microrheology using two complementary techniques: diffusive wave spectroscopy (DWS) and multiple particles tracking (MPT). DWS, by allowing probing the mechanical properties of the network at high frequency, gave information on its microstructure. Furthermore, the motion of the casein micelles/micelle aggregates themselves (thus the protein network) is probed. However, by scattering, the average motion of a high number of scatterers was obtained, which means that the heterogeneity of the system e.g. the properties of the void and any distributions of the casein micelles, were not investigated. Multiple particle tracking was used to probe this heterogeneity by following the distribution of the displacements of beads (added to the system) at a given time lag during the gelation using the Van Hove distribution. Furthermore, the surface chemistry of the probes was modified in an attempt to control their location in the system. Finally, the mean square displacements of the casein micelles obtained by DWS and, of κ-casein coated particles obtained by MPT were compared for the same acid milk system.

Secondly, we aimed to gain understanding of the interaction between pectin and casein micelles by investigating the interfacial interaction between κ-casein and pectin (avoiding the complication of the presence of calcium). Two approaches were envisaged: the direct study of the interaction by surface plasmon resonance and indirectly by probing the motion of 'calcium-free casein micelles' in pectin solutions. With SPR, pectins with different fine structures were flown over κ-casein coated gold surface and the resonance angle, reflecting changes in the refractive index, was recorded versus time. It is thus the relative number of polymers binding to the surface and the effect of this binding on the state of the κ-casein layer that is reported rather than directly the strength of the interaction. With the 'calcium-free casein micelles', the interaction is not probed directly but is inferred from the way a κ-casein coating affects the motion of latex beads in pectin solutions.

2 Main conclusions and further suggested work

Firstly, the determination of the degree of methylesterification using capillary electrophoresis has been improved. The reliability and repeatability of the CE methods have been reinforced. Furthermore, an empirical fit of the experimentally measured electromobility versus ratio of charges gave a more precise relation between electromobility and degree of methylesterification (DM) valid for a bigger range of DM. Using this the pectin fine structure of homogalacturonan modified by alkali treatment was then investigated. For homogalacturonan, the intermolecular charge distribution was shown to contain information on the intramolecular distribution as they result from the same process and their random distribution was confirmed by comparison with the predicted distribution based on the binomial theorem. The intermolecular charge distribution of PME modified pectins versus degree of methylesterification during the enzymatic processing showed that at first only selected regions of the sample are modified while others remain intact. The rate of modification is not uniform for each pectin chain in the sample which is reflected by the increase of the broadness of the charge distribution with the enzymatic action at the beginning of the process. Furthermore, the charge distribution of the non-digestible fraction by endoPGII

was found to be similar to the mother pectin (before modification by PME). It means that the area on the backbone de-methylesterified by PME is accessible to endo-PGII which is fitting well with a pectin chain having a highly blocky distribution. The pectin chain parts on which PME has acted seems to be almost if not completely de-esterified and the other parts of the chain seem in contrast intact. It showed that PME has a really stepwise action pattern. However, to draw a more precise pattern of the distribution of the charges on the backbone, apart from saying that its not random and inferring that it is indeed blocky would require computer modelling on the PME action and comparison of the model with the experimental data.

Secondly, the study of the effect of pectin on acid milk gels showed that the interaction between pectin and casein micelles is strongly dependant on pectin's availability e.g. whether it was trapped by binding with calcium. For acid milk systems without pectin, a fractal signature is transiently observed at pH 4.8 which corresponds to the percolation point, using DWS. The effect of pectin on the behaviour at high frequency was dependant on the pectin fine structure. In the presence of high methoxyl pectin, insensitive to calcium, a characteristic modified shape of the mean square displacement was observed at high frequency using DWS and interpreted as a signature of bridging of the casein aggregates by pectin. In presence of low methoxyl pectin, the MSD shape at high frequency was not distinguishable from the shape obtained for a sample without pectin. LM pectins sensitive to calcium, were hypothesised to be trapped and were not able to interact with the casein micelles. These findings were supported by the study of the calcium balance by phosphorus NMR in milk systems at pH 6.8: LM pectin shifts the serum/micelle calcium balance and more calcium is leaking from the casein micelles in presence of LM pectin.

With multiple particle tracking and controlling the position of the probes by modifying their surface to include them in the network, the network formation was shown to be a homogeneous process and the final gel network, homogeneous. However, probing the mechanical properties of the voids by modifying the probes surfaces with PEG (which has shown to inhibit protein absorption from solution) wasn't successful. In further works, it could be considered to use an active strategy to drag the probes in the voids by optical tweezers for example or to

maintain the particle at a fixed position during the gelation considering that some of the held particles might be located in the void at the end of the gelation. Furthermore, by modulating the force used to hold the beads in the optical traps, information could be gained on the strength of the force acting on the beads at the void/protein network interface.

The comparison of the mean square displacements obtained by DWS and MPT with κ-casein coated probes gave good agreement. Furthermore, the comparison allowed us insight on the state of the casein micelle during acid milk gelation and justified their use as probes for the DWS experiment. It also evaluated the validity of κ-casein coated particles as a synthetic casein model.

Thirdly, the interfacial interaction between pectin and κ-casein, studied by SPR has shown that the amount of pectin binding on a κ-casein coated gold surface is strongly dependant on the pectin fine structure. The highest SPR signal was observed for an unusually high methoxyl pectin with a degree of methylesterifiaction of 90%, which gave information on the size of the 'epitopes' on the polymer backbone needed for the interaction. Indeed, a small negative patch on the pectin backbone likely to comprise of around two consecutive unmethylesterified acid galacturonics seems effective for the pectin binding on the κ-casein. The lower amount of bound pectin for the less methylesterified polymer at pH 4.5 has been explained by a multiple patch binding on the κ-casein layer.

Finally, the study of the motion of calcium-free model casein micelles in pectin solutions with different fine structures have shown that high methoxyl (DM 78) and low methoxyl (DM 28) pectin are bridging the casein micelles at every pH except pH 3.5. However, bridging was not observed for less charged HM (DM90%) even though SPR measurements have shown that this pectin structure was binding heavily on the κ-casein coated surface. This pectin structure with a limited number of negative patches on its backbone limits the potential for destabilization via bridging (and maximises the number of chains stuck to the surface).

In this thesis, the interaction between pectin and casein micelles has been studied directly and indirectly using different casein micelles systems and analogues. However, the strength of the interaction hasn't been investigated

directly. Indeed by SPR, even if it is a direct method, the result obtained is the amount of polymer bound to the κ-casein coated surface and changes in the state of this surface. Further works could study the direct interaction using atomic force measurement (AFM) by coating the surface with κ-casein or casein micelles, and the cantilever with pectin.

Another interesting route would be to gain further information on the 'epitope' on the pectin backbone needed for the interaction. The SPR data could be further analyzed using more modelling and comparing the relative amount of polymer bound for the different fine pectin structures.

In this thesis we have shown that an unusually highly methylesterified pectins seems the best candidates to stabilize casein micelles in an acid milk system. It will be interesting to give further details on this optimal structure by further controlling the pectin pattern and test the designed structures by combining calcium sensitivity measurements and binding ability. We could for example answer if all the negative charges on the backbone of the pectin with a DM 90 are important for the interaction or if it is only one 'epitope' composed of two consecutive negative charges which is determinant for the interaction.